MODELING PULMONARY TUBERCULOSIS AND PNEUMONIA CO-INFECTION INCORPORATING AN ASYMPTOMATIC COMPONENT AND NATURAL IMMUNITY

ERICK MUTWIRI KIRIMI

A Thesis Submitted in Partial Fulfillment of the Requirements for the Conferment of the Degree of Doctor of Philosophy in Mathematics of Meru University of Science and Technology

2025

DECLARATION

This thesis is my original work and has not been presented for a degree in any other Institution.

SC502/200924/20

Erick Mutwiri Kirimi

Signed: . . . . . Date: . . . . . .

This thesis has been submitted with our approval as university supervisors.

Signed: . . . . . Date: . . . . . .

Dr. Grace Gakii Muthuri, PhD

Meru University of Science and Technology, Kenya.

Signed: . . . . . Date: . . . . . .

Dr. Stephen Karanja, PhD

Meru University of Science and Technology, Kenya.

Signed: . . . . . Date: . . . . . .

Dr. Cyrus Gitonga Ngari, PhD

Kirinyaga University, Kenya

DEDICATION

To my parents, Mr. and Mrs. Kirimi, for your encouragement and support towards my education. To my wife, Jane, for your prayers, and to my daughter, Meghan, for your patience.

ACKNOWLEDGEMENTS

I thank Almighty God for His grace, which has enabled me to carry out this study. My sincere gratitude goes to my supervisors, Dr. Grace Gakii Muthuri, Dr. Stephen Karanja, and Dr. Cyrus Gitonga Ngari, whose guidance, advice, and inspiration were invaluable throughout the research period. Their unwavering support ensured I remained on the right track, and their timely feedback motivated me to maintain a spirit of diligence. I extend my heartfelt thanks to my lecturers, Prof. Eustace Mwenda, Dr. Karanja, Dr. Gakii, Dr. Njagi, Dr. Mutua, and Dr. Ngari, for their professional assistance during the coursework. Special appreciation goes to my wife, Jane, for her steadfast support throughout this journey. Her prayers and encouragement were my source of strength. I am also deeply grateful to my other family members for their constant support and encouragement. I remain indebted to my classmates, Vincent, James, Kariuki, and Makembo, for their invaluable contributions and encouragement during the progressive stages of this study. Lastly, I am grateful for the financial support provided by the Higher Education Loans Board Postgraduate Scholarship, which enabled me to pursue my PhD studies.

TABLE OF CONTENTS

LIST OF TABLES

LIST OF FIGURES

ABBREVIATION AND ACRONYMS

AIDS	Acquired Immune Deficiency Syndrome
CRS	Civil Registration Services
ECDC	European Centre for Disease Control
KNBS	Kenya National Bureau of Statistics
MATLAB	Matrix Laboratory
NTLLDP	National Tuberculosis Leprosy and Lung Disease Program
SDG	Sustainable Development Goals
SSD	Sum of Square Difference
SIS	Susceptible-Infected-Susceptible
SIR	Susceptible-Infected-recovered
SIRS	Susceptible-Infected-recovered-Susceptible
SEIS	Susceptible-Exposed-Infected-Susceptible
SEIR	Susceptible-Exposed-Infected-Recovered
SEIRS	Susceptible-Exposed-Infected-Recovered-Susceptible
SVEIR	Susceptible-Vaccinated-Exposed-Infected-Recovered
SVEIRE	Susceptible-Vaccinated-Exposed-Infected-Recovered-Exposed
TB	Tuberculosis
UHC	Universal Health Coverage
UNEP	United Nations Environment Program
WHO	World Health Organization

DEFINITION OF TERMS

Asymptomatic Infectious TB	Refers to a condition where an individual has pulmonary TB but does not exhibit any symptoms typically associated with the disease.
Basic Reproduction Number	It is the average number of secondary infections caused by an index case in a completely susceptible population.
Co-infection	This is the simultaneous infection of the same host with two or more different pathogens leading to co-existence of pathogens in a population.
Control Reproduction Number	It is the average number of secondary infected cases due to each infectious case in the presence of control measures such as vaccination.
Endemic	Refers to constant prevalence of a disease in a population within a geographical area.
Epidemic	This is widespread occurrence of disease in a population at a particular time.
Epidemiology	The study of the determinants, occurrence, and distribution of disease in a defined population.
Latent TB Infection	Refers to a condition where a person carries the bacteria that cause tuberculosis in their body, but the bacteria are in an inactive or dormant state.
Pulmonary TB	It is a form of tuberculosis that primarily affects the lungs caused by the bacterium *Mycobacterium tuberculosis*.

Symptomatic TB	Refers to a condition where an individual with tuberculosis shows clinical signs and symptoms of the disease, such as persistent cough, chest pain, fever, night sweats, fatigue, or weight loss.

ABSTRACT

Pulmonary tuberculosis is one of the leading infectious diseases causing mortality worldwide, and its impact is exacerbated by opportunistic infections such as pneumonia. The lethal synergism between pulmonary tuberculosis and pneumonia contributes to increased mortality in endemic regions. Existing models of pulmonary tuberculosis do not incorporate the screening of asymptomatic infectious individuals, despite their significant contribution to disease transmission within the population. Additionally, these models do not account for the impact of natural immunity in controlling or reducing the spread of infections. The aim of this study was to model pulmonary tuberculosis and pneumonia co-infection incorporating an asymptomatic infectious component and natural immunity. The study objectives included: formulating a pulmonary tuberculosis model that incorporates an asymptomatic infectious component and natural immunity; formulating a co-infection model that also incorporates an asymptomatic infectious component and natural immunity; determining the reproduction numbers for analyzing the formulated models; and investigating the effects of varying model parameters on the control of pulmonary tuberculosis. A population-based compartmental approach was employed to formulate the models, from which differential equations were derived. The progression from latent infection to pulmonary tuberculosis disease was modeled using Holling's saturation term to account for natural immunity. The Next-Generation Matrix method was used to determine reproduction numbers, while stability was analyzed using the Routh–Hurwitz criteria, the Castillo–Chavez method, and Lyapunov functions. Sensitivity analyses of the reproduction numbers in relation to the model parameters were conducted using the normalized sensitivity index method. The model equations were solved numerically using fourth- and fifth-order Runge-Kutta methods in MATLAB software to identify effective intervention strategies for significantly reducing disease transmission. Secondary data from National Tuberculosis, Leprosy, and Lung Disease Program (NTLLDP) in Kenya were utilized to perform numerical simulations, with 2022 data serving as the initial conditions. The co-infection model was fitted to NTLLDP prevalence data from 2012 to 2022 using the fminsearch algorithm in MATLAB software to estimate specific parameters. The results predicted that combining vaccination, screening, and treatment for all forms of pulmonary tuberculosis is the most effective intervention for reducing transmission. Enhancing natural immunity, increasing screening rates for latently infected individuals, and improving vaccine efficacy were also shown to reduce the co-infected population. Specifically, a 10% increase in vaccine efficacy was predicted to reduce co-infections by 6.67%, while the same increase in the screening rate for latent infections reduced them by 6.73%. Furthermore, doubling the screening rate for individuals with asymptomatic infectious pulmonary tuberculosis was shown to reduce the population with severe co-infections and those undergoing treatment for severe conditions by 53.2%. These findings offer valuable guidance to healthcare officials in making informed decisions about screening latently infected and asymptomatic infectious tuberculosis patients, thereby contributing to the fight against epidemics of this disease. The results also underscore the importance of accurate diagnosis and effective treatment of tuberculosis and pneumonia co-infections, which contribute to reducing infection transmission. Lastly, the study emphasizes the need to enhance the natural immunity of latently infected individuals to reduce disease progression and transmission.

CHAPTER ONE: INTRODUCTION

1.1 Background Information

This section presents background information on pulmonary tuberculosis and pneumonia as major public health concerns. It also examines the role of natural immunity in tuberculosis transmission and outlines key mathematical epidemiological modeling approaches relevant to the study. Finally, it highlights the significance of the research within national and global development frameworks, with particular reference to Kenya Vision 2030 and the United Nations Sustainable Development Goals.

1.1.1 Tuberculosis

Tuberculosis (TB) is a disease that primarily affects the lungs but can also impact other parts of the body, such as the brain, kidneys, bones, and spine. Pulmonary TB specifically affects the lungs, while extra-pulmonary TB, which is non-infectious, affects other areas of the body (Nyerere et al., 2016). In this research, contagious pulmonary TB was considered, as it is one of the leading causes of morbidity and mortality globally. According to the World Health Organization (WHO) fact sheet for 2024, in 2023, 10.8 million people worldwide fell ill with pulmonary TB, and about 1.2 million succumbed to the disease. Furthermore, the fact sheet asserts that each year, an average of 10 million people globally contract pulmonary TB, with approximately 15% losing their lives despite the availability of effective treatment and affordable prevention strategies aimed at halting its transmission.

The glaring public health threat posed by pulmonary TB underscores the urgent need to intensify efforts to control its global spread. Notably, a significant knowledge gap persists in controlling or reducing pulmonary TB transmission, particularly in sub-Saharan Africa (World Health Organization, 2025). In addition to the failure to address the resurgence of pulmonary TB, researchers have attributed this knowledge gap to an overly simplistic view of its transmission mechanisms (Wilcox and Colwell, 2019). This suggests that effectively addressing the challenge of pulmonary TB requires a precise description of its transmission mechanisms, which can be achieved through new conceptual frameworks and the development of improved theories and models.

For a long time, the description of pulmonary TB transmission mechanisms has primarily relied on censored medical surveillance data, which are not entirely accurate (Dowdy et al., 2017). However, mathematical modeling, which combines the power of multivariate data analysis with the realism of complex epidemiological dynamical systems, offers a promising alternative (Wilcox and Colwell, 2019). Recognizing the potential of mathematical modeling provides an opportunity to understand the underlying causes of the recent increase in pulmonary TB incidences. Consequently, accurately describing pulmonary TB transmission mechanisms through mathematical modeling is essential for developing effective strategies to combat its spread. This realization motivated the current research study, which aimed to provide a realistic depiction of pulmonary TB transmission mechanisms and to formulate new mathematical models.

Pulmonary TB is caused by bacteria known as Mycobacterium tuberculosis. These bacteria are airborne and spread from one person to another when individuals with pulmonary TB cough, sneeze, spit, talk, laugh, or sing, releasing TB germs into the air. When inhaled, these germs can cause infection. Infected individuals may develop symptoms, including coughing with sputum, chest pains, weakness, weight loss, fever, and night sweats (World Health Organization, 2020a). However, researchers estimate that about one-quarter of the world's population is infected with pulmonary TB but shows no symptoms, a condition known as latent TB infection (Barry et al., 2019). Individuals with latent TB are neither infectious nor clinically ill, but if left untreated, they may progress to pulmonary TB disease. Preventing the progression of latent TB infection to pulmonary TB disease reduces the risk of further transmission within the population (Madhukar et al., 2016). This study, therefore, investigated the effects of screening latently infected individuals on the transmission of pulmonary TB using mathematical modeling approach.

Although approximately one-quarter of the world's population is latently infected with TB, some individuals with pulmonary TB are asymptomatic but infectious in its early stages. As a result, they delay seeking healthcare, leading to limited treatment options and adverse social and economic consequences (World Health Organization, 2015). This was confirmed by the National TB Prevalence Survey report of 2016 in Kenya, which revealed that 26% of

the prevalent cases diagnosed during the survey were asymptomatic, infectious, and did not seek medical care (National Tuberculosis, Leprosy and Lung Disease Program, 2016). Additionally, a study conducted by the European Centre for Disease Prevention and Control in 2018 showed that several individuals not only had a positive chest X-ray for pulmonary TB before developing symptoms but were also infectious (Verver et al., 2018). Furthermore, a report by (World Health Organization, 2025) asserts that approximately 50% of people with pulmonary TB detected through global prevalence surveys are asymptomatic. The presence of asymptomatic infectious patients underscores the need for tracing and quarantining contacts of infected individuals based on localized pulmonary tuberculosis epidemiology.

Asymptomatic infectiousness plays a significant role in the spread of contagious diseases such as pulmonary TB, as infections can be transmitted within the population undetected (Mathur and Narayan, 2018). Therefore, efforts to eradicate pulmonary TB must address the heterogeneities in transmission mechanisms and the drivers of localized epidemics. This study incorporated asymptomatic infectious individuals into a transmission mathematical model to more accurately represent the natural history of pulmonary TB. Specifically, numerical simulations were used to evaluate the impact of screening and treating asymptomatic infectious individuals on controlling pulmonary TB. This research addresses a gap in the existing literature, as the study of this aspect through mathematical modeling had not been previously explored.

The study considered pneumonia as an opportunistic infection to accurately describe the pulmonary TB transmission mechanism. A brief overview of pneumonia is provided in the following subsection.

1.1.2 Pneumonia

Pneumonia is a respiratory infection in which the alveoli of an infected individual become inflamed and filled with pus or fluid instead of air, resulting in painful breathing due to limited oxygen intake. It has been identified as one of the most life-threatening illnesses for people of all ages. In 2023, pneumonia accounted for 15% of all reported deaths among children under 5 years of age (World Health Organization, 2024).

Pneumonia is commonly caused by bacteria, along with other microorganisms such as

viruses and fungi. Bacterial and viral pneumonia are contagious and spread from person to person through inhalation of airborne droplets released when an infected individual sneezes or coughs. An infected person may develop symptoms ranging from mild to severe, which can result in hospitalization or even death. Symptoms include a cough with sputum, fever, sweating, shortness of breath, chest pain, fatigue, loss of appetite, nausea or vomiting, and headaches. Children under five years old often exhibit rapid breathing or wheezing (World Health Organization, 2020b).

In resource-limited settings with poor healthcare systems, the impact of pneumonia as an opportunistic infection on other respiratory diseases cannot be underestimated. Notably, individuals with pulmonary TB are particularly vulnerable to opportunistic pneumonia due to compromised immune systems (Garcia, 2019). Several clinical studies and reports have documented the occurrence of opportunistic pneumonia among pulmonary TB patients (Chavarría and Laura, 2018; Garcia, 2019; Oliwa et al., 2019; Xiao-Ying et al., 2016), despite both conditions being independent global causes of mortality. These studies and reports indicate a lethal synergism between pulmonary TB and pneumonia, driven primarily by their overlapping symptoms.

Epidemiological data on pulmonary TB in the presence of opportunistic pneumonia are limited due to challenges in simultaneous diagnosis. However, such epidemiological patterns can be inferred using structured mathematical models. This study formulated a mathematical model for pulmonary TB that incorporated opportunistic pneumonia to suggest appropriate intervention strategies for halting the global spread of infections. Specifically, through numerical simulations, the study determined the effects of screening and treating co-morbidities of pulmonary TB and pneumonia on controlling infection transmission.

1.1.3 The role of natural immunity in pulmonary TB transmission

Epidemiological evidence suggests that the suppression of natural immunity significantly accelerates the progression of latent infections to pulmonary tuberculosis disease (Chandra et al., 2022). This rapid progression, in turn, catalyzes transmission within the population. Increased incidences of pulmonary TB are commonly observed among individuals whose natural immunity is compromised by factors such as malnutrition, alcoholism, drug abuse,

opportunistic infections, and psychological stress (Aparicio and Castillo-Chavez, 2021). The importance of improving living conditions or utilizing immunotherapy for latently infected individuals becomes apparent in reducing the transmission of pulmonary tuberculosis infections. Therefore, it is essential to incorporate the effects of natural immunity into a mathematical model to accurately represent the transmission mechanisms of pulmonary TB disease. In this study, the dynamics governing the progression of latent infections to pulmonary TB disease were investigated to control transmission. Specifically, the study rigorously evaluated, through mathematical modeling, the impact of natural immunity on the reactivation of latent infections and its role in controlling or reducing transmission to the susceptible population. This addresses a gap in the existing literature, as it had not been extensively explored previously.

1.1.4 Mathematical epidemiological modeling

Infectious diseases remain among the leading causes of mortality worldwide, primarily due to their complex transmission dynamics. Additionally, the adaptation of pathogens to prevailing conditions has led to the emergence of new diseases and the reemergence of existing ones (Hethcote, 2009). This has reignited interest in epidemiological studies, which have long played a crucial role in analyzing the spread and control of infections globally. However, epidemiological patterns and disease control theories can often be complex, necessitating a strong reliance on mathematical model analysis (Hethcote, 2004). Compartmental mathematical models, in particular, represent real-world events through mathematical expressions (Biswas et al., 2018). Thus, mathematical modeling is essential in infectious disease epidemiological studies. One of the primary roles of mathematical models is to predict the potential impact of interventions or the interactions between multiple interventions during epidemics, while effectively capturing nonlinear transmission dynamics.

Since the inception of mathematical modeling theory, various classical epidemiological models for infectious diseases have been formulated based on compartmental transitions, including SI, SIR, SIS, SIRS, SEIS, SEIR, and SEIRS models (Zhang et al., 2022). Advancements in these classical models are fundamentally significant due to the growing understanding of pathogen evolution. Consequently, efforts have been made to formulate

models that accurately represent the transmission mechanisms of various infectious diseases. These models have been widely used to gain insights into the spread and control of infections within populations.

The dynamics of these models are typically governed by a threshold quantity known as the basic reproduction number. The basic reproduction number is defined as the average number of secondary infections caused by an index case in a completely susceptible population. In infectious disease epidemiology, the reproduction number suggests that controlling disease spread does not require the complete elimination of infected cases; rather, it requires reducing the number of infections below a critical threshold, such that, on average, an index case infects fewer than one individual during the infectious period (Safi and Garba, 2017). In this study, a classical SEIRS transmission mechanism was employed to formulate a mathematical model for pulmonary TB, with the goal of accurately representing its natural progression and controlling the spread of infections.

1.1.5 Kenya's Vision 2030 and Sustainable Development Goals

Kenya Vision 2030 emphasizes the need to transition from a curative to a preventive approach in order to provide a high-quality healthcare system. tuberculosis, HIV/AIDS, and malaria were identified for special attention due to their significant impact on the population (Government of Kenya, 2008). In the Big Four Agenda, the Government of Kenya aims to achieve affordable Universal Health Coverage (UHC) by providing a 100% cost subsidy on essential health packages. Pulmonary tuberculosis treatment is one of the key indicators of UHC, as it is fully subsidized. Consequently, the Big Four Agenda is closely aligned with the goals of Kenya Vision 2030 (National Tuberculosis, Leprosy and Lung Disease Program, 2019).

Globally, the United Nations' 'Agenda 2030 Sustainable Development Goals (SDGs)' has identified TB as one of the communicable diseases that must be eradicated by 2030 to achieve sustainable development (United Nations Environment Programme (UNEP), 2015). Therefore, it is crucial to identify effective approaches to translate this global health goal into actionable practices in local settings. However, Kenya faces numerous challenges, including a lack of adequately disaggregated data. Despite this, mathematical modeling

research has been recognized as playing a pivotal role in predicting the behavior of dynamical systems, particularly in scenarios with insufficient disaggregated data, through numerical simulations.

This study sought to use mathematical modeling to identify intervention strategies that could significantly reduce the transmission of pulmonary TB within the population. In doing so, it aligns with the Big Four Agenda, Kenya Vision 2030, and the United Nations Agenda 2030 Sustainable Development Goals (SDGs).

1.2 Statement of the Problem

Pulmonary TB is one of the leading infectious diseases causing mortality worldwide. According to the World Health Organization (World Health Organization, 2024), the disease claimed approximately 1.2 million lives globally in 2023. In Kenya, data from the Civil Registration Services (CRS) indicate that pulmonary TB accounted for about 5.4% of all reported deaths in 2022 (Civil Registration Services, 2023). The impact of pulmonary TB is further exacerbated by opportunistic infections such as pneumonia. Clinical studies have highlighted that the lethal synergism between pulmonary TB and pneumonia has significantly contributed to mortality in endemic regions. While previous studies have incorporated either asymptomatic infection or natural immunity when modeling single-disease or co-infection systems, few, if any, have explicitly integrated both features in the context of pulmonary TB and pneumonia co-infection. This study seeks to fill that gap by presenting models that simultaneously consider both components, with a focus on their combined epidemiological impact. Specifically, the dynamics of pulmonary TB, along with the co-dynamics of pulmonary TB and pneumonia, were formulated with the goal of controlling and reducing their spread. The study determined the reproduction numbers, which were then used to analyze the formulated models. Furthermore, the effects of varying model parameters on the control of pulmonary TB and opportunistic pneumonia were investigated through numerical simulations.

1.3 Objectives of the Study

The general and specific objectives that guided this study are outlined as follows:

1.3.1 General objective

The main objective of this study was to model pulmonary TB and pneumonia co-infection, incorporating an asymptomatic component and natural immunity.

1.3.2 Specific objectives

The specific objectives of this study were to:

i. Formulate a pulmonary TB model incorporating an asymptomatic component and natural immunity.

ii. Formulate a pulmonary TB and pneumonia co-infection model, incorporating an asymptomatic component and natural immunity.

iii. Determine the reproduction numbers for analyzing the formulated models.

iv. Investigate the effects of varying model parameters on the control of pulmonary TB and opportunistic pneumonia.

1.4 Significance of the Study

The findings of this study are expected to support healthcare policymakers and practitioners in making evidence-based decisions on the screening of latently infected and asymptomatic infectious pulmonary TB patients, thereby strengthening efforts to control epidemics of the disease. In addition, the study underscores the critical role of enhancing the natural immunity of latently infected individuals as a complementary strategy for reducing disease progression and transmission.

The outcomes underscore the importance of accurate diagnosis and effective treatment of TB and pneumonia co-infections to control transmission and support the global eradication of these diseases. Furthermore, this study provides public health officials with valuable insights into the epidemiological patterns and underlying mechanisms of TB and pneumonia co-infections. These findings are crucial for formulating effective prevention and intervention strategies aimed at reducing transmission, particularly in resource-limited settings in developing countries.

The results further emphasize the need for healthcare authorities to assemble multidisciplinary research teams consisting of mathematicians and infectious disease experts. These

teams can play a pivotal role in reducing the global transmission of pulmonary TB and pneumonia infections.

CHAPTER TWO: LITERATURE REVIEW

2.1 Introduction

In this section, literature on the mathematical modeling of pulmonary TB dynamics is presented, followed by studies on the mathematical modeling of pneumonia transmission dynamics, particularly those addressing the effects of various control strategies. Next, literature on pulmonary TB and pneumonia co-infection is reviewed, with a focus on clinical studies and reports, as mathematical models remain limited. In addition, studies on natural immunity, the progression from latent infection to active disease, screening for asymptomatic pulmonary TB, and reproduction numbers are discussed. Finally, attention is directed toward current research efforts aimed at addressing the identified gaps in the literature.

2.2 Tuberculosis

This section reviews the work conducted by researchers on the mathematical modeling of pulmonary TB, focusing on strategies to control infection transmission. These strategies include screening and treating latent infections, vaccination, early diagnosis, social protection, education and counseling, treatment of drug-resistant strains, and the effects of awareness levels.

Liu and Wang (2017) conducted a study to investigate the effect of treatment interruptions on tuberculosis transmission dynamics. They developed a mathematical model incorporating treatment interruptions and two latent periods. They determined the control reproduction number and analyzed the global asymptotic stabilities of the equilibria by constructing the proper Lyapunov functions. The reproduction numbers, as well as the numerical simulations, showed that complete treatment of active tuberculosis patients generally helps to contain the tuberculosis epidemic, whereas treatment interruptions sustain the transmission of infection to susceptible populations during epidemics.

Egonmwan and Okuonghae (2019) formulated and analyzed a mathematical model to determine the impact of diagnosis and treatment on a population using first-order ordinary differential equations that were analyzed qualitatively and numerically. Their results revealed that the model undergoes backward bifurcation whenever a stable disease-free equilibrium coexists with a stable endemic equilibrium when the associated reproduction number is less

than unity. In the absence of exogenous reinfection, this phenomenon does not exist. The analysis of the model further showed that the parameters that have the most influence on the reproduction number are the transmission rates, the fraction of fast disease progression, and the detection rate of active tuberculosis cases. Numerical results indicated that diagnosis and treatment of both latent and active TB cases result in a significant decrease in TB prevalence in a population.

A study investigating the effects of awareness levels on the transmission dynamics of pulmonary TB was conducted by Okuonghae and Ikhimwin (2019) using a deterministic mathematical model. In their study, they classified both susceptible and latently infected individuals according to their level of awareness of TB. Furthermore, they included a TB disease case-finding parameter, in addition to using chronic cough as a sign for identifying potential TB cases. Their results showed that backward bifurcation due to exogenous reinfection was sustained by latently infected individuals with low awareness levels. Model results further revealed that incidences of TB in the population can be decreased by intensifying awareness campaigns for both susceptible and latently infected individuals, coupled with increasing the rate of TB disease case finding.

The effect of screening and treating latent tuberculosis infection in the elderly in Hong Kong city was modeled by Chong et al. (2019). They used annual age-stratified tuberculosis notifications from 1965-2013 obtained from the health department to calibrate the model. The population under study was subdivided into susceptible, recently latent infected, remotely latent infected, infectious, latent infected treated, infectious treated, completed treatment, and recovered individuals. Their results revealed that the highest percentage of all tuberculosis incidences was contributed by the reactivation of latent infections among the elderly population. Furthermore, their results indicated that screening and complete treatment of more than 50% of the latently infected elderly population significantly reduces new TB cases.

A study to model the transmission dynamics of pulmonary tuberculosis considering drug-resistant strains was conducted by Mishra and Srivastava (2019). Their model divided the population into susceptible, exposed, infectious, quarantined, recovered, and susceptible

with vaccination categories. Thresholds and equilibria were obtained, and the conditions for an epidemic under different threshold conditions were established. The system of ordinary differential equations obtained was simulated using real parametric values of the Jharkhand state in India, which is highly epidemic with the disease. Their results indicated that by quarantining multi-drug-resistant tuberculosis patients, a rapid recovery, which almost ends the spread of infection, is achieved. Vaccination was shown to immunize the population against infections, which provides an enabling guideline for active tuberculosis control.

The role of vaccinating newborn babies and treating both latent infection and tuberculosis disease in controlling the spread of infections was investigated by Kalu and Inyama (2020). In their study, they formulated an SEIR mathematical model of disease transmission dynamics and derived first-order ordinary differential equations that were analyzed qualitatively and numerically. They established the disease-free equilibrium state of the model and analyzed its stability using the Routh-Hurwitz theorem. Their results suggested the possibility of eradicating tuberculosis by ensuring that the recovery rate of latent infections is high, coupled with lowering the rate at which latent infections are activated.

A study by Eguda et al. (2020) sought to explain the risk factors for drug resistance to tuberculosis in society using a mathematical transmission dynamics model incorporating first and second-line treatment. In their study, the total human population was divided into susceptible (S), latent (E), infectious (I), first-line treatment (R_1), second-line treatment (R_2), and recovered (R) classes. A system of ordinary differential equations was derived to describe the model, which was then analyzed qualitatively and numerically. Their results showed that complete treatment of infectious individuals leads to a drastic reduction in drug-resistant tuberculosis incidences in the population, which in turn reduces disease burden.

A mathematical tuberculosis model incorporating exogenous reinfection was formulated by Feng et al. (2020). They investigated the effects of reinfections on the transmission dynamics of tuberculosis in an attempt to control its spread. In their model, the total population was subdivided into susceptible (S), exposed (E), infectious (I), and effectively

treated (T) individuals. They derived first-order ordinary differential equations to describe the model and analyzed them qualitatively and numerically. Their results showed that exogenous reinfection increases the number of active TB cases. Therefore, they emphasized the reduction of exogenous reinfection as a key strategy to eliminate TB disease in the population.

A study comparing the effects of educational counseling, treatment, and vaccination as intervention strategies to reduce the transmission of TB was conducted by Fatima et al. (2020). In their study, they modified the SEIR epidemic TB model to incorporate the aforementioned disease control aspects and used a system of first-order linear equations for model analysis. The disease-free equilibrium was established, and the effective reproduction number was obtained using the next-generation operator. This study revealed that the disease dies out when the effective reproduction number is less than unity with the implementation of intervention strategies. Further results indicated that educational counseling is the most effective strategy in controlling TB, and a significant reduction in the spread of the disease was achieved by combining it with treatment compared to vaccination.

Trauer et al. (2022) simulated a mathematical model of tuberculosis transmission dynamics using data from the endemic region of the Asia-Pacific. Their deterministic model considered partial and temporal vaccine efficacy, the risk of active disease following infection, re-infection during the latent infection period and after treatment, and multi-drug-resistant tuberculosis during treatment. Sensitivity analyses of the parameters showed that the rate of detection and treatment is the most important factor in determining disease incidence in a population. It was also revealed that there was an increase in multi-drug-resistant tuberculosis rates due to the replacement of drug-susceptible individuals by multidrug-resistant ones within the pool of latently infected individuals as a result of poor treatment options. Vaccination was reported to have little impact because of a significantly smaller population that was unvaccinated in society. Progression from latent to active infection was shown to be responsible for a higher percentage of new cases.

Fröberg et al. (2022) formulated a mathematical model to estimate the likelihood of an in-

dividual being infected with recent and remote latent TB independent of diagnostic tools. They observed that current diagnostic tests for latent tuberculosis infection have poor predictive values for tuberculosis activation. In their study, they estimated recent latent TB infections based on the infectiousness of the index case, proximity and time of exposure, and environmental factors, whereas estimation of remote latent tuberculosis infection was based on the country of origin for immigrants and previous stays in high-risk environments. Individual estimations were calculated and compared with diagnostic test results for 162 contacts of 42 index TB cases. The mathematical model results showed that 35% of recent latent tuberculosis infections were found among smear microscopy-positive index case contacts. Further results showed that a higher chance of remote latent TB was seen among tuberculin skin test-positive contacts.

Research to determine the effect of an imperfect vaccine on the transmission dynamics of tuberculosis was conducted by Sulayman et al. (2023). They developed and analyzed the SVEIRE mathematical model and determined its effective reproduction number using the next-generation matrix. Their results showed that the model exhibited backward bifurcation, which could be prevented through organizing education programs aimed at changing members of the public behavior to decrease disease contact and subsequently reduce transmission. Backward bifurcation could also be prevented by increasing the vaccination threshold value. Vaccination of a population above the critical value with an imperfect vaccine of high efficacy was shown to significantly control the transmission of TB.

The impact of social protection on reducing the transmission rate of tuberculosis in society was modeled by Boccia et al. (2023). They studied the effect of cash transfers to the underprivileged in society as an example of social protection intervention in reducing TB transmission. Their results showed that improving household income, and thus their nutritional status, reduces tuberculosis transmission by 4%. The study further indicated that social protection contributes to poverty elimination, which in turn prevents TB transmission since the infected will get timely access to quality TB care.

2.3 Pneumonia

This section highlights previous research on the mathematical modeling of pneumonia. Since this study examines the impact of opportunistic pneumonia on pulmonary tuberculosis transmission mechanisms, it is essential to analyze the transmission dynamics of pneumonia as an independent disease, as outlined by the researchers referenced in this study.

The effects of screening and treatment on the transmission dynamics of pneumonia were studied by Ndelwa et al. (2015). In their research, they formulated a mathematical model of pneumonia transmission dynamics and analyzed it numerically. The transmission model divided the population into susceptible, asymptomatic infective, symptomatic infective, and treated. Numerical simulations of the ordinary differential equations describing the model were conducted to determine the effects of screening and treatment in controlling the epidemic. Their results indicated that the combination of both screening and treatment is the best strategy to eradicate the pneumonia epidemic compared to the deployment of only one of the interventions.

A study to investigate cost-effective strategies for controlling the transmission of pneumonia infections in a population was conducted by Tilahun et al. (2017). In their research, they formulated and analyzed a deterministic mathematical model using ordinary differential equations. They compared several control strategies to establish the most cost-effective approach to combat pneumonia in a population. The strategies considered included screening, prevention, and treatment. Their numerical findings suggested that a combination of prevention and treatment is the most cost-effective intervention strategy to contain the pneumonia pandemic at the population level.

A combination of treatment and vaccination interventions was compared with treatment alone by Kizito and Tumwiine (2018) to investigate the best strategies for controlling the spread of pneumonia infections. In their research, they used compartmental models to investigate pneumonia infection control strategies among children less than five years old. They developed two models: the first considered treatment intervention alone, while the second combined both vaccination and treatment interventions. They carried out numerical simulations of the models on the effective reproduction number, revealing that the combi-

nation of treatment and vaccination has a greater impact on the eradication of Streptococcus pneumoniae than treatment alone. The study suggested that for significant control of pneumonia in the population, infected individuals should be completely treated, and those with suppressed immune systems should be adequately vaccinated.

Otieno and Paul (2018) developed and analyzed a mathematical model of pneumonia transmission dynamics, taking into consideration infectious carriers. In their study, the population was divided into four compartments: susceptible, carriers, infectious, and recovered. They analyzed their model using ordinary differential equations. Their findings emphasized the reduction of transfer rates between carriers and the infected to minimize the prevalence of pneumonia in the population. They suggested that early diagnoses, isolation of the infected, and adequate treatment of infectious carriers are appropriate strategies for ensuring pneumonia infections are eliminated in the population.

A study to investigate the effects of vaccine efficacy and treatment on pneumonia transmission dynamics was conducted by Zephaniah et al. (2020). They formulated and analyzed the SVEIR model for pneumonia with the saturated force of infection in the presence of a preventive vaccine. The non-linear differential equations governing the model were solved using the Adomian decomposition method. The study revealed that improving vaccine efficacy and expanding treatment capacity are important strategies for eradicating the disease in a population. Furthermore, the study showed that with vaccination covering a critical percentage of the population, the disease will die out.

Research to determine the effects of asymptomatic carriers on pneumonia transmission dynamics and vaccination was carried out by Otoo et al. (2020). They formulated and analyzed a deterministic mathematical model that incorporated symptomatic, asymptomatic carriers, and vaccinated compartments. Numerical simulations of the ordinary differential equations describing the model revealed that the effective contact rates of both asymptomatic and symptomatic infectives fuel the spread of the disease. The study observed that since vaccine efficacy is not 100%, multiple doses of the vaccine are necessary to prevent the pneumonia pandemic in the population.

To investigate the effects of health intervention measures, Soliman and Bueno (2021) com-

pared quarantine and vaccination strategies in reducing the spread of pneumonia infections. In their study, they used the SIR model to analyze and predict the rate of transmission of pneumonia in the Philippines, incorporating demographic changes in the population. The model's differential equations were solved assuming exponential population growth, and the results were compared with real-world epidemic data. Their findings showed a positive correlation between the real-world and the modeled data. Furthermore, their results indicated that reducing the contact rate through quarantine between the infected and susceptible populations significantly reduces the transmission rate compared to vaccinating the susceptible population. However, the study showed that a combination of isolation and vaccination is the most effective strategy for controlling the transmission of pneumonia infections in a population.

Research targeting the control of pneumonia transmission among toddlers was conducted by Imran et al. (2022). In their study, they formulated and analyzed a mathematical model incorporating immunization and treatment to reduce the rate of spread of pneumonia among children under five years old. Stability analysis and numerical simulation revealed that increasing the rate of treating infected individuals, coupled with immunizing a higher percentage of the susceptible population, suppresses the basic reproduction number, which accelerates the eradication of the disease.

2.4 Tuberculosis and Pneumonia Co-infection

In this section, most of the reviewed studies focus on clinical research and reports on pulmonary tuberculosis in the presence of opportunistic pneumonia, as mathematical models in this area remain limited.

A clinical etiology investigation of all cases of co-existing pulmonary tuberculosis and bacterial pneumonia at the National Tuberculosis Clinical Centre of China from June 2009 to June 2012 was conducted by Xiao-Ying et al. (2016). In their clinical research, the co-existences were confirmed using results from microbiology, radiology, diagnostic treatment, and clinical symptoms. Their study revealed that 80% of all investigated cases were found to be co-infected with pulmonary tuberculosis and pneumonia. Furthermore, the results pointed out that the risk factors for co-existence include female gender, age 40 and

above, and the presence of pulmonary cavities. However, diabetes and liver disorders were not associated with the co-existence as hypothesized. The study underscored the importance of accurate diagnosis and effective treatment of co-existing pulmonary tuberculosis and pneumonia.

A clinical case report of co-infection with community-acquired pneumonia and Mycobacterium tuberculosis was reported in Costa Rica by Chavarría and Laura (2018). They described a case involving a 36-year-old male patient with respiratory distress, whose radiological tests indicated the presence of pulmonary tuberculosis and pneumonia infections. Further laboratory tests, including sputum analysis by smear microscopy, molecular techniques, and culture, were conducted. The sputum analysis by culture and smear microscopy detected pneumonia, while molecular techniques indicated the presence of pulmonary tuberculosis infections. Subsequently, the patient received treatment for both pneumonia and pulmonary tuberculosis in an isolation room to prevent the transmission of infection to both healthcare workers and patients in proximity. The report reinforced the importance of actively searching for pulmonary tuberculosis in patients with acute pneumonia, especially in tuberculosis-endemic regions.

The review of clinical and autopsy studies in tuberculosis endemic settings was conducted by Oliwa et al. (2019). Their review focused on published literature reporting severe pneumonia in children younger than 5 years who were also tested for multiple infections, including tuberculosis. The reviewed autopsy studies indicated that 21% of the sampled population died as a result of tuberculosis and pneumonia co-existence. The study recommended improved diagnostics for TB in infants and young children, especially those who present with acute severe pneumonia in countries with a high incidence of tuberculosis.

A clinical case report from the United States of America, in which a patient was diagnosed with the co-existence of Streptococcus pneumoniae and active pulmonary tuberculosis in the absence of HIV infection, was presented by Garcia (2019). The patient was diagnosed with pneumonia upon admission to the hospital and was immediately put under treatment with the appropriate regimens. Despite receiving treatment, his condition deteriorated, prompting additional microbiology and computed tomography tests to be conducted. Sub-

sequently, he died, and test results returned positive for Mycobacterium tuberculosis. It was reported that the delay in diagnosing active pulmonary tuberculosis placed other patients in close proximity, as well as healthcare providers, at a high risk of contracting infections. The report emphasized testing all individuals presenting with pneumonia in healthcare centers for pulmonary tuberculosis to ensure the appropriate isolation of positive cases.

A study on pulmonary tuberculosis and other bacterial co-infections was conducted by Attia et al. (2023). In their study, they analyzed the clinical characteristics of patients presenting with respiratory infections at a referral hospital in Cambodia. Additionally, mycobacterium and bacterial sputum tests, along with chest radiography results, were analyzed. Their findings revealed that 9% of tuberculosis patients had co-infection with pulmonary tuberculosis and pneumonia. An interesting observation from their results was that clinical symptoms did not differ among individuals with pulmonary TB, pneumonia, or co-infection of the two diseases. However, the findings indicated that co-infection was common among patients with pulmonary cavities on chest radiography. Their study advocated for robust microbiology and radiology diagnoses for pulmonary tuberculosis and pneumonia co-infection to ensure appropriate diagnosis and treatment.

A model of tuberculosis and pneumonia co-infection dynamics was formulated by Gweryina et al. (2023). Their study utilized the SEIR mathematical model with ordinary differential equations. They employed partial rank correlation coefficients to perform a sensitivity analysis, and their results indicated that increasing infection recovery is the most influential parameter in reducing the magnitude of the disease. The cost-benefit analysis revealed that treating tuberculosis alone is the most effective strategy for reducing co-infection.

2.5 Natural Immunity and the Progression from Latent Infection to Tuberculosis Disease

Flores-Garza et al. (2022) studied the immunopathological progression of tuberculosis using an integrative systems biology approach, analyzing the key interactions between the cells involved in the different phases of the infectious process. Their study integrated multiple in vivo and in vitro data from immunohistochemical, serological, molecular biology, and cell count assays into a mechanistic mathematical model. The ordinary differential

equation model captured the regulatory interplay between the phenotypic variation of the main cells involved in disease progression and the inflammatory microenvironment. The simulations demonstrated how genotypic variations shaped the transitions across phases, showing that 100% of the evaluated genotypes eventually progressed to phase two of the disease, suggesting that activation of the adaptive immune response was unavoidable.

Darboe et al. (2024) focused on accumulating scientific evidence indicating that viral infections contribute to the progression of latent tuberculosis due to a compromised immune system. They used the example of HIV/AIDS–related immune suppression, which is associated with increased cases of tuberculosis resulting from the reactivation of latent infections. Their study recommended enhancing natural immunity among individuals latently infected with tuberculosis as an appropriate measure to reduce the transmission of the disease.

Kudryavtsev et al. (2024) investigated the role of the immune response in the development of active tuberculosis from latent infection. Their research presented data on the pathogenesis of latent tuberculosis infection, particularly focusing on the immune response in the interaction between Mycobacterium tuberculosis and the host. The study described the mechanisms of T-cell immunity and cytokine activation, supporting the concept of type 1, type 2, and type 3 immune responses. Their results indicated that the reactivation of latent tuberculosis is primarily caused by damage to the immune mechanisms responsible for containing Mycobacterium tuberculosis.

Hu et al. (2024), in their study, investigated the role of natural immunity in the progression of latent tuberculosis infection. Their study focused on clinical case reports that highlighted factors promoting the progression of latent infections to tuberculosis disease. The results indicated that the main contributing factor to this progression is a compromised immune system.

Cao et al. (2025) formulated and analyzed a mathematical model describing the immune response during the latent stage of tuberculosis infection. The study aimed to explore the sustained immune response of the immune system against invading Mycobacterium tuberculosis during latent infection. Their results showed that when tuberculosis bacteria invade

the host's lungs, the immune system may clear the invading pathogens, preventing the development of active TB. This corresponds to the stable sterile equilibrium of the formulated model. During latent tuberculosis infection, the immune system initiates a sustained immune response to control the growth and reproduction of the bacteria in the lungs, leading to the formation of TB granulomas

Halabitska et al. (2025) reported a case demonstrating the reactivation of latent tuberculosis following co-infection with a viral disease. The report highlighted a clinical scenario in which immune dysregulation likely facilitated tuberculosis progression. The case underscored the importance of considering latent tuberculosis reactivation in patients with viral infections, particularly in regions with high tuberculosis prevalence. The study indicated that tuberculosis reactivation can occur as a result of immune system compromise.

Nieto Ramirez et al. (2025) conducted a systematic review of the immune response against tuberculosis complex infection in animal models. The review focused on immune mediators associated with either protection or disease progression in animal models of tuberculosis infection. The results indicated that approximately 60% of latent tuberculosis reactivations occur as a result of a compromised immune system. The study emphasized that understanding the role of the immune response in tuberculosis infection is crucial for preventing disease progression.

2.6 Screening for Asymptomatic Pulmonary Tuberculosis

Ryckman et al. (2022) formulated a mathematical model to track the future trajectories of individuals with asymptomatic tuberculosis. Their study used Bayesian methods to calibrate the model to targets derived from historical survival data, notifications, mortality, and prevalence data from five countries. The results indicated that screening for asymptomatic tuberculosis could contribute to a 35–50% reduction in future transmissions. They recommended screening asymptomatic individuals as a strategy to reduce the tuberculosis burden in the population.

Mahmoudi et al. (2024) determined the prevalence of minimal and asymptomatic tuberculosis and evaluated the positivity rates of current diagnostic tests. The study conducted a meta-analysis of research published between January 2000 and December 2022, ana-

lyzing prevalence rates and diagnostic test results, with pooled prevalence calculated and comparisons made across geographical regions. The results indicated that the prevalence of minimal tuberculosis ranged from 0.9% to 22.9% in the general population, while the prevalence of asymptomatic tuberculosis ranged from 1.57% to 14.63%. The study highlighted the need to screen the general population for asymptomatic tuberculosis to reduce undetected cases, especially in high-risk populations.

Schwalb et al. (2024) assessed the impact and cost-effectiveness of annual rounds of different population-wide screening algorithms using a mathematical model calibrated to tuberculosis epidemiology in Viet Nam. Their model incorporated the recent spectrum of tuberculosis disease, including the relative contribution of asymptomatic tuberculosis to transmission. The results indicated that a substantial reduction in tuberculosis prevalence could be achieved through repeated annual rounds of asymptomatic population-wide screening. A two-step algorithm, which uses chest radiography as the initial screening method followed by a sputum nucleic acid amplification test, was projected to avert 1.31 million cases of severe tuberculosis and prevent 171,000 tuberculosis-related deaths by 2050.

Kuddus et al. (2024) formulated a tuberculosis model to investigate the potential influence of asymptomatic carriers, symptomatic infections, and overall tuberculosis prevalence on different treatment and prevention approaches in Thailand. They used annual tuberculosis incidence data from 2000 to 2022 in Thailand to calibrate the model parameters. Their results showed that reducing only the progression rate of symptomatic tuberculosis infections is insufficient to control asymptomatic carriers and overall tuberculosis prevalence, even when the relative infectiousness of carriers is less than unity.

MacPherson et al. (2024) in their study, synthesized evidence and experiences from implementing active case-finding programs to provide guidance on screening algorithms. Their results indicated that with careful planning and substantial investment, community-based active case finding for tuberculosis can be an impactful approach to accelerating progress toward the elimination of tuberculosis in high-burden countries. The study highlighted the screening of asymptomatic tuberculosis as a potential measure to enable early diagnosis and, consequently, reduce transmission of infections.

Mandal et al. (2025) formulated a mathematical model that incorporated enhanced features, including an explicit representation of asymptomatic tuberculosis. The model was calibrated to country-specific data using Bayesian adaptive Markov Chain Monte Carlo methods. It was then applied to assess the impact of national strategic plans and the bold initiative to end tuberculosis by mapping interventions to WHO guidelines through a target population component. The results indicated that the enhanced tuberculosis model provides a flexible, policy-relevant framework for evaluating the epidemiological impact of tuberculosis interventions at both national and global levels.

2.7 Reproduction Numbers

Diekmann et al. (2020) presented a clear and practical recipe for constructing the Next Generation Matrix from basic ingredients derived directly from the specifications of the model. They showed that two related matrices exist, which they define as the Next Generation Matrix with a large domain and the Next Generation Matrix with a small domain. Together with the original formulation, these three matrices reflect the range of possibilities encountered in the literature for the characterization of the reproduction number. They further demonstrated how the matrices are connected, how their construction follows from the basic model ingredients, and established that they share the same non-zero eigenvalues, the largest of which corresponds to the reproduction number.

Avram et al. (2023), in their study, made new contributions to the literature on the basic reproduction number. First, they provided a universal algorithm for defining the Jacobian matrix gradient decomposition, and second, they introduced a fixed-point equation for estimating the probabilities of a stochastic model, which can be expressed in terms of the Jacobian matrix decomposition. Lastly, they developed Mathematica scripts and implemented them for a wide variety of examples. Their results showed that the Next Generation Matrix approach quickly leads to most of the results reported in the literature.

Avram et al. (2024) showed that for a large class of ordinary differential equation epidemic models, in addition to the rank-one formula, an integral renewal representation of the reproduction number with respect to explicit age kernels, expressed in a matrix exponential form can be provided. They also extended their approach to cases with several susceptible

classes. The results suggested an interesting alternative to classical statistical approaches in mathematical epidemiology, which usually start by postulating an epidemiological model and then estimating its parameters.

Jang et al. (2024) conducted a comparative analysis of time-varying reproduction numbers, taking into account population immunity and variant differences. They incorporated regional heterogeneity, age distribution, evolving variants, and vaccination rates over time. The reproduction number was computed both with and without considering variant-based immunity. Their results showed that reproduction number values differed significantly by variant, emphasizing the importance of immunity.

Hill et al. (2025), in their study, estimated the effective reproduction number using wastewater-based methods. They reviewed different approaches for estimating the effective reproduction number of SARS-CoV-2 from wastewater. Using wastewater data collected between August 1, 2022, and February 2024, they fitted eight wastewater-based effective reproduction number models identified in the literature. Their results showed a high degree of similarity across all eight methods. They concluded that, while not all methods for estimating the effective reproduction number from wastewater yield identical results, they all provide a useful way to incorporate wastewater concentration data into epidemic modeling.

Anazawa (2025) proposed multiple simplified approaches for estimating the reproduction number of infectious diseases and compared their effectiveness. These approaches include methods based on exponential, fixed, normal, and gamma distributions for the generation time. The exponential and fixed generation time methods were shown to offer convenience, as they rely solely on the mean generation time and the number of new infections. The exponential method tended to underestimate the reproduction number when the variance was small, while the fixed generation time method tended to overestimate it when the variance was large. The normal distribution method sometimes resulted in underestimation, depending on the growth rate. In contrast, the gamma distribution method demonstrated greater robustness and accuracy across a variety of scenarios.

Bajaj et al. (2025) introduced a method to estimate reproduction numbers that makes use of retrospective updates to case time series, which occur as more historically delayed cases en-

ter the health system. The method simultaneously estimates reporting delays, true historical case counts, and the reproduction number within a single Bayesian framework, allowing uncertainty in each of these quantities to be accounted for. They applied their method to both simulated and real outbreak data, and their results showed that it substantially improves upon naïve estimates of the reproduction number that do not account for reporting delays.

2.8 Research Gaps

Despite the extensive research conducted on the mathematical modeling of pulmonary TB transmission dynamics, the following research gaps remain unexplored:

1. The combined effects of screening asymptomatic infectious individuals and the influence of natural immunity on the progression from latent infection to disease in a pulmonary TB model.

2. The formulation of a model for pulmonary TB that considers the presence of opportunistic pneumonia while incorporating the screening of asymptomatic individuals and the impact of natural immunity.

Therefore, this study is a valuable endeavor to address the aforementioned gaps by modeling pulmonary TB transmission dynamics in the presence of opportunistic pneumonia, incorporating the screening of asymptomatic infectious populations, and assessing the impact of natural immunity on controlling the transmission of infections to susceptible populations.

CHAPTER THREE: METHODOLOGY

3.1 Introduction

This chapter describes the methodology used to conduct the research. The chapter is organized as follows: first, the justification for addressing the research gaps in the formulation of the two models is provided; next, the formulation of a model for pulmonary TB transmission mechanisms incorporating an asymptomatic infectious component and natural immunity is presented; this is followed by the formulation of a model for pulmonary TB and pneumonia co-infection; then the method for determining control reproduction numbers is outlined; and finally, the approach to data fitting and parameter estimation for the co-infection model is presented.

3.2 Justification of the Research Gaps in the Formulation of the Models

This study adopts a classical SEIRS transmission framework to model pulmonary TB dynamics. The models incorporate an asymptomatic infectious class, as these individuals contribute to sustained transmission by spreading infection undetected. The inclusion is justified by the Kenya National TB Prevalence Survey (2016), which reported that 26% of prevalent TB cases were asymptomatic and infectious (National Tuberculosis, Leprosy and Lung Disease Program, 2016). Similarly, World Health Organization (2025) estimates that nearly 50% of pulmonary TB cases identified in global prevalence surveys are asymptomatic. These findings highlight that targeting only symptomatic individuals is insufficient, as asymptomatic carriers sustain ongoing transmission.

Previous models often assume that progression from latent infection to pulmonary TB is proportional to the number of latently infected individuals. In reality, this progression is strongly influenced by host immunity (Barry et al., 2019). To reflect this, the present models incorporate a saturated progression rate using Holling's function, $\frac{\chi E}{1+mE}$ (Banerjee, 2021). This formulation captures the delay in reactivation conferred by stronger immunity, where χ denotes the reactivation rate, E denotes the latently infected population, and m represents the effect of immune protection. As m approaches zero, reflecting low immunity, the function approximates χE. Two disease states are considered: asymptomatic infectious and symptomatic. The respective reactivation rates are given by $\frac{\chi_1 E}{1+mE}$ and $\frac{\chi_2 E}{1+mE}$.

Clinical studies have reported a lethal synergism between pulmonary TB and pneumonia, with each accelerating the progression of the other. Individuals with TB are particularly vulnerable to severe pneumonia due to compromised immunity (Garcia, 2019). To capture this interaction and assess its impact on transmission, the pulmonary TB model was extended to incorporate opportunistic pneumonia.

3.3 A Model of Pulmonary Tuberculosis Incorporating an Asymptomatic Component and Natural Immunity

In this section, the assumptions underlying the model formulation, the model description, and the equations are presented.

3.3.1 Assumptions for model formulation

The formulation of the new model was guided by the following assumptions:

i. The successful treatment of pulmonary TB disease is assumed.

ii. The progression from latent infection to pulmonary TB disease depends on natural immunity.

iii. Individuals who are latently infected do not transmit the infection.

iv. When latently infected individuals are screened and treated, they cannot develop pulmonary TB.

v. Recovered individuals do not acquire permanent immunity and can become susceptible to reinfection.

vi. The impact of drug-resistant pulmonary TB in the population is minimal.

3.3.2 Model description

The model categorizes the total population size at time t, denoted as $N(t)$, into nine subclasses based on their disease status: susceptible individuals $S(t)$, vaccinated individuals $V(t)$, latently infected individuals $E(t)$, asymptomatic infectious individuals $I_a(t)$, symptomatic individuals $I_S(t)$, latently infected individuals undergoing treatment $T_E(t)$, asymptomatic infectious individuals undergoing treatment $T_a(t)$, symptomatic individuals undergoing treatment $T_S(t)$, and recovered individuals $R(t)$. Therefore, the total population

satisfies equation (3.1) given by:

$$N(t) = S(t) + V(t) + E(t) + I_a(t) + I_S(t) + T_E(t) + T_a(t) + T_S(t) + R(t) \quad (3.1)$$

The transitions and interactions between these compartments are described as follows:
Individuals are recruited into the population at a constant rate, π. A fraction of the recruits is vaccinated at a constant rate, P, and enters the vaccinated class, while the remaining individuals become susceptible.
Susceptible individuals become latently infected after effective contact with infectious cases. The force of infection is given by equation (3.2) as follows:

$$\lambda = \beta(I_S + \eta_1 I_a + \eta_2 T_S + \eta_3 T_a) \quad (3.2)$$

where β denotes the transmission rate of pulmonary TB infections, and η_1, η_2, and η_3 are dimensionless transmission coefficients. These coefficients account for the relative infectiousness of individuals in different classes, with:
$0 < \eta_3 < \eta_2 < \eta_1 < 1$.
This hierarchy assumes that asymptomatic individuals denoted by (I_a) are more infectious than symptomatic individuals undergoing treatment (T_S), who are, in turn, more infectious than asymptomatic individuals undergoing treatment (T_a).
The model considers that vaccination is not 100% effective; therefore, vaccinated individuals may still become latently infected. The force of infection for vaccinated individuals is given in equation (3.3) as follows:

$$\lambda_v = (1 - \rho) = (1 - \rho)\lambda(I_S + \eta_1 I_a + \eta_2 T_S + \eta_3 T_a) \quad (3.3)$$

where ρ is the vaccine efficacy, such that $0 \leq \rho \leq 1$.
Latently infected individuals (E) can either be screened at a constant rate, θ_1 and move to the latent infected undergoing treatment class (T_E), or progress to the asymptomatic infectious class (I_a) at a rate of $\frac{\chi_1 E}{1+mE}$. Alternatively, they may develop severe disease and

transition to the symptomatic class (I_S) at a rate of $\frac{\chi_2 E}{1+mE}$.

Asymptomatic infectious individuals (I_a) can either be screened at a rate, θ_2, and move to the asymptomatic infectious undergoing treatment class (T_a), or progress to severe disease and join the symptomatic class (I_S) at a rate, ω. Symptomatic individuals (I_S) are identified for treatment at a rate, θ_3 and move to the symptomatic undergoing treatment class (T_S).

The rate of disease-induced deaths for individuals in the symptomatic class (I_S) is denoted by δ_1, while the rate of disease-induced deaths for symptomatic individuals undergoing treatment (T_S) is denoted by δ_2.

Treatment for different forms of pulmonary TB is considered to be successful, with latent infected individuals undergoing treatment (T_E), asymptomatic infectious individuals undergoing treatment (T_a), and symptomatic individuals undergoing treatment (T_S) recovering at rates, ξ_1, ξ_2, and ξ_3, respectively, and moving to the recovered class (R).

The model considers that recovered individuals become susceptible again after their immunity wanes at a rate, σ. The rate at which individuals die from causes other than pulmonary TB is denoted by μ.

Considering the assumptions, variables, and parameters, the flowchart of the formulated model is presented in Figure 3.1, from which the system of differential equations (3.4) is derived.

System (3.4) presents the differential equations derived from the model.

Figure 3.1

The flow chart for the TB transmission model

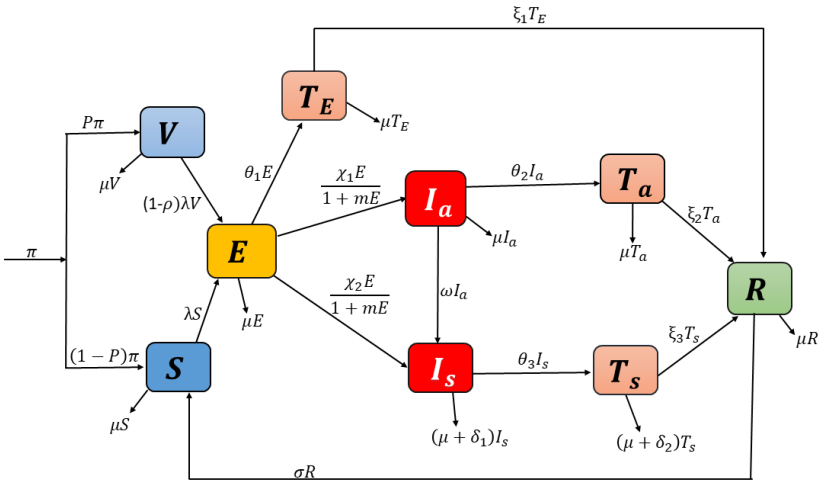

Source: Researcher (2024)

$$
\begin{cases}
\frac{dS}{dt} = (1-P)\pi + -(\lambda+\mu)S, \\
\frac{dV}{dt} = P\pi - ((1-\rho)\lambda+\mu)V, \\
\frac{dE}{dt} = +(1-\rho) - (\frac{\chi_1}{1+mE} + \frac{\chi_2}{1+mE} + \theta_1 + \mu)E, \\
\frac{dI_a}{dt} = \frac{\chi_1 E}{1+mE} - (\theta_2+\omega+\mu)I_a, \\
\frac{dI_S}{dt} = \frac{\chi_2 E}{1+mE} +_a -(\theta_3+\delta_1+\mu)I_S, \\
\frac{dT_E}{dt} = \theta_1 E - (\xi_1+\mu)T_E, \\
\frac{dT_a}{dt} = \theta_2 I_a - (\xi_2+\mu)T_a, \\
\frac{dT_S}{dt} = \theta_3 I_S - (\delta_2+\xi_3+\mu)T_S, \\
\frac{dR}{dt} = \xi_1 T_E + \xi_2 T_a + \xi_3 T_S - (\sigma+\mu).
\end{cases}
\tag{3.4}
$$

3.4 A Co-infection Model of Pulmonary Tuberculosis and Pneumonia

The assumptions, model description, and equations for pulmonary TB and pneumonia co-infection are presented in this section.

3.4.1 Assumptions for the formulation of the model

The formulation of the co-infection model was guided by the following assumptions:

i. Pneumonia is an opportunistic infection affecting pulmonary TB patients.

ii. The progression from latent infection to pulmonary TB disease occurs due to compromised immunity in individuals.

iii. Treatment for both pulmonary TB and pneumonia infections is assumed to be successful.

iv. Individuals undergoing treatment for pulmonary TB and pneumonia co-infection recover from pneumonia first, as it is an acute disease.

3.4.2 Model description

The population-based compartmental model divides the total human population into the following subclasses: susceptible (S), vaccinated (V), pulmonary TB latently infected (E), asymptomatic pulmonary TB infectious individuals (I_a), symptomatic pulmonary TB individuals (I_S), individuals co-infected with asymptomatic pulmonary TB and pneumonia (I_{aP}), individuals co-infected with symptomatic pulmonary TB and pneumonia (I_{SP}), latently pulmonary TB infected individuals undergoing treatment (T_E), individuals infected with asymptomatic pulmonary TB alone who are undergoing treatment (T_a), individuals infected with symptomatic pulmonary TB alone who are undergoing treatment (T_S), individuals co-infected with asymptomatic pulmonary TB and pneumonia who are undergoing treatment (T_{aP}), individuals co-infected with symptomatic pulmonary TB and pneumonia who are undergoing treatment (T_{SP}), and recovered individuals (R).

Individuals are recruited into the model either through birth or immigration at a constant rate, Λ. The co-infection model assumes that a fraction of the recruits is vaccinated at a constant rate, Q, and enters the vaccinated class.

The susceptible population becomes latently infected with pulmonary TB after effective contact with any of the infectious cases. The force of infection with pulmonary TB is given by equation (3.5) as follows:

$$\lambda_1 = \beta_1 \left(I_{SP} + \eta_4 I_S + \eta_5 T_{aP} + \eta_6 I_a + \eta_7 T_{SP} + \eta_8 T_S + \eta_9 T_{aP} + \eta_{10} T_a \right) \tag{3.5}$$

where β_1 denotes the transmission rate of TB infections, and $\eta_4, \eta_5, \eta_6, \eta_7, \eta_8, \eta_9, \eta_{10}$ account for the relative infectiousness of individuals with pulmonary TB in various categories. These parameters are assumed to satisfy:

$0 < \eta_{10} < \eta_9 < \eta_8 < \eta_7 < \eta_6 < \eta_5 < \eta_4 < 1.$

The model considers that vaccine efficacy is not 100%; therefore, vaccinated individuals can become latently infected at a force of infection given by equation (3.6) as follows:

$$(1-\rho)\lambda_1 = (1-\rho)\beta_1(I_{SP} + \eta_4 I_S + \eta_5 T_{aP} + \eta_6 I_a + \eta_7 T_{SP} + \eta_8 T_S + \eta_9 T_{aP} + \eta_{10} T_a) \quad (3.6)$$

where ρ is the vaccine efficacy, such that $0 \leq \rho \leq 1$.

Latently infected individuals are either screened at a constant rate of ϑ_1 and move to the class of latently infected individuals undergoing treatment (T_E), or progress to the symptomatic pulmonary TB class (I_S) at a rate of $\frac{\varepsilon_1 E}{1+nE}$, where ε_1 represents the progression rate of latent infections to symptomatic disease, and n measures the extent of delay in latent infection progression due to enhanced immunity. Alternatively, latently infected individuals can become asymptomatic infectious at a rate of $\frac{\varepsilon_2 E}{1+nE}$, where ε_2 represents the progression rate of latent TB infections to asymptomatic infectious disease. Asymptomatic infectious individuals may develop symptoms and join the symptomatic class (I_S) at a rate of ϕ_1.

Individuals with pulmonary TB disease may contract secondary pneumonia infections after effective contact with any pneumonia-infectious cases. The force of infection is represented by equation (3.7) as follows:

$$\lambda_2 = \beta_2 \left(I_{SP} + \epsilon_1 I_{aP} + \epsilon_2 T_{SP} + \epsilon_3 T_{aP}\right) \quad (3.7)$$

where β_2 denotes the transmission rate of pneumonia, and $\epsilon_1, \epsilon_2, \epsilon_3$ represent the relative infectiousness of individuals with pneumonia infections in different categories.

Alternatively, individuals with either asymptomatic or symptomatic TB may be identified for treatment before contracting opportunistic pneumonia and transition to the treatment classes at rates ϑ_2 and ϑ_3, respectively.

Individuals co-infected with either asymptomatic or symptomatic TB and pneumonia are identified at rates ϑ_4 and ϑ_5, respectively, and move to the treated classes. Additionally, individuals co-infected with asymptomatic TB and pneumonia may progress to symptomatic TB-pneumonia co-infection before being identified for treatment at a rate of ϕ_2. Individuals undergoing treatment for the co-infections recover from pneumonia first, as it is an acute disease, and join either the class of individuals with asymptomatic TB undergoing treatment (T_a) at a rate of ϕ_3, or the class of individuals with symptomatic TB undergoing treatment (T_S) at a rate of ϕ_4.

The rate of disease-induced deaths due to symptomatic TB is denoted by γ_1, while the rate of disease-induced deaths for individuals undergoing treatment for symptomatic TB is γ_4. Additionally, the rates of disease-induced deaths due to co-infection with TB and pneumonia are γ_2 and γ_5 for symptomatic and asymptomatic TB, respectively, whereas the rate of disease-induced deaths for individuals undergoing treatment for co-infection is γ_3.

Treatment for different forms of pulmonary TB is assumed to be successful. Consequently, latently infected individuals undergoing treatment, asymptomatic pulmonary TB individuals undergoing treatment, and symptomatic pulmonary TB individuals undergoing treatment recover at rates of α_1, α_2, and α_3, respectively, and transition to the recovered class (R). The model assumes that recovered individuals become susceptible again after their immunity wanes at a rate of κ.

The rate at which individuals die from causes other than pulmonary TB or TB-pneumonia co-infection is denoted by μ. It is worth noting that all parameters are positive constants.

Based on the assumptions, variables, and parameters, the flowchart for the formulated model is presented in Figure 3.2, which serves as the basis for deriving the differential equations given by system (3.8).

Figure 3.2

The flowchart for the TB and pneumonia co-infection model

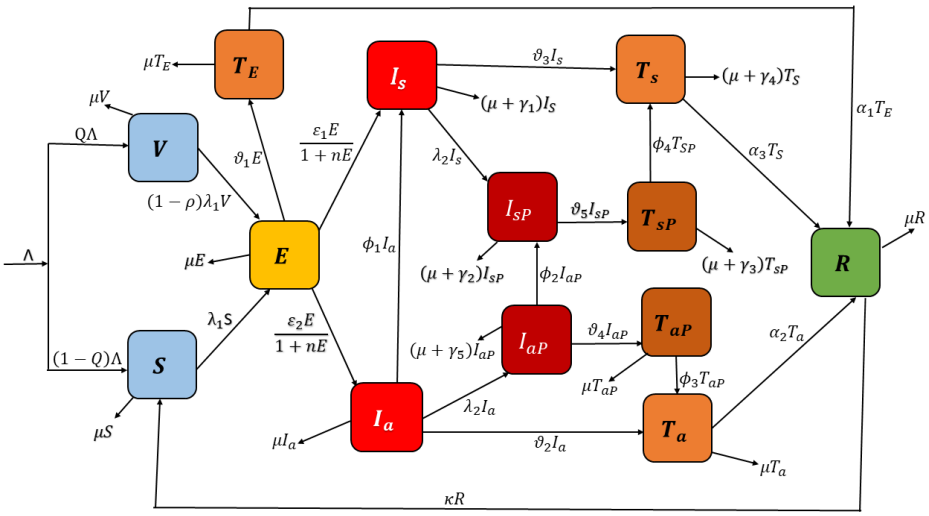

Source: Researcher (2024)

$$
\begin{cases}
\frac{dS}{dt} &= (1-Q)\Lambda + \kappa R - (\lambda_1 + \mu)S, \\
\frac{dV}{dt} &= Q\Lambda - \left[(1-\rho)\lambda_1 + \mu\right]V, \\
\frac{dE}{dt} &= \lambda_1 S + (1-\rho)\lambda_1 V - \left(\frac{\varepsilon_1}{1+nE} + \frac{\varepsilon_2}{1+nE} + \vartheta_1 + \mu\right)E, \\
\frac{dI_a}{dt} &= \frac{\varepsilon_2 E}{1+nE} - (\lambda_2 + \phi_1 + \mu + \vartheta_2)I_a, \\
\frac{dI_S}{dt} &= \frac{\varepsilon_1 E}{1+nE} + \phi_1 I_a - (\lambda_2 + \vartheta_3 + \mu + \gamma_1)I_S, \\
\frac{dI_{aP}}{dt} &= \lambda_2 I_a - (\mu + \gamma_5 + \phi_2 + \vartheta_4)I_{aP}, \\
\frac{dI_{SP}}{dt} &= \lambda_2 I_S + \phi_2 I_{aP} - (\gamma_2 + \vartheta_5 + \mu)I_{SP}, \\
\frac{dT_E}{dt} &= \vartheta_1 E - (\mu + \alpha_1)T_E, \\
\frac{dT_a}{dt} &= \vartheta_2 I_a + \phi_3 T_{aP} - (\mu + \alpha_2)T_a, \\
\frac{dT_S}{dt} &= \vartheta_3 I_S + \phi_4 T_{SP} - (\mu + \gamma_4 + \alpha_3)T_S, \\
\frac{dT_{aP}}{dt} &= \vartheta_4 I_{aP} - (\mu + \phi_3)T_{aP}, \\
\frac{dT_{SP}}{dt} &= \vartheta_5 I_{SP} - (\mu + \phi_4 + \gamma_3)T_{SP}, \\
\frac{dR}{dt} &= \alpha_1 T_E + \alpha_2 T_a + \alpha_3 T_S - (\mu + \kappa)R.
\end{cases}
\tag{3.8}
$$

3.5 Determining the Control Reproduction Numbers

The control reproduction numbers of the formulated models were determined using the Next-Generation Matrix method. The Next-Generation Matrix provides a systematic way to compute reproduction numbers, which represent the expected number of new infections caused by a single infected individual. This method is particularly useful when the model has multiple infectious compartments (e.g., asymptomatic, symptomatic, and treated) and when the model represents nonlinear and complex disease dynamics (Driessche et al., 2020).

The method begins by identifying the set of compartments that contain infected individuals (e.g., latent, infectious, and treated). These compartments are written in vector form as shown in equation (3.9):

$$X = (x_1, x_2, ..., x_n) \tag{3.9}$$

where n is the number of infected compartments.

The system in equation (3.9) is then rewritten in the form:

$$\frac{dX}{dt} = f(x) - v(x) \tag{3.10}$$

where $f(x)$ is the rate of appearance of new infections in each compartment, and $v(x)$ is the rate of transfer into and out of compartments by all other means (e.g., progression, recovery, death, or treatment).

Equation (3.10) is then linearized at the disease-free equilibrium by computing the Jacobian matrices F and V at the disease-free equilibrium, as shown in equation (3.11):

$$\begin{cases} F = \left[\dfrac{\partial F_i}{\partial x_j}\right] \\ V = \left[\dfrac{\partial V_i}{\partial x_j}\right] \end{cases} \tag{3.11}$$

where i represents the infected compartment being affected, and j represents the infected compartment causing the effect.

The control reproduction number is then given by the spectral radius of FV^{-1}, as shown

in equation (3.12):

$$R_C = \rho(FV^{-1}) \tag{3.12}$$

3.6 Data Fitting and Parameter Estimation

The NTLLDP data on pulmonary TB and pneumonia co-infection in Kenya were used to fit the prevalence of the formulated model. The NTLLDP prevalence data from 2012 to 2022 were considered, as presented in Tables 3.1 and 3.2.

Table 3.1

TB-Pneumonia prevalence by year (2012–2017)

Year	2012	2013	2014	2015	2016	2017
TB-Pneumonia Prevalence	42440	48555	50599	54345	56795	59529

Source: Researcher (2024)

Table 3.2

TB-Pneumonia prevalence by year (2018–2022)

Year	2018	2019	2020	2021	2022
TB-Pneumonia Prevalence	60615	62146	62022	66106	68100

Source: Researcher (2024)

The pulmonary TB and pneumonia co-infection model prevalence was defined as follows:

$$\text{TB and Pneumonia Model Prevalence} = \frac{\text{Total number of TB and pneumonia co-infection cases}}{\text{Total population}}$$

or

$$\text{TB and Pneumonia Model Prevalence} = \frac{I_{aP}+I_{SP}+T_{aP}+T_{SP}}{N} \tag{3.13}$$

where N represents the total population size.

The pulmonary TB and pneumonia co-infection model prevalence, described in equation (3.13), was fitted to the NTLLDP prevalence data in Tables 3.1 and 3.2 to estimate the parameters. Using MATLAB's built-in functions, ODE45 and `fminsearch`, the parameters were estimated by minimizing the sum of squared differences (SSD) between the co-infection model prevalence solution and the NTLLDP prevalence data, following the approaches

outlined by Kim et al. (2020) and Khan et al. (2015). The SSD is defined as follows:

$$SSD = \sum_{q=1}^{11} \left(\frac{\left(\frac{I_{aP}^q + I_{SP}^q + T_{aP}^q + T_{SP}^q}{N^q} - C_1^q \right)^2}{\left(\max(C_1^q, C_2^q) \right)^2} \right) \tag{3.14}$$

where:

$N^q = S^q + V^q + E^q + I_a^q + I_S^q + I_{aP}^q + I_{SP}^q + T_E^q + T_a^q + T_S^q + T_{aP}^q + T_{SP}^q + R^q$

In Equation (3.14), q represents the time period from 2012 to 2022. C_1^q denotes the yearly pulmonary TB and pneumonia co-infection prevalence data from NTLLDP, while C_2^q represents the corresponding yearly model prevalence. Additionally, the variables S^q, V^q, E^q, I_a^q, I_S^q, I_{aP}^q, I_{SP}^q, T_E^q, T_a^q, T_S^q, T_{aP}^q, T_{SP}^q, and R^q represent the numerically computed solutions at each time point q.

The parameters of the model were estimated using MATLAB's `fminsearch` algorithm, which minimizes uncertainty by computing the goodness of fit via the sum of squared errors. The estimated parameters include β_2, η_4, η_5, η_6, η_7, η_8, η_9, η_{10}, ϵ_1, ϵ_2, ϵ_3, ϑ_4, ϑ_5, ϕ_2, ϕ_3, ϕ_4, γ_2, γ_3, γ_5, and n.

4.1 Introduction

This chapter presents the results and discussion of the analysis and numerical simulations for the formulated models. The aim is to determine the threshold conditions for the persistence and control of the disease. The chapter is organized as follows. First, the model analysis and numerical simulation results for pulmonary TB incorporating an asymptomatic component and natural immunity are presented. Thereafter, the analysis and numerical results for the co-infection model are provided.

4.2 Pulmonary TB Model Analysis

In this section, a pulmonary TB model is analyzed, focusing on several aspects: the positivity of model solutions, the invariant region, the disease-free and endemic equilibrium points, the reproduction numbers of the model, bifurcation analysis, and sensitivity analysis.

4.2.1 Positivity of the model solutions

The dynamical system (3.4) illustrates the changes in the human population. Therefore, it is essential to prove that, given non-negative initial conditions, its solutions remain positive for all $t > 0$, as demonstrated by Theorem 4.1.

Theorem 4.1. *Given that the initial conditions* $S(0) \geq 0$, $V(0) \geq 0$, $E(0) \geq 0$, $I_a(0) \geq 0$, $I_S(0) \geq 0$, $T_E(0) \geq 0$, $T_a(0) \geq 0$, $T_S(0) \geq 0$, *and* $R(0) \geq 0$, *the solutions* $S(t)$, $V(t)$, $E(t)$, $I_a(t)$, $I_S(t)$, $T_E(t)$, $T_a(t)$, $T_S(t)$, *and* $R(t)$ *remain non-negative for all* $t > 0$.

Proof. The first equation of the model system (3.4) is considered to demonstrate the positivity of the solutions using the integrating factor method. To simplify the computations, let $y(t) = \lambda(t) + \mu$; thus, the first equation of the model system (3.4) is rewritten as:

$$\frac{ds}{dt} = (1 - P)\pi + \sigma R - y(t)S \tag{4.1}$$

The integrating factor (IF) of equation (4.1) is given as:

$$\text{IF} = e^{\int y(t)\, dt} \tag{4.2}$$

Multiplying equation (4.1) by the integrating factor gives:

$$e^{\int y(t)\,dt}\frac{dS}{dt} + e^{\int y(t)\,dt}y(t)S = \big((1-P)\pi + \sigma R\big)\,e^{\int y(t)\,dt} \tag{4.3}$$

Equation (4.3) simplifies to:

$$\frac{d}{dt}\Big(S(t)\,e^{\int y(t)\,dt}\Big) = \big((1-P)\pi + \sigma R\big)\,e^{\int y(t)\,dt} \tag{4.4}$$

Integrating equation (4.4) yields:

$$S(t) = e^{-\int y(t)\,dt}\left[\int \big((1-P)\pi + \sigma R\big)\,e^{\int y(t)\,dt}\,dt + C\right] \tag{4.5}$$

where C is the constant of integration. Applying the initial condition at $t = 0$, $S(t) = S(0)$, yields $C = S(0)$. Substituting C into equation (4.5) results in:

$$S(t) = e^{-\int y(t)\,dt}\left[\int \big((1-P)\pi + \sigma R\big)\,e^{\int y(t)\,dt}\,dt + S(0)\right] \geq 0 \tag{4.6}$$

Since $S(0) \geq 0$, the solution $S(t)$ of the differential equation is non-negative and remains positive for all $t > 0$. The same approach can be applied to demonstrate the positivity of solutions for all other differential equations in system (3.4). Thus,

$$\{S(t), V(t), E(t), I_a(t), I_S(t), T_E(t), T_a(t), T_S(t), R(t)\} \geq 0, \quad \forall\, t > 0 \tag{4.7}$$

This confirms that the solutions of the model system (3.4) remain positive for all $t > 0$.

4.2.2 Boundedness of the solution

The model system (3.4) pertains to the human population; therefore, it is necessary to demonstrate that its solutions are bounded for all $t > 0$. The following theorem is used to prove the boundedness of the solutions:

Theorem 4.2. *Given the positive initial conditions, the feasible region is defined as:*

$$\Omega = \left\{(S(t), V(t), E(t), I_a(t), I_S(t), T_E(t), T_a(t), T_S(t), R(t)) \in \mathbb{R}^9_+ : N \leq \frac{\pi}{\mu}\right\} \tag{4.8}$$

Proof. The sum of all equations in system (3.4) represents the total human population in the model and satisfies the following equation:

$$\frac{dN}{dt} = \pi - \mu N - \delta_1 I_S - \delta_2 T_S \tag{4.9}$$

In the absence of mortality due to pulmonary TB infections, $\delta_1 = \delta_2 = 0$. Therefore, equation (4.9) simplifies to:

$$\frac{dN}{dt} = \pi - \mu N \tag{4.10}$$

By integrating equation (4.10) and applying the initial condition at $t = 0$,
$N(t) = N(0)$, yields:

$$N(t) = \frac{\pi}{\mu} + \left(N(0) - \frac{\pi}{\mu} \right) e^{-\mu t} \tag{4.11}$$

As $t \to \infty$, the population $N(t) \to \frac{\pi}{\mu}$, implying that $0 \leq N(t) \leq \frac{\pi}{\mu}$. Thus, the feasible solution of the system enters and remains in the region:

$$\Omega = \left\{ (S(t), V(t), E(t), I_a(t), I_S(t), T_E(t), T_a(t), T_S(t), R(t)) \in \mathbb{R}^9_+ : N \leq \tfrac{\pi}{\mu} \right\}$$

Therefore, the basic model is well-posed epidemiologically and mathematically, and it is sufficient to study its dynamics in Ω.

4.2.3 The disease-free equilibrium point

The disease-free equilibrium is a fundamental concept in the analysis of epidemiological mathematical models. It represents a state where the entire population is free of infection, with only the susceptible and potentially vaccinated compartments populated. This equilibrium serves as a baseline to assess whether a disease can invade and persist in a population or eventually die out.

The disease-free equilibrium point of the system (3.4) is obtained by setting the latently infected class, all infectious classes, all classes undergoing treatment, and the recovered class to zero, i.e., $E = I_a = I_S = T_E = T_a = T_S = R = 0$. Therefore, the following

equations are obtained:

$$\begin{cases} (1-P)\pi - \mu S = 0 \\ P\pi - \mu V = 0 \end{cases} \tag{4.12}$$

Solving system (4.12) yields:

$$S^0 = \frac{(1-P)\pi}{\mu}, \qquad V^0 = \frac{P\pi}{\mu}.$$

The disease-free equilibrium is thus given by:

$$B^0 = (S^0, V^0, E^0, I_a^0, I_S^0, T_E^0, T_a^0, T_S^0, R^0) = \left(\frac{(1-P)\pi}{\mu}, \frac{P\pi}{\mu}, 0, 0, 0, 0, 0, 0, 0\right) \tag{4.13}$$

where: $B^0 = (S^0, V^0, E^0, I_a^0, I_S^0, T_E^0, T_a^0, T_S^0, R^0)$

denotes the disease-free equilibrium of the formulated model.

4.2.4 The control reproduction number and basic reproduction number

The control reproduction number is a threshold parameter that governs the spread of diseases. It is defined as the expected number of secondary infections produced by an index infected individual during his entire period of infectiousness in a population that is not entirely susceptible due to the presence of control efforts. The basic reproduction number is defined as the average number of secondary infections caused by a single infectious individual during his entire infectious period in a population that is entirely susceptible (Driessche et al., 2020).

The Next-Generation Matrix method, as outlined by Driessche et al. (2020), was used to determine the control reproduction number, derived from the matrix's spectral radius. The model equations for the infected classes are rewritten as follows:

$$
\begin{cases}
\frac{dE}{dt} &= \lambda S + (1-\rho)\lambda V - \left(\frac{\chi_1}{1+mE} + \frac{\chi_2}{1+mE} + \theta_1 + \mu\right) E, \\
\frac{dI_a}{dt} &= \frac{\chi_1 E}{1+mE} - (\theta_2 + \omega + \mu) I_a, \\
\frac{dI_S}{dt} &= \frac{\chi_2 E}{1+mE} + \omega I_a - (\theta_3 + \delta_1 + \mu) I_S, \\
\frac{dT_a}{dt} &= \theta_2 I_a - (\xi_2 + \mu) T_a, \\
\frac{dT_S}{dt} &= \theta_3 I_S - (\delta_2 + \xi_3 + \mu) T_S.
\end{cases} \tag{4.14}
$$

Applying the principle of the next-generation matrix, the matrix of new infection terms, denoted by f, and the matrix of remaining transfer terms, denoted by v, are obtained as follows:

$$
f = \begin{bmatrix} \lambda S + (1-\rho)\lambda V \\ 0 \\ 0 \\ 0 \\ 0 \end{bmatrix}, \qquad v = \begin{bmatrix} \left(\frac{\chi_1}{1+mE} + \frac{\chi_2}{1+mE} + \theta_1 + \mu\right) E \\ (\theta_2 + \omega + \mu) I_a - \dfrac{\chi_1 E}{1+mE} \\ (\theta_3 + \delta_1 + \mu) I_S - \dfrac{\chi_2 E}{1+mE} - \omega I_a \\ (\xi_2 + \mu) T_a - \theta_2 I_a \\ (\delta_2 + \xi_3 + \mu) T_S - \theta_3 I_S \end{bmatrix}.
$$

The Jacobian matrices of f and v with respect to E, I_a, I_S, T_a, and T_S at the disease-free equilibrium (4.13) are then obtained. This process is simplified by assigning f and v as follows:

$$
f = \begin{bmatrix} f_1 \\ f_2 \\ f_3 \\ f_4 \\ f_5 \end{bmatrix}, \qquad v = \begin{bmatrix} v_1 \\ v_2 \\ v_3 \\ v_4 \\ v_5 \end{bmatrix}.
$$

where:

$$
\begin{aligned}
f_1 &= \lambda S + (1-\rho)\lambda V, & v_1 &= \left(\frac{\chi_1}{1+mE} + \frac{\chi_2}{1+mE} + \theta_1 + \mu\right) E, \\
f_2 &= 0, & v_2 &= (\theta_2 + \omega + \mu) I_a - \frac{\chi_1 E}{1+mE}, \\
f_3 &= 0, & v_3 &= (\theta_3 + \delta_1 + \mu) I_S - \frac{\chi_2 E}{1+mE} - \omega I_a, \\
f_4 &= 0, & v_4 &= (\xi_2 + \mu) T_a - \theta_2 I_a, \\
f_5 &= 0, & v_5 &= (\delta_2 + \xi_3 + \mu) T_S - \theta_3 I_S.
\end{aligned}
$$

Here:

$\lambda = bT_a + cT_S + dI_a + eI_S$

where:

$b = \beta\eta_3$, is the transmission rate for asymptomatic individuals undergoing treatment.

$c = \beta\eta_2$, is the transmission rate for symptomatic individuals undergoing treatment.

$d = \beta\eta_1$, is the transmission rate for asymptomatic individuals.

$e = \beta$, is the transmission rate for symptomatic individuals.

The Jacobians of f and v are obtained by differentiating each function with respect to their respective variables. These Jacobians are denoted by F and V, respectively, and are determined as follows:

$$
F = \begin{bmatrix}
\frac{\partial f_1}{\partial E} & \frac{\partial f_1}{\partial I_a} & \frac{\partial f_1}{\partial I_S} & \frac{\partial f_1}{\partial T_a} & \frac{\partial f_1}{\partial T_S} \\
\frac{\partial f_2}{\partial E} & \frac{\partial f_2}{\partial I_a} & \frac{\partial f_2}{\partial I_S} & \frac{\partial f_2}{\partial T_a} & \frac{\partial f_2}{\partial T_S} \\
\frac{\partial f_3}{\partial E} & \frac{\partial f_3}{\partial I_a} & \frac{\partial f_3}{\partial I_S} & \frac{\partial f_3}{\partial T_a} & \frac{\partial f_3}{\partial T_S} \\
\frac{\partial f_4}{\partial E} & \frac{\partial f_4}{\partial I_a} & \frac{\partial f_4}{\partial I_S} & \frac{\partial f_4}{\partial T_a} & \frac{\partial f_4}{\partial T_S} \\
\frac{\partial f_5}{\partial E} & \frac{\partial f_5}{\partial I_a} & \frac{\partial f_5}{\partial I_S} & \frac{\partial f_5}{\partial T_a} & \frac{\partial f_5}{\partial T_S}
\end{bmatrix},
$$

$$V = \begin{bmatrix} \frac{\partial v_1}{\partial E} & \frac{\partial v_1}{\partial I_a} & \frac{\partial v_1}{\partial I_S} & \frac{\partial v_1}{\partial T_a} & \frac{\partial v_1}{\partial T_S} \\ \frac{\partial v_2}{\partial E} & \frac{\partial v_2}{\partial I_a} & \frac{\partial v_2}{\partial I_S} & \frac{\partial v_2}{\partial T_a} & \frac{\partial v_2}{\partial T_S} \\ \frac{\partial v_3}{\partial E} & \frac{\partial v_3}{\partial I_a} & \frac{\partial v_3}{\partial I_S} & \frac{\partial v_3}{\partial T_a} & \frac{\partial v_3}{\partial T_S} \\ \frac{\partial v_4}{\partial E} & \frac{\partial v_4}{\partial I_a} & \frac{\partial v_4}{\partial I_S} & \frac{\partial v_4}{\partial T_a} & \frac{\partial v_4}{\partial T_S} \\ \frac{\partial v_5}{\partial E} & \frac{\partial v_5}{\partial I_a} & \frac{\partial v_5}{\partial I_S} & \frac{\partial v_5}{\partial T_a} & \frac{\partial v_5}{\partial T_S} \end{bmatrix}.$$

The Jacobian matrices of F and V at the disease-free equilibrium are then expressed as:

$$F = \begin{bmatrix} 0 & dS^0 + (1-\rho)\, dV^0 & eS^0 + (1-\rho)\, eV^0 & bS^0 + (1-\rho)\, bV^0 & cS^0 + (1-\rho)\, cV^0 \\ 0 & 0 & 0 & 0 & 0 \\ 0 & 0 & 0 & 0 & 0 \\ 0 & 0 & 0 & 0 & 0 \\ 0 & 0 & 0 & 0 & 0 \end{bmatrix}$$

$$\mathrm{V} = \begin{bmatrix} \chi_1 + \chi_2 + \theta_1 + \mu & 0 & 0 & 0 & 0 \\ -\chi_1 & \theta_2 + \omega + \mu & 0 & 0 & 0 \\ -\chi_2 & -\omega & \theta_3 + \delta_1 + \mu & 0 & 0 \\ 0 & -\theta_2 & 0 & \xi_2 + \mu & 0 \\ 0 & 0 & -\theta_3 & 0 & \delta_2 + \xi_3 + \mu \end{bmatrix}$$

Using Mathematica software, the inverse of V was found to be:

$$\mathrm{V}^{-1} = \begin{bmatrix} \frac{1}{\chi_1 + \chi_2 + \theta_1 + \mu} & 0 & 0 & 0 & 0 \\ \frac{\chi_1}{c_1} & \frac{1}{\theta_2 + \mu + \omega} & 0 & 0 & 0 \\ \frac{\chi_1\omega + \chi_2(\theta_2 + \mu + \omega)}{c_2} & \frac{\omega}{c_3} & \frac{1}{\theta_3 + \delta_1 + \mu} & 0 & 0 \\ \frac{\theta_2\chi_1}{c_4} & \frac{\theta_2}{c_5} & 0 & \frac{1}{\mu + \xi_2} & 0 \\ \frac{\theta_3\chi_1\omega + \theta_3\chi_2(\theta_2 + \mu + \omega)}{c_6} & \frac{\theta_3\omega}{c_7} & \frac{\theta_3}{c_8} & 0 & \frac{1}{\xi_3 + \delta_2 + \mu} \end{bmatrix}$$

where:

$$c_1 = (\chi_1 + \chi_2 + \theta_1 + \mu)(\theta_2 + \mu + \omega),$$

$$c_2 = (\theta_3 + \delta_1 + \mu)(\chi_2 + \chi_1 + \theta_1 + \mu)(\theta_2 + \mu + \omega),$$

$$c_3 = (\theta_3 + \delta_1 + \mu)(\delta_2 + \mu + \omega),$$

$$c_4 = (\chi_2 + \chi_1 + \theta_1 + \mu)(\mu + \xi_2)(\theta_2 + \mu + \omega),$$

$$c_5 = (\mu + \xi_2)(\theta_2 + \mu + \omega),$$

$$c_6 = (\xi_3 + \delta_2 + \mu)(\theta_3 + \delta_1 + \mu)(\chi_2 + \chi_1 + \theta_1 + \mu)(\theta_2 + \mu + \omega),$$

$$c_7 = (\xi_3 + \delta_2 + \mu)(\theta_3 + \delta_1 + \mu)(\theta_2 + \mu + \omega),$$

$$c_8 = (\xi_3 + \delta_2 + \mu)(\theta_3 + \delta_1 + \mu).$$

The product of F and V^{-1} then becomes:

$$FV^{-1} = \begin{bmatrix} a_1 + a_2 + a_3 + a_4 & a_5 + a_6 + a_7 + a_8 & a_9 + a_{10} & a_{11} & a_{12} \\ 0 & 0 & 0 & 0 & 0 \\ 0 & 0 & 0 & 0 & 0 \\ 0 & 0 & 0 & 0 & 0 \\ 0 & 0 & 0 & 0 & 0 \end{bmatrix}$$

where:

$$
\begin{aligned}
a_1 &= \frac{\chi_1 d}{(\theta_2+\mu+\omega)(\chi_1+\chi_2+\theta_1+\mu)}\,[S^0+(1-\rho)V^0],\\
a_2 &= \frac{e\,[\chi_1\omega+\chi_2(\theta_2+\mu+\omega)]}{(\theta_3+\delta_1+\mu)(\theta_2+\mu+\omega)(\chi_1+\chi_2+\theta_1+\mu)}\,[S^0+(1-\rho)V^0],\\
a_3 &= \frac{b\chi_1\theta_2}{(\theta_2+\mu+\omega)(\chi_1+\chi_2+\theta_1+\mu)(\mu+\xi_2)}\,[S^0+(1-\rho)V^0],\\
a_4 &= \frac{c[\theta_3\chi_1\omega+\theta_3\chi_2(\theta_2+\mu+\omega)]}{(\xi_3+\delta_2+\mu)(\theta_3+\delta_1+\mu)(\theta_2+\mu+\omega)(\chi_1+\chi_2+\theta_1+\mu)}\,[S^0+(1-\rho)V^0],\\
a_5 &= \frac{d}{\theta_2+\mu+\omega}\,[S^0+(1-\rho)V^0],\\
a_6 &= \frac{\omega e}{(\theta_3+\delta_1+\mu)(\delta_2+\mu+\omega)}\,[S^0+(1-\rho)V^0],\\
a_7 &= \frac{\theta_2 b}{(\theta_2+\mu+\omega)(\xi_2+\mu)}\,[S^0+(1-\rho)V^0],\\
a_8 &= \frac{\omega\theta_3 c}{(\xi_3+\delta_2+\mu)(\theta_3+\delta_1+\mu)(\theta_2+\mu+\omega)}\,[S^0+(1-\rho)V^0],\\
a_9 &= \frac{e}{\xi_3+\delta_2+\mu}\,[S^0+(1-\rho)V^0],\\
a_{10} &= \frac{\theta_3 c}{(\xi_3+\delta_2+\mu)(\theta_3+\delta_1+\mu)}\,[S^0+(1-\rho)V^0],\\
a_{11} &= \frac{b}{\xi_2+\mu}\,[S^0+(1-\rho)V^0],\\
a_{12} &= \frac{c}{\xi_3+\delta_2+\mu}\,[S^0+(1-\rho)V^0].
\end{aligned}
$$

The eigenvalues of matrix FV^{-1} are determined as follows:

$$
\begin{vmatrix}
(a_1+a_2+a_3+a_4)-\lambda & a_5+a_6+a_7+a_8 & a_9+a_{10} & a_{11} & a_{12}\\
0 & 0-\lambda & 0 & 0 & 0\\
0 & 0 & 0-\lambda & 0 & 0\\
0 & 0 & 0 & 0-\lambda & 0\\
0 & 0 & 0 & 0 & 0-\lambda
\end{vmatrix} = 0
$$

$$\Rightarrow \ ((a_1+a_2+a_3+a_4)-\lambda)\begin{vmatrix} 0-\lambda & 0 & 0 & 0 \\ 0 & 0-\lambda & 0 & 0 \\ 0 & 0 & 0-\lambda & 0 \\ 0 & 0 & 0 & 0-\lambda \end{vmatrix} = 0$$

$$\Rightarrow \ \big[(a_1+a_2+a_3+a_4)-\lambda\big]\lambda^4 = 0$$

Either

$$\lambda^4 = 0 \quad \Rightarrow \quad \lambda_1=\lambda_2=\lambda_3=\lambda_4=0$$

or

$$(a_1+a_2+a_3+a_4)-\lambda = 0 \quad \Rightarrow \quad \lambda_5 = a_1+a_2+a_3+a_4.$$

Among the eigenvalues λ_1, λ_2, λ_3, λ_4, and λ_5, the dominant eigenvalue is λ_5.
Therefore, the control reproduction number is given by the following equation:

$$R_C = \lambda_5 = a_1+a_2+a_3+a_4 \tag{4.15}$$

By substituting $a_1, a_2, a_3, a_4, b, c, d, e,\ V^0,$ and S^0 into equation (4.15), the control reproduction number (R_{CVST}) with vaccination, screening, and treatment of all forms of pulmonary tuberculosis as intervention strategies is expressed as:

$$\mathrm{R}_{CVST} = \frac{\beta\left[(\eta_1\chi_1x_3+\chi_1\omega+\chi_2x_2)x_5x_6+\eta_3\theta_2\chi_1x_3x_6+\eta_2\theta_3x_5(\chi_1\omega+\chi_2x_2)\right]\left[\frac{(1-P)\pi}{\mu}+\frac{(1-\rho)P\pi}{\mu}\right]}{x_1x_2x_3x_5x_6} \tag{4.16}$$

where:

$$x_1=\chi_1+\chi_2+\theta_1+\mu, \quad x_2=\theta_2+\omega+\mu, \quad x_3=\theta_3+\delta_1+\mu, \quad x_5=\xi_2+\mu, \quad x_6=\delta_2+\xi_3+\mu.$$

Without vaccination intervention, the fraction of recruits vaccinated, P, equals zero. Consequently, the parameter ρ, representing vaccine efficacy, also becomes zero since there will be no vaccinated population. Substituting $P=\rho=0$ into equation (4.16) gives the

control reproduction number (R_{CST}) with screening and treatment as the only intervention strategies. R_{CST} is thus expressed as:

$$R_{CST} = \frac{\beta\Big[(\eta_1\chi_1 x_3 + \chi_1\omega + \chi_2 x_2)x_5x_6 + \eta_3\theta_2\chi_1 x_3x_6 + \eta_2\theta_3 x_5(\chi_1\omega + \chi_2 x_2)\Big]\frac{\pi}{\mu}}{x_1x_2x_3x_5x_6} \tag{4.17}$$

Considering the presence of latently infected and asymptomatic infectious individuals in the population without their screening, the parameters θ_1, θ_2, and ξ_2 become zero. Substituting $\theta_1 = \theta_2 = \xi_2 = 0$ into equation (4.16) gives the control reproduction number (R_{CVT_S}) with vaccination and treatment of the symptomatic population as the only intervention strategies. R_{CVT_S} is expressed as:

$$R_{CVT_S} = \frac{\beta\Big[(\eta_1\chi_1(\theta_3+\delta_1+\mu)+\chi_1\omega+\chi_2(\mu+\omega))(\xi_3+\delta_2+\mu)+\eta_2\theta_3(\chi_1\omega+\chi_2(\mu+\omega))\Big]\Big[(1-P)\frac{\pi}{\mu}+(1-\rho)P\frac{\pi}{\mu}\Big]}{(\chi_1+\chi_2+\mu)(\omega+\mu)(\theta_3+\delta_1+\mu)(\delta_2+\xi_3+\mu)} \tag{4.18}$$

When there is no vaccination of recruits and screening of both latent infected and asymptomatic infectious populations, the parameters θ_1, θ_2, ξ_2, P, and ρ become zero. Substituting $\theta_1 = \theta_2 = \xi_2 = P = \rho = 0$ into equation (4.16) gives the control reproduction number (R_{CT_S}) with the treatment of the symptomatic population as the only intervention strategy. R_{CT_S} is expressed as:

$$R_{CT_S} = \frac{\beta\Big[(\eta_1\chi_1(\theta_3 + \delta_1 + \mu) + \chi_1\omega + \chi_2(\mu+\omega))(\xi_3 + \delta_2 + \mu) + \eta_2\theta_3(\chi_1\omega + \chi_2(\mu+\omega))\Big]\frac{\pi}{\mu}}{(\chi_1 + \chi_2 + \mu)(\omega+\mu)(\theta_3 + \delta_1 + \mu)(\delta_2 + \xi_3 + \mu)} \tag{4.19}$$

Finally, considering the absence of any intervention measures, meaning no vaccination of recruits, no screening of latently infected or asymptomatic infectious populations, and no treatment of pulmonary tuberculosis, the parameters P, ρ, θ_1, θ_2, θ_3, ξ_2, ξ_3, and δ_2 become zero. Substituting $P = \rho = \theta_1 = \theta_2 = \theta_3 = \xi_2 = \xi_3 = \delta_2 = 0$ into equation (4.16) gives the basic reproduction number (R_0) as:

$$R_0 = \frac{\beta\Big[\eta_1\chi_1(\delta_1 + \mu) + \chi_1\omega + \chi_2(\mu+\omega)\Big]\frac{\pi}{\mu}}{(\chi_1 + \chi_2 + \mu)(\omega+\mu)(\delta_1 + \mu)} \tag{4.20}$$

4.2.5 Local stability of disease-free equilibrium

The local stability of the disease-free equilibrium is a critical aspect of analyzing the dynamics of infectious diseases within a population. This stability analysis helps determine whether small perturbations around the disease-free state result in the system returning to equilibrium or deviating toward disease prevalence. The following theorem is employed to illustrate the stability of the disease-free equilibrium point:

Theorem 4.3. *The disease-free equilibrium point is locally asymptotically stable if* $R_{CVST} < 1$ *and unstable if* $R_{CVST} > 1$.

Proof. To prove the local stability of the disease-free equilibrium, the Jacobian matrix of system (3.4), evaluated at the disease-free equilibrium point B^0, is derived as follows:

$$J(B^0) = \begin{bmatrix} -\mu & 0 & 0 & -dS^0 & -eS^0 & 0 & -bS^0 & -cS^0 & \sigma \\ 0 & -\mu & 0 & -H_1 & -H_2 & 0 & -H_3 & -H_4 & 0 \\ 0 & 0 & -x_1 & H_5 & H_6 & 0 & H_7 & H_8 & 0 \\ 0 & 0 & \chi_1 & -x_2 & 0 & 0 & 0 & 0 & 0 \\ 0 & 0 & \chi_2 & \omega & -x_3 & 0 & 0 & 0 & 0 \\ 0 & 0 & \theta_1 & 0 & 0 & -x_4 & 0 & 0 & 0 \\ 0 & 0 & 0 & \theta_2 & 0 & 0 & -x_5 & 0 & 0 \\ 0 & 0 & 0 & 0 & \theta_3 & 0 & 0 & -x_6 & 0 \\ 0 & 0 & 0 & 0 & 0 & \xi_1 & \xi_2 & \xi_3 & -x_7 \end{bmatrix} \tag{4.21}$$

where:

$$\begin{aligned} &x_1 = \chi_1 + \chi_2 + \theta_1 + \mu, && x_2 = \theta_2 + \omega + \mu, && x_3 = \theta_3 + \delta_1 + \mu, \\ &x_4 = \xi_1 + \mu, && x_5 = \xi_2 + \mu, && x_6 = \delta_2 + \xi_3 + \mu, \\ &x_7 = \sigma + \mu, && H_1 = (1-\rho)dV^0, && H_2 = (1-\rho)eV^0, \\ &H_3 = (1-\rho)bV^0, && H_4 = (1-\rho)cV^0, && H_5 = dS^0 + (1-\rho)dV^0, \\ &H_6 = eS^0 + (1-\rho)eV^0, && H_7 = bS^0 + (1-\rho)bV^0, && H_8 = cS^0 + (1-\rho)cV^0. \end{aligned}$$

Then, the eigenvalues of equation (4.21) are determined as follows:

Either,

$$(-(\mu+\lambda))(-(\mu+\lambda))(-(x_7+\lambda)) = 0 \tag{4.22}$$

Or

$$\begin{vmatrix} -x_1-\lambda & H_5 & H_6 & 0 & H_7 & H_8 \\ \chi_1 & -x_2-\lambda & 0 & 0 & 0 & 0 \\ \chi_2 & \omega & -x_3-\lambda & 0 & 0 & 0 \\ \theta_1 & 0 & 0 & -x_4-\lambda & 0 & 0 \\ 0 & \theta_2 & 0 & 0 & -x_5-\lambda & 0 \\ 0 & 0 & \theta_3 & 0 & 0 & -x_6-\lambda \end{vmatrix} = 0 \tag{4.23}$$

Using the Routh–Hurwitz criterion, which states that all eigenvalues of the Jacobian matrix must have negative real parts for stability, the roots of equation (4.22) are determined to be strictly negative, as follows:

$$\lambda_1 = \lambda_2 = -\mu < 0, \quad \lambda_3 = -x_7 = -(\sigma + \mu). \tag{4.24}$$

The characteristic polynomial of equation (4.23) is given as follows:

$$M_1\lambda^6 + M_2\lambda^5 + M_3\lambda^4 + M_4\lambda^3 + M_5\lambda^2 + M_6\lambda + M_7 = 0 \tag{4.25}$$

The coefficients M_1, M_2, M_3, M_4, M_5, M_6, and M_7 are determined using Mathematica software, as shown below:

$M_1 = 1 > 0$,

$M_2 = x_1 + x_2 + x_3 + x_4 + x_5 + x_6$,

$M_3 = x_6(x_1 + x_2 + x_3 + x_4 + x_5) + x_5(x_1 + x_2 + x_4) + x_4(x_1 + x_2 + x_3) + x_3(x_1 + x_2) + x_1x_2 - H_5\chi_1 - H_6\chi_2$,

$M_4 = x_6[x_5(x_1 + x_2 + x_3 + x_4) + x_4(x_1 + x_2 + x_3) + x_3(x_1 + x_2) + x_1x_2 - (H_5\chi_1 + H_6\chi_2)] + x_5[x_4(x_1 + x_2 + x_3) + x_3(x_1 + x_2) + x_1x_2 - (H_5\chi_1 + H_6\chi_2)] + x_4[x_3(x_1 + x_2) + x_1x_2 - (H_5\chi_1 + H_5\chi_2)] + x_3(x_1x_2 - H_5\chi_1) - x_2H_6\chi_2 - \omega H_6\chi_1 - \theta_2H_7\chi_1 - \theta_3H_8\chi_2$,

$M_5 = x_6[x_4x_5(x_1 + x_2 + x_3) + x_3x_5(x_1 + x_2) + x_2x_5x_1 + x_3x_4(x_1 + x_2) + x_1x_2(x_3 + x_4) - H_5\chi_1(x_3 + x_4 + x_5) - H_6\omega\chi_1 - H_6\chi_2(x_2 + x_4 + x_5) - H_7\theta_2\chi_1] + x_5[x_1x_2(x_3 + x_4) + x_3x_4(x_1 + x_2) - H_5\chi_1(x_3 + x_4) - H_6\omega\chi_1 - H_6\chi_2(x_2 + x_4) - H_8\theta_3\chi_2] + x_4[x_3x_2x_1 -$

$H_5\chi_1 x_3 - H_6\omega\chi_1 - H_6\chi_2 x_2 - H_7\theta_2\chi_1 - H_8\theta_3\chi_2] - H_7\theta_2\chi_1 x_3 - H_8\theta_{32}x_2 - H_8\theta_3\omega\chi_1,$

$M_6 = x_6[x_1x_2(x_3x_4 + x_3x_5 + x_4x_5) + x_3x_4(x_1x_5 + x_2x_5) - H_5\chi_1(x_3x_4 + x_3x_5 + x_4x_5) - H_6\omega\chi_1(x_4 + x_5) - H_6\chi_2(x_2x_4 + x_2x_5 + x_4x_5) - H_7\theta_2\chi_1(x_3 + x_4)] + x_5[x_1x_2x_3x_4 - H_5\chi_1x_3x_4 - H_6\chi_2x_4x_5 - H_6\omega\chi_1x_4 - H_8\omega_3\chi_2(x_2 + x_4) - H_8\omega\theta_3\chi_1] + x_4[-H_7\theta_2\chi_1x_3 - H_8\theta_3(x_2\chi_2 + \chi_1\omega)],$

$M_7 = x_1x_2x_3x_4x_5x_6 - x_4[x_5x_6[x_3H_5\chi_1 + H_6(\chi_2x_2 + \chi_1\omega)] + H_7\chi_{12}x_3x_6 + H_8\omega_3x_5(\chi_2x_2 + \chi_1\omega)].$

According to the Routh-Hurwitz criteria, $M_1 > 0$, $M_2 > 0$, $M_3 > 0$, $M_5 > 0$, $M_6 > 0$, and $M_7 > 0$.

From $M_7 > 0$, it follows that:

$x_1x_2x_3x_4x_5x_6 - x_4[x_5x_6[x_3H_5\chi_1 + H_6(\chi_2x_2 + \chi_1\omega)] + H_7\chi_1\theta_2x_3x_6 + H_8\theta_3x_5(\chi_2x_2 + \chi_1\omega)] > 0$

$\Rightarrow [x_5x_6[x_3H_5\chi_1 + H_6(\chi_2x_2 + \chi_1\omega)] + H_7\chi_1\omega_2x_3x_6 + H_8\omega_3x_5(\chi_2x_2 + \chi_1\omega)] < x_1x_2x_3x_5x_6$

$$\Rightarrow \frac{\left[x_5x_6\big(x_3H_5\chi_1 + H_6(\chi_2x_2 + \chi_1\omega)\big) + H_7\chi_1\theta_2x_3x_6 + H_8\theta_3x_5(\chi_2x_2 + \chi_1\omega)\right]}{x_1x_2x_3x_5x_6} < 1 \quad (4.26)$$

Substituting, H_5, H_6, H_7, H_8, S^0 and V^0 in inequality (4.26), and rearranging yields:

$$\frac{\beta\left[(\eta_1\chi_1x_3 + \chi_1\omega + \chi_2x_2)x_5x_6 + \eta_3\theta_2\chi_1x_3x_6 + \eta_2\theta_3x_5(\chi_1\omega + \chi_2x_2)\right]\left[\frac{(1-P)\pi}{\mu} + \frac{(1-\rho)P\pi}{\mu}\right]}{x_1x_2x_3x_5x_6} < 1 \quad (4.27)$$

Comparing equation (4.16) and inequality (4.27), it follows that $R_{CVST} < 1$.

The disease-free equilibrium point is considered to be locally asymptotically stable if the control reproduction number R_{CVST} is less than 1, indicating that the disease will die out over time. Conversely, it is deemed unstable if R_{CVST} is greater than 1, suggesting that the disease will persist and potentially lead to an outbreak.

4.2.6 Global stability of disease-free equilibrium

The global stability of the disease-free equilibrium is crucial for understanding the long-term behavior of infectious diseases within a population. Analyzing global stability involves assessing whether the disease-free state is stable under all possible conditions and perturbations.

The Castillo-Chavez method was used to investigate the global stability of the disease-

free equilibrium, as illustrated in Castillo-Chavez and Song (2004).This method involves decomposing the system into uninfected and infected compartments and applying sufficient conditions under which the disease-free equilibrium is globally asymptotically stable whenever the basic reproduction number $R_{CVST} < 1$.

The model system (3.4) is first written as:

$$\begin{cases} \dfrac{dX}{dt} = F(X, Z), \\ \dfrac{dZ}{dt} = G(X, Z). \end{cases} \tag{4.28}$$

where:

$X = (S, V, R)^T$ represents the uninfected population, while

$Z = (E, I_a, I_S, T_E, T_a, T_S)^T$ represents the infected population.

The fixed point of system (3.4) is denoted by: $U = (X^*, 0) = (\frac{(1-P)\pi}{\mu}, \frac{P\pi}{\mu}, 0, 0, 0, 0, 0, 0, 0)$.

The global stability of the disease-free equilibrium is established by theorem 4.4.

Theorem 4.4. *The equilibrium point $U = (X^*, 0)$ is globally asymptotically stable if $R_{CVST} < 1$ and satisfies the conditions L_1 and L_2; otherwise, it is unstable.* ***Condition*** ***L_1:***

$$\frac{dX}{dt} = F(X, 0), \quad X^* \textit{ is globally asymptotically stable.}$$

Condition ***L_2:***

$$G(X, Z) = AZ - \hat{G}(X, Z), \quad \hat{G}(X, Z) \geq 0 \textit{ for } (X, Z) \in \mathbb{R}^9_+.$$

where, $A = D_Z G(X, Z)$ is a Metzler matrix.

Proof. From the system (3.4), $F(X, Z)$ and $G(X, Z)$ are obtained as follows:

$$F(X, Z) = \begin{bmatrix} (1-P)\pi + \sigma R - (\lambda + \mu)S \\ P\pi - \big[(1-\rho)\lambda + \mu\big]V \\ \xi_1 T_E + \xi_2 T_a + \xi_3 T_S - (\sigma + \mu)R \end{bmatrix} \tag{4.29}$$

$$G(X,Z) = \begin{bmatrix} \lambda S + (1-\rho)\lambda V - \left(\frac{\chi_1}{1+mE} + \frac{\chi_2}{1+mE} + \theta_1 + \mu\right) E \\ \frac{\chi_1 E}{1+mE} - (\theta_2 + \omega + \mu) I_a \\ \frac{\chi_2 E}{1+mE} + \omega I_a - (\theta_3 + \delta_1 + \mu) I_S \\ \theta_1 E - (\xi_1 + \mu) T_E \\ \theta_2 I_a - (\xi_2 + \mu) T_a \\ \theta_3 I_S - (\delta_2 + \xi_3 + \mu) T_S \end{bmatrix} \tag{4.30}$$

The first condition L_1, which states that X^* is globally asymptotically stable, is investigated to determine whether it is satisfied. Considering the first, second and ninth equations of system (3.4), when there is no infection (i.e., $\lambda = 0$, $T_E = T_a = T_S = R = 0$), it follows that:

$$\left.\frac{dX}{dt}\right|_{Z=0} = \begin{bmatrix} (1-P)\pi - \mu S \\ P\pi - \mu V \\ 0 \end{bmatrix} \tag{4.31}$$

The first equation of system (4.31) is given by:

$$\frac{dS}{dt} = (1-P)\pi - \mu S \tag{4.32}$$

By separating variables and integrating, equation (4.32) can be written as

$$\int \frac{dS}{(1-P)\pi - \mu S} = \int dt \tag{4.33}$$

This yields:

$$\frac{-1}{\mu} \ln\left((1-P)\pi - \mu S\right) = t + c$$

where c is a constant of integration. Hence,

$$(1-P)\pi - \mu S(t) = Ae^{-\mu t}$$

where A is a constant. Therefore,

$$S(t) = \frac{(1-P)\pi - Ae^{-\mu t}}{\mu}$$

At $t = 0$, $A = (1-P)\pi - \mu S(0)$

Therefore, the solution of equation (4.32) is:

$$S(t) = \frac{(1-P)\pi}{\mu} + \left(S(0) - \frac{(1-P)\pi}{\mu}\right) e^{-\mu t} \tag{4.34}$$

As $t \to \infty$, $S(t) \to \dfrac{(1-P)\pi}{\mu}$. Hence,
$S^* = \frac{(1-P)\pi}{\mu}$ is the limiting (equilibrium) value of $S(t)$ as $t \to \infty$.

Applying the same approach to the second equation of system (4.32) shows that

$V^* = \frac{P\pi}{\mu}$ is the equilibrium value of $V(t)$ as $t \to \infty$.

Therefore, $X^* = \left(\frac{(1-P)\pi}{\mu},\ \frac{P\pi}{\mu},\ 0\right)$ is globally asymptotically stable and satisfies condition L_1.

The second condition L_2 is investigated to determine whether it is satisfied as follows: Let

$$A = \begin{bmatrix} -x_1 & H_5 & H_6 & 0 & H_7 & H_8 \\ \gamma & -x_2 & 0 & 0 & 0 & 0 \\ \alpha & \omega & -x_3 & 0 & 0 & 0 \\ \theta_1 & 0 & 0 & -x_4 & 0 & 0 \\ 0 & \theta_2 & 0 & 0 & -x_5 & 0 \\ 0 & 0 & \theta_3 & 0 & 0 & -x_6 \end{bmatrix} \tag{4.35}$$

where

$$x_1 = (\gamma + \alpha + \theta_1 + \mu), \qquad x_2 = (\theta_2 + \omega + \mu), \qquad x_3 = (\theta_3 + \delta_1 + \mu),$$

$$x_4 = (\xi_1 + \mu), \qquad x_5 = (\xi_2 + \mu), \qquad x_6 = (\delta_2 + \xi_3 + \mu),$$

$$\gamma = \frac{\chi_1}{1+mE}, \qquad \alpha = \frac{\chi_2}{1+mE}, \qquad H_5 = \beta\eta_1\big(S^0 + (1-\rho)V^0\big),$$

$$H_6 = \beta\big(S^0 + (1-\rho)V^0\big), \quad H_7 = \beta\eta_3\big(S^0 + (1-\rho)V^0\big), \quad H_8 = \beta\eta_2\big(S^0 + (1-\rho)V^0\big).$$

The product of A and Z is given as follows:

$$AZ = \begin{bmatrix} -x_1E + \beta\big(S^0 + (1-\rho)V^0\big)\big(\eta_1 I_a + I_S + \eta_3 T_a + \eta_2 T_S\big) \\ \gamma E - x_2 I_a \\ \alpha E + \omega I_a - x_3 I_S \\ \theta_1 E - x_4 T_E \\ \theta_2 I_a - x_5 T_a \\ \theta_3 I_S - x_6 T_S \end{bmatrix} \tag{4.36}$$

$\hat{G}(X,Z) = AZ - G(X,Z)$, which upon computation yields:

$$\hat{G}(X,Z) = \begin{bmatrix} \hat{G}_1(X,Z) \\ \hat{G}_2(X,Z) \\ \hat{G}_3(X,Z) \\ \hat{G}_4(X,Z) \\ \hat{G}_5(X,Z) \\ \hat{G}_6(X,Z) \end{bmatrix} = \begin{bmatrix} \beta(\eta_1 I_a + I_S + \eta_3 T_a + \eta_2 T_S)\big[(S^0 - S) + (V^0 - V)(1-\rho)\big] \\ 0 \\ 0 \\ 0 \\ 0 \\ 0 \end{bmatrix} \tag{4.37}$$

Since both the susceptible and vaccinated populations are bounded by $S \leq S^0$ and $V \leq V^0$, and since $0 \leq \rho \leq 1$, it follows that $\hat{G}_1(X,Z) \geq 0$, $\hat{G}_2(X,Z) = 0$, $\hat{G}_3(X,Z) = 0$, $\hat{G}_4(X,Z) = 0$, $\hat{G}_5(X,Z) = 0$, and $\hat{G}_6(X,Z) = 0$. Thus, $\hat{G}(X,Z) \geq 0$, and condition L_2 is satisfied.

Since both conditions L_1 and L_2 are satisfied, the point $U = (X^*, 0)$ is globally asymptotically stable whenever $R_{CVST} < 1$. Therefore, a disease-free equilibrium exists when $R_{CVST} < 1$. This implies that each infectious case infects, on average, fewer than one susceptible individual during the infectious period, indicating that the disease can be eradicated from the population.

4.2.7 The endemic equilibrium

The steady state at which pulmonary TB persists in the community is referred to as the endemic equilibrium of the system (3.4). At this equilibrium, the rate of change in the pop-

ulation in each class is zero. Hence, the model system (3.4) can be represented as:

$$\begin{cases} 0 = (1-P)\pi + \sigma R^* - (\lambda+\mu)S^*, \\ 0 = P\pi - \big((1-\rho)\lambda+\mu\big)V^*, \\ 0 = \lambda S^* + (1-\rho)\lambda V^* - \left(\frac{\chi_1}{1+mE} + \frac{\chi_2}{1+mE} + \theta_1 + \mu\right)E^*, \\ 0 = \gamma E^* - (\theta_2+\omega+\mu)I_a^*, \\ 0 = \alpha E^* + \omega I_a^* - (\theta_3+\delta_1+\mu)I_S^*, \\ 0 = \theta_1 E^* - (\xi_1+\mu)T_E^*, \\ 0 = \theta_2 I_a^* - (\xi_2+\mu)T_a^*, \\ 0 = \theta_3 I_S^* - (\delta_2+\xi_3+\mu)T_S^*, \\ 0 = \xi_1 T_E^* + \xi_2 T_a^* + \xi_3 T_S^* - (\sigma+\mu)R^*. \end{cases} \tag{4.38}$$

The steady state solution for system (4.38) is:

$B^* = \big(S^*, V^*, E^*, I_a^*, I_S^*, T_E^*, T_a^*, T_S^*, R^*\big)$

Here:

$S^* = \frac{(1-P)\pi+\sigma R^*}{\lambda^{**}+\mu}$,

$V^* = \frac{P\pi}{(1-\rho)\lambda^{**}+\mu}$,

$E^* = \frac{\lambda^{**}\Big[(1-\rho)\lambda^{**}+\mu\Big]\Big[(1-P)\pi+\sigma R^*\Big]+(\lambda^{**}+\mu)(1-\rho)P\pi\lambda^{**}}{(\lambda^{**}+\mu)(\gamma+\alpha+\theta_1+\mu)\Big((1-\rho)\lambda^{**}+\mu\Big)}$,

$I_a^* = \frac{\gamma\lambda^{**}\Big[(1-\rho)\lambda^{**}+\mu\Big]\Big[(1-P)\pi+\sigma R^*\Big]+\gamma(\lambda^{**}+\mu)(1-\rho)P\pi\lambda^{**}}{(\lambda^{**}+\mu)(\gamma+\alpha+\theta_1+\mu)\Big((1-\rho)\lambda^{**}+\mu\Big)(\theta_2+\omega+\mu)}$,

$I_s^* = \frac{\lambda^{**}\Big(\Big[(1-\rho)\lambda^{**}+\mu\Big]\Big[(1-P)\pi+\sigma R^*\Big]+(\lambda^{**}+\mu)(1-\rho)P\pi\Big)\Big[\alpha(\theta_2+\omega+\mu)+\omega\gamma\Big]}{(\theta_3+\delta_1+\mu)(\lambda^{**}+\mu)(\gamma+\alpha+\theta_1+\mu)\Big((1-\rho)\lambda^{**}+\mu\Big)(\theta_2+\omega+\mu)}$,

$T_E^* = \frac{\theta_1\lambda^{**}\Big(\Big[(1-\rho)\lambda^{**}+\mu\Big]\Big[(1-P)\pi+\sigma R^*\Big]+(\lambda^{**}+\mu)(1-\rho)P\pi\lambda^{**}\Big)}{(\xi_1+\mu)(\lambda^{**}+\mu)(\gamma+\alpha+\theta_1+\mu)\Big((1-\rho)\lambda^{**}+\mu\Big)}$,

$T_a^* = \frac{\theta_2\gamma\lambda^{**}\Big(\Big[(1-\rho)\lambda^{**}+\mu\Big]\Big[(1-P)\pi+\sigma R^*\Big]+(\lambda^{**}+\mu)(1-\rho)P\pi\lambda^{**}\Big)}{(\xi_2+\mu)(\lambda^{**}+\mu)(\gamma+\alpha+\theta_1+\mu)\Big((1-\rho)\lambda^{**}+\mu\Big)(\theta_2+\omega+\mu)}$,

$$T_s^* = \frac{\theta_3\lambda^{**}\Big(\Big[(1-\rho)\lambda^{**}+\mu\Big]\Big[(1-P)\pi+\sigma R^*\Big]+(\lambda^{**}+\mu)(1-\rho)P\pi\Big)\Big(\alpha(\theta_2+\omega+\mu)+\omega\gamma\Big)}{(\delta_2+\xi_3+\mu)(\theta_3+\delta_1+\mu)(\lambda^{**}+\mu)(\gamma+\alpha+\theta_1+\mu)\Big((1-\rho)\lambda^{**}+\mu\Big)(\theta_2+\omega+\mu)},$$

$$R^* = \frac{\lambda^{**}\Big(\Big[(1-\rho)\lambda^{**}+\mu\Big]S^*+(\lambda^{**}+\mu)(1-\rho)P\pi\lambda^{**}\Big)\Big(D_1+D_2+D_3\Big)}{\Big((1-\rho)\lambda^{**}+\mu\Big)(\alpha+\gamma+\theta_1+\mu)(\theta_2+\omega+\mu)(\theta_3+\delta_1+\mu)A_1A_2A_3A_4},$$

where:

$D_1 = \theta_1(\theta_3+\delta_1+\mu)(\theta_2+\omega+\mu)(\delta_2+\xi_3+\mu)(\xi_2+\mu),$

$D_2 = \theta_2\gamma(\theta_3+\delta_1+\mu)(\delta_2+\xi_3+\mu)(\xi_1+\mu),$

$D_3 = \theta_3\big[\alpha(\theta_2+\omega+\mu)+\omega\gamma\big](\xi_1+\mu)(\xi_2+\mu),$

$A_1 = (\xi_1+\mu),\ A_2 = (\xi_2+\mu),\ A_3 = (\delta_2+\xi_3+\mu),$

$A_4 = (\sigma+\mu),\ \gamma = \frac{\chi_1}{1+mE},\ \alpha = \frac{\chi_2}{1+mE}.$

4.2.8 Local stability of endemic equilibrium

The local stability of an endemic equilibrium in a mathematical model refers to the behavior of the system in the vicinity of this equilibrium. Specifically, it involves determining whether small perturbations or deviations from the equilibrium decay over time, indicating stability, or grow, indicating instability. The following theorem establishes the local stability of the endemic equilibrium point:

Theorem 4.5. *A positive endemic equilibrium exists and is locally asymptotically stable whenever* $R^*_{CVST} > 1$.

Proof. For the disease to be endemic, the following conditions must hold:

$$\begin{cases} \dfrac{dE}{dt} = \lambda S + (1-\rho)\lambda V - \left(\dfrac{\chi_1}{1+mE} + \dfrac{\chi_2}{1+mE} + \theta_1 + \mu\right)E\ > 0, \\ \dfrac{dI_a}{dt} = \dfrac{\chi_1 E}{1+mE} - (\theta_2+\omega+\mu)I_a\ > 0, \\ \dfrac{dI_S}{dt} = \dfrac{\chi_2 E}{1+mE} + \omega I_a - (\theta_3+\delta_1+\mu)I_S\ > 0, \\ \dfrac{dT_E}{dt} = \theta_1 E - (\xi_1+\mu)T_E\ > 0, \\ \dfrac{dT_a}{dt} = \theta_2 I_a - (\xi_2+\mu)T_a\ > 0, \\ \dfrac{dT_S}{dt} = \theta_3 I_S - (\delta_2+\xi_3+\mu)T_S\ > 0. \end{cases} \tag{4.39}$$

By letting the natural immunity parameter $m \to 0$ at the endemic equilibrium, the first inequality in system (4.39) reduces to

$$(\chi_1 + \chi_2 + \theta_1 + \mu)E \ < \ \lambda S + (1-\rho)\lambda V. \tag{4.40}$$

Hence, we obtain

$$E \ < \ \frac{\lambda S + (1-\rho)\lambda V}{\chi_1 + \chi_2 + \theta_1 + \mu} \tag{4.41}$$

Substituting equation (3.2) into inequality (4.41) yields:

$$E \ < \ \frac{\beta\big(I_S + \eta_1 I_a + \eta_2 T_S + \eta_3 T_a\big)S + (1-\rho)\beta\big(I_S + \eta_1 I_a + \eta_2 T_S + \eta_3 T_a\big)V}{\chi_1 + \chi_2 + \theta_1 + \mu} \tag{4.42}$$

Inequality (4.42) simplifies to:

$$E \ < \ \frac{\beta\big(I_S + \eta_1 I_a + \eta_2 T_S + \eta_3 T_a\big)\left[S + (1-\rho)V\right]}{\chi_1 + \chi_2 + \theta_1 + \mu} \tag{4.43}$$

From the steady state system (4.38), I_a^*, I_S^*, T_a^* and T_S^* are respectively given as:

$$I_a^* = \frac{\gamma E^*}{\theta_2 + \omega + \mu}, \tag{4.44}$$

$$I_S^* = \frac{\alpha E^* + \omega I_a^*}{\theta_3 + \delta_1 + \mu}, \tag{4.45}$$

$$T_a^* = \frac{\theta_2 I_a^*}{\xi_2 + \mu}, \tag{4.46}$$

$$T_S^* = \frac{\theta_3 I_S^*}{\xi_3 + \delta_2 + \mu}. \tag{4.47}$$

Substituting equations (4.44), (4.45), (4.46), and (4.47) into inequality (4.43) gives:

$$E^* < \frac{\beta\left[\dfrac{\chi_2 E^* + \omega I_a^*}{\theta_3 + \delta_1 + \mu} + \dfrac{\eta_1\chi_1 E^*}{\theta_2 + \omega + \mu} + \dfrac{\eta_2\theta_3 I_S^*}{\delta_2 + \xi_3 + \mu} + \dfrac{\eta_3\theta_2 I_a^*}{\xi_2 + \mu}\right]\big(S + (1-\rho)V\big)}{\chi_1 + \chi_2 + \theta_1 + \mu} \tag{4.48}$$

Inequality (4.48) is simplified to obtain:

$$E^* < \frac{\beta\Big[(\eta_1\chi_1 x_3 + \chi_1\omega + \chi_2 x_2)x_5 x_6 + \eta_3\theta_2\chi_1 x_3 x_6 + \eta_2\theta_3 x_5(\chi_1\omega + \chi_2 x_2)\Big]\left(\dfrac{(1-P)\pi}{\mu} + \dfrac{(1-\rho)P\pi}{\mu}\right)E^*}{x_1 x_2 x_3 x_5 x_6} \tag{4.49}$$

After further simplification, inequality (4.49) is written as:

$$1 < \frac{\beta\Big[(\eta_1\chi_1 x_3 + \chi_1\omega + \chi_2 x_2)x_5x_6 + \eta_3\theta_2\chi_1 x_3 x_6 + \eta_2\theta_3 x_5(\chi_1\omega + \chi_2 x_2)\Big]\left(\frac{(1-P)\pi}{\mu} + \frac{(1-\rho)P\pi}{\mu}\right)}{x_1x_2x_3x_5x_6} \tag{4.50}$$

However,

$$\frac{\beta\Big[(\eta_1\chi_1 x_3+\chi_1\omega+\chi_2 x_2)x_5x_6+\eta_3\theta_2\chi_1 x_3 x_6+\eta_2\theta_3 x_5(\chi_1\omega+\chi_2 x_2)\Big]\left(\frac{(1-P)\pi}{\mu}+\frac{(1-\rho)P\pi}{\mu}\right)}{x_1x_2x_3x_5x_6} = R_{CVST}$$

Therefore, inequality (4.50) can be expressed as:

$$1 < R_{CVST} \quad \Longleftrightarrow \quad R_{CVST} > 1 \tag{4.51}$$

Thus, when the reproduction number $R_{CVST} > 1$, the system reaches an endemic equilibrium. This equilibrium occurs when the number of new infections generated by an infected individual exceeds one, leading to the sustained spread of the disease within the population.

4.2.9 Global stability of endemic equilibrium

The global stability of an endemic equilibrium in epidemiological modeling implies that the disease will persist at a constant level over time from any starting point within the population, provided the initial conditions lie within a realistic and meaningful range. This concept is crucial for understanding the long-term outcomes of disease spread and for developing effective public health strategies.

Global stability is demonstrated by constructing a Lyapunov function, which shows that, regardless of the system's initial state, the solutions converge to the endemic equilibrium. A Lyapunov function $V(x)$ is a scalar function that maps the state of the system $x(t)$ to a real number and satisfies the following conditions:

(i) $V(x) > 0 \quad$ for all $x \neq x^*$,

(ii) $V(x^*) = 0$,

(iii) $\dfrac{dV}{dt} \leq 0$,

where x^* is the equilibrium point.

A negative derivative of the Lyapunov function with respect to time indicates that the endemic equilibrium attracts all trajectories in the invariant set, thereby proving that the endemic equilibrium is globally asymptotically stable within that set.

The following theorem illustrates the global stability of the endemic equilibrium:

Theorem 4.6. *If $R_{CVST} > 1$, the endemic equilibrium B^* of the system* (3.4) *is globally asymptotically stable.*

Proof. The method of Lyapunov functions was used to prove the global asymptotic stability of the endemic equilibrium. A Lyapunov function was proposed and defined as follows:

$$\begin{aligned} L = &(S - S^* + S^* \ln \tfrac{S^*}{S}) + (V - V^* + V^* \ln \tfrac{V^*}{V}) + (E - E^* + E^* \ln \tfrac{E^*}{E}) \\ &+ (I_S - I_S^* + I_S^* \ln \tfrac{I_S^*}{I_S}) + (T_E - T_E^* + T_E^* \ln \tfrac{T_E^*}{T_E}) \\ &+ (T_a - T_a^* + T_a^* \ln \tfrac{T_a^*}{T_a}) + (T_S - T_S^* + T_S^* \ln \tfrac{T_S^*}{T_S}) + (R - R^* + R^* \ln \tfrac{R^*}{R}) \end{aligned} \tag{4.52}$$

where,

$S^*, V^*, E^*, I_a^*, I_S^*, T_E^*, T_a^*, T_S^*, R^*$ are constants.

The derivative of equation (4.52) with respect to time was determined as follows:

$$\begin{aligned} \frac{dL}{dt} = &\frac{S - S^*}{S}\frac{dS}{dt} + \frac{V - V^*}{V}\frac{dV}{dt} + \frac{E - E^*}{E}\frac{dE}{dt} + \frac{I_a - I_a^*}{I_a}\frac{dI_a}{dt} + \frac{I_S - I_S^*}{I_S}\frac{dI_S}{dt} \\ &+ \frac{T_E - T_E^*}{T_E}\frac{dT_E}{dt} + \frac{T_a - T_a^*}{T_a}\frac{dT_a}{dt} + \frac{T_S - T_S^*}{T_S}\frac{dT_S}{dt} + \frac{R - R^*}{R}\frac{dR}{dt} \end{aligned} \tag{4.53}$$

Substituting system (3.4) equation (4.53) yields:

$$\frac{dL}{dt} = K - Y \tag{4.54}$$

where:

$$K = \pi + \sigma R + \frac{\sigma R^* S^*}{S} + \frac{\lambda S^* E^*}{E} + (1-\rho)\lambda V + \frac{(1-\rho)\lambda V^* E^*}{E} + \gamma E + \frac{\gamma I_a^* E^*}{I_a} + \alpha E + \frac{\alpha I_S^* E^*}{I_S} + \omega I_a + \frac{\omega I_S^* I_a^*}{I_S} + \theta_1 E + \frac{\theta_1 T_E^* E^*}{T_E} + \theta_2 I_a + \frac{\theta_2 I_a^* T_a^*}{T_a} + \theta_3 T_S + \frac{\theta_3 I_S^* T_S^*}{T_S} + \xi_1 T_E + \frac{\xi_1 T_E^* R^*}{R} + \xi_2 T_a + \frac{\xi_2 T_a^* R^*}{R} + \xi_3 T_S + \frac{\xi_3 T_S^* R^*}{R} + \frac{\pi P V^*}{V} + \lambda S$$

$$Y = \frac{\pi S^*}{S} + \frac{\pi P S^*}{S} + \frac{\sigma R S^*}{S} + \frac{\lambda S E^*}{E} + (1-\rho)\lambda V^* + \frac{(1-\rho)\lambda E^*}{E^*} + \gamma E^* + \frac{\gamma E I_a^*}{I_a} + \alpha E^* + \alpha E I_S^* + \omega I_a^* + \frac{\omega I_a I_S^*}{I_S} + \theta_1 E^* + \frac{\theta_1 E T_E^*}{T_E} + \theta_2 I_a^* + \frac{\theta_2 I_a T_a^*}{T_a} + \theta_3 I_S^* + \frac{\theta_3 I_S T_S^*}{T_S} + \xi_1 T_E^* + \frac{\xi_1 T_E R^*}{R} + \xi_2 T_a^* + \frac{\xi_2 T_a R^*}{R} + \xi_3 T_S^* + \frac{\xi_2 T_S R^*}{R} + \lambda S^* + \frac{(S-S^*)^2}{S}[\lambda + \mu] + \frac{(V-V^*)^2}{V}[(1-\rho)\lambda + \mu] + \frac{(E-E^*)^2}{E}[\gamma + \alpha + \theta_1 + \mu] + \frac{(I_a - I_a^*)^2}{I_a}[\theta_2 + \omega + \mu] + \frac{(I_S - I_S^*)^2}{I_S}[\theta_3 + \delta_1 + \mu] + \frac{(T_E - T_E^*)^2}{T_E}[\xi_1 + \mu] + \frac{(T_a - T_a^*)^2}{T_a}[\xi_2 + \mu] + \frac{(T_S - T_S^*)^2}{T_S}[\delta_2 + \xi_3 + \mu] + \frac{(R-R^*)^2}{R}[\sigma + \mu]$$

If $K \leq Y$, then $\frac{dL}{dt} \leq 0$, and $\frac{dL}{dt} = 0$ if and only if:

$S = S^*, \quad V = V^*, \quad E = E^*, \quad I_a = I_a^*, \quad I_S = I_S^*, \quad T_E = T_E^*, \quad T_a = T_a^*,$

$T_S = T_S^*, \quad R = R^*.$

Therefore, the largest compact invariant set in:

$(S^*, V^*, E^*, I_a^*, I_S^*, T_E^*, T_a^*, T_S^*, R^*) \in \Omega : \frac{dL}{dt} = 0\}$ is the singleton endemic equilibrium point B^*. Thus, from LaSalle's invariance principle (La Salle, 1976), it is concluded that as $t \to \infty$, the solution of the model system (3.4) approaches the endemic equilibrium B^* when the control reproduction number $R^*_{CVST} > 1$. Therefore, the endemic equilibrium point B^* is globally asymptotically stable in the invariant set Ω if $K < Y$.

The global stability is crucial for designing and evaluating intervention strategies. For instance, if an intervention can alter the system's parameters such that a disease-free equilibrium becomes globally stable instead of an endemic equilibrium, it would imply that the disease could be eradicated.

4.2.10 Bifurcation analysis of the model

Bifurcation analysis in epidemiological modeling refers to the study of qualitative changes in the behavior of a system as key parameters are varied. Backward bifurcation occurs when a stable disease-free equilibrium coexists with a stable endemic equilibrium. In such cases, reproduction numbers being less than one remain a necessary but not sufficient condition for disease eradication. The possibility of bifurcation is explored using Centre Manifold theory Castillo-Chavez and Song (2004). The analysis of the model's bifurcation considers two quantities: the coefficients a and b of the normal form representing the dynamics of the system on the center manifold. Then, if $a < 0$ and $b > 0$, the bifurcation is forward. Conversely, if $a > 0$ and $b > 0$, the bifurcation is backward. The coefficients a and b are defined by the Castillo–Chavez theorem as follows:

$$\begin{cases} a = \sum_{k,j,i=1}^{n} v_k w_i w_j \frac{\partial^2 f_k}{\partial y_i \, \partial y_j}, \\ b = \sum_{k,i=1}^{n} v_k w_i \frac{\partial^2 f_k}{\partial y_i \, \partial \beta}. \end{cases} \tag{4.55}$$

Here, w is a right eigenvector of the Jacobian $J(B^*)$ for the system (3.14) at the disease-free equilibrium, associated with the zero eigenvalue, while v is a left eigenvector of the Jacobian $J(B^*)$ associated with the same zero eigenvalue, and β is the bifurcation parameter. The derivation of y_i and f_k follows.

To determine the bifurcation of the model system (3.4), the variables are transformed as follows:

$S = y_1, V = y_2, E = y_3, I_a = y_4, I_S = y_5, T_E = y_6, T_a = y_7, T_S = y_8, R = y_9.$

Vector notation is introduced to represent multiple variables simultaneously as follows:

$y = (y_1, y_2, y_3, y_4, y_5, y_6, y_7, y_8, y_9)^T$

The system of equations (3.4) can then be expressed as:

$\frac{dy}{dt} = F(y)$, where: $F = (f_1, f_2, f_3, f_4, f_5, f_6, f_7, f_8, f_9)^T$

It follows that:

$$
\begin{cases}
\frac{dy_1}{dt} = f_1 = (1-P)\pi + \sigma y_9 - (\lambda+\mu)y_1, \\
\frac{dy_2}{dt} = f_2 = P\pi - \big((1-\rho)\lambda + \mu\big)y_2, \\
\frac{dy_3}{dt} = f_3 = \lambda y_1 + (1-\rho)\lambda y_2 - \Big(\frac{\chi_1}{1+my_3} + \frac{\chi_2}{1+my_3} + \theta_1 + \mu\Big)y_3, \\
\frac{dy_4}{dt} = f_4 = \frac{\chi_1 y_3}{1+my_3} - (\theta_2 + \omega + \mu)y_4, \\
\frac{dy_5}{dt} = f_5 = \frac{\chi_2 y_3}{1+my_3} + \omega y_4 - (\theta_3 + \delta_1 + \mu)y_5, \\
\frac{dy_6}{dt} = f_6 = \theta_1 y_3 - (\xi_1 + \mu)y_6, \\
\frac{dy_7}{dt} = f_7 = \theta_2 y_4 - (\xi_2 + \mu)y_7, \\
\frac{dy_8}{dt} = f_8 = \theta_3 y_5 - (\delta_2 + \xi_3 + \mu)y_8, \\
\frac{dy_9}{dt} = f_9 = \xi_1 y_6 + \xi_2 y_7 + \xi_3 y_8 - (\delta + \mu)y_9.
\end{cases} \tag{4.56}
$$

here, $\lambda = \beta(y_5 + \eta_1 y_4 + \eta_2 y_8 + \eta_3 y_7)$

where: $N = y_1 + y_2 + y_3 + y_4 + y_5 + y_6 + y_7 + y_8 + y_9$

The Jacobian of the system (4.56) at the disease-free equilibrium point, denoted by $J(B^*)$, is given as follows:

$$
J(B^0) = \begin{bmatrix}
-\mu & 0 & 0 & -\beta\eta_1 S^0 & -\beta S^0 & 0 & -\beta\eta_3 S^0 & -\beta\eta_2 S^0 & \sigma \\
0 & -\mu & 0 & -H_1 & -H_2 & 0 & -H_3 & -H_4 & 0 \\
0 & 0 & -x_1 & H_5 & H_6 & 0 & H_7 & H_8 & 0 \\
0 & 0 & \chi_1 & -x_2 & 0 & 0 & 0 & 0 & 0 \\
0 & 0 & \chi_2 & \omega & -x_3 & 0 & 0 & 0 & 0 \\
0 & 0 & \theta_1 & 0 & 0 & -x_4 & 0 & 0 & 0 \\
0 & 0 & 0 & \theta_2 & 0 & 0 & -x_5 & 0 & 0 \\
0 & 0 & 0 & 0 & \theta_3 & 0 & 0 & -x_6 & 0 \\
0 & 0 & 0 & 0 & 0 & \xi_1 & \xi_2 & \xi_3 & -x_7
\end{bmatrix} \tag{4.57}
$$

The control reproduction number was considered to be equal to one, i.e $R^*_{CVST} = 1$ and $\beta = \beta^*$ was chosen as a bifurcation parameter. Then, the value of β^* was determined when $R^*_{CVST} = 1$ from:

$$1 = \beta \frac{\left((\eta_1\chi_1 x_3 + \chi_1\omega + \chi_2 x_2)x_5x_6 + \eta_3\theta_2\chi_1 x_3x_6 + \eta_2\theta_3 x_5(\chi_1\omega + \chi_2 x_2)\right)\left[\frac{(1-P)\pi}{\mu} + \frac{(1-\rho)P\pi}{\mu}\right]}{x_1x_2x_3x_5x_6}$$

which yields:

$$\beta^* = \frac{x_1x_2x_3x_5x_6}{\left[(\eta_1\chi_1 x_3 + \chi_1\omega + \chi_2 x_2)x_5x_6 + \eta_3\theta_2\chi_1 x_3x_6 + \eta_2\theta_3 x_5(\chi_1\omega + \chi_2 x_2)\right]\left[\frac{(1-P)\pi}{\mu} + \frac{(1-\rho)P\pi}{\mu}\right]}$$

Using Mathematica software, it was determined that the Jacobian of $\frac{dy}{dt} = F(y)$ at the disease-free equilibrium point with $\beta = \beta^*$ has one of the eigenvalues equal to zero. Hence, the Center Manifold theory is applied to analyze the dynamics of the system near $\beta = \beta^*$. The Jacobian $[J(B^0)]$ near $\beta = \beta^*$ has a right eigenvector associated with the zero eigenvalue, denoted by:

$w = (w_1, w_2, w_3, w_4, w_5, w_6, w_7, w_8, w_9)^T$,

which satisfies the system:

$$\begin{bmatrix} -\mu & 0 & 0 & -\beta\eta_1 S^0 & -\beta S^0 & 0 & -\beta\eta_3 S^0 & -\beta\eta_2 S^0 & \sigma \\ 0 & -\mu & 0 & -H_1 & -H_2 & 0 & -H_3 & -H_4 & 0 \\ 0 & 0 & -x_1 & H_5 & H_6 & 0 & H_7 & H_8 & 0 \\ 0 & 0 & \chi_1 & -x_2 & 0 & 0 & 0 & 0 & 0 \\ 0 & 0 & \chi_2 & \omega & -x_3 & 0 & 0 & 0 & 0 \\ 0 & 0 & \theta_1 & 0 & 0 & -x_4 & 0 & 0 & 0 \\ 0 & 0 & 0 & \theta_2 & 0 & 0 & -x_5 & 0 & 0 \\ 0 & 0 & 0 & 0 & \theta_3 & 0 & 0 & -x_6 & 0 \\ 0 & 0 & 0 & 0 & 0 & \xi_1 & \xi_2 & \xi_3 & -x_7 \end{bmatrix} \begin{bmatrix} w_1 \\ w_2 \\ w_3 \\ w_4 \\ w_5 \\ w_6 \\ w_7 \\ w_8 \\ w_9 \end{bmatrix} = \begin{bmatrix} 0 \\ 0 \\ 0 \\ 0 \\ 0 \\ 0 \\ 0 \\ 0 \\ 0 \end{bmatrix} \quad (4.58)$$

From this system, the following equations are obtained:

$$\begin{cases} -\mu w_1 - \beta\eta_1 S^0 w_4 - \beta S^0 w_5 - \beta\eta_3 S^0 w_7 - \beta\eta_2 S^0 w_8 + \sigma w_9 = 0, \\ -\mu w_2 - H_1 w_4 - H_2 w_5 - H_3 w_7 - H_4 w_8 = 0, \\ -x_1 w_3 + H_5 w_4 + H_6 w_5 + H_7 w_7 + H_8 w_8 = 0, \\ \chi_1 w_3 - x_2 w_4 = 0, \\ \chi_2 w_3 + \omega w_4 - x_3 w_5 = 0, \\ \theta_1 w_3 - x_4 w_6 = 0, \\ \theta_2 w_4 - x_5 w_7 = 0, \\ \theta_3 w_5 - x_6 w_8 = 0, \\ \xi_1 w_6 + \xi_2 w_7 + \xi_3 w_8 - x_7 w_9 = 0. \end{cases} \tag{4.59}$$

Solving the system of equations, yields:

$$w_1 = \frac{-(\beta\eta_1 S^0 w_4 + \beta S^0 w_5 + \beta\eta_3 S^0 w_7 + \beta\eta_2 S^0 w_8) + \sigma w_9}{\mu} < 0, w_2 = w_2 > 0,$$

$$w_4 = \frac{\chi_1 w_3}{x_2} > 0, \quad w_5 = \frac{\chi_2 w_3 + \omega w_4}{x_3} > 0, w_6 = \frac{\theta_1 w_3}{x_4} > 0, \quad w_7 = \frac{\theta_2 w_4}{x_5} > 0,$$

$$w_8 = \frac{\theta_3 w_5}{x_6} > 0, \quad w_9 = \frac{\xi_1 w_6 + \xi_2 w_7 + \xi_3 w_8}{x_7} > 0.$$

Furthermore, the Jacobian $[J(B^0)]$ of the model near $\beta = \beta^*$ has a left eigenvector associated with the zero eigenvalue, given by:

$v = (v_1, v_2, v_3, v_4, v_5, v_6, v_7, v_8, v_9)^T$,

which satisfies the system,

$$J(B^0) = \begin{bmatrix} -\mu & 0 & 0 & 0 & 0 & 0 & 0 & 0 & 0 \\ 0 & -\mu & 0 & 0 & 0 & 0 & 0 & 0 & 0 \\ 0 & 0 & -x_1 & \chi_1 & \chi_2 & \theta_1 & 0 & 0 & 0 \\ -\beta\eta_1 S^0 & -H_1 & H_5 & -x_2 & \omega & 0 & \theta_2 & 0 & 0 \\ -\beta S^0 & -H_2 & H_6 & 0 & -x_3 & 0 & 0 & \theta_3 & 0 \\ 0 & 0 & 0 & 0 & 0 & -x_4 & 0 & 0 & \xi_1 \\ -\beta\eta_3 S^0 & -H_3 & H_7 & 0 & 0 & 0 & -x_5 & 0 & \xi_2 \\ -\beta\eta_2 S^0 & -H_4 & H_8 & 0 & 0 & 0 & 0 & -x_6 & \xi_3 \\ \sigma & 0 & 0 & 0 & 0 & 0 & 0 & 0 & -x_7 \end{bmatrix} \begin{bmatrix} v_1 \\ v_2 \\ v_3 \\ v_4 \\ v_5 \\ v_6 \\ v_7 \\ v_8 \\ v_9 \end{bmatrix} = \begin{bmatrix} 0 \\ 0 \\ 0 \\ 0 \\ 0 \\ 0 \\ 0 \\ 0 \\ 0 \end{bmatrix} \tag{4.60}$$

From system (4.60), the following system of equations is obtained:

$$\begin{cases} -\mu v_1 = 0, \\ -\mu v_2 = 0, \\ -x_1 v_3 + \chi_1 v_4 + \chi_2 v_5 + \theta_1 v_6 = 0, \\ -\beta\eta_1 S^0 v_1 - H_1 v_2 + H_5 v_3 - x_2 v_4 + \omega v_5 + \theta_2 v_7 = 0, \\ -\beta S^0 v_1 - H_2 v_2 + H_6 v_3 - x_3 v_5 + \theta_3 v_8 = 0, \\ -x_4 v_6 + \xi_1 v_9 = 0, \\ -\beta\eta_3 S^0 v_1 - H_3 v_2 + H_7 v_3 - x_5 v_7 + \xi_2 v_9 = 0, \\ -\beta\eta_2 S^0 v_1 - H_4 v_2 + H_8 v_3 - x_6 v_8 + \xi_3 v_9 = 0, \\ \sigma v_1 - x_7 v_9 = 0. \end{cases} \tag{4.61}$$

Solving system of equation (4.61) yields:

$v_1 = 0, v_2 = 0, v_3 = v_3 > 0, v_4 = \frac{H_5 v_3 + \omega v_5 + \theta_2 v_7}{x_2} > 0, v_5 = \frac{H_6 v_3 + \theta_3 v_8}{x_3} > 0, v_6 = 0,$

$v_7 = \frac{H_7 v_3}{x_5} > 0, v_8 = \frac{H_8 v_3}{x_6} > 0, v_9 = 0.$

Equations (4.55) are then used to compute a and b. To compute a , $\frac{\partial^2 f_k}{\partial y_i \partial y_j}$ was determined as follows:

$\frac{\partial^2 f_3}{\partial y_1 \partial y_4} = \frac{\partial^2 f_3}{\partial y_4 \partial y_1} = \beta\eta_1$, $\frac{\partial^2 f_3}{\partial y_1 \partial y_5} = \frac{\partial^2 f_3}{\partial y_5 \partial y_1} = \beta$, $\frac{\partial^2 f_3}{\partial y_1 \partial y_7} = \frac{\partial^2 f_3}{\partial y_7 \partial y_1} = \beta\eta_3$, and
$\frac{\partial^2 f_3}{\partial y_1 \partial y_8} = \frac{\partial^2 f_3}{\partial y_8 \partial y_1} = \beta\eta_2$.

Thus,

$a = 2v_3 w_1 \beta w_4 \eta_1 + w_5 + w_7\eta_3 + w_8\eta_2 < 0$

To compute b, $\frac{\partial^2 f_k}{\partial y_i \partial \beta}$ was determined as follows:

$\frac{\partial^2 f_3}{\partial y_1 \partial \beta} = y_5 + \eta_1 y_4 + \eta_2 y_8 + \eta_3 y_7$, $\frac{\partial^2 f_3}{\partial y_2 \partial \beta} = (1-\rho)(y_5 + \eta_1 y_4 + \eta_2 y_8 + \eta_3 y_7)$,
$\frac{\partial^2 f_3}{\partial y_4 \partial \beta} = \eta_1(y_1 + (1-\rho)y_2)$, $\frac{\partial^2 f_3}{\partial y_5 \partial \beta} = y_1 + (1-\rho)y_2$, $\frac{\partial^2 f_3}{\partial y_7 \partial \beta} = \eta_3(y_1 + (1-\rho)y_2)$, and
$\frac{\partial^2 f_3}{\partial y_8 \partial \beta} = \eta_2(y_1 + (1-\rho)y_2)$.

Thus,

$b = v_3\big[w_1(y_5 + \eta_1 y_4 + \eta_2 y_8 + \eta_3 y_7) + w_2(1-\rho)(y_5 + \eta_1 y_4 + \eta_2 y_8 + \eta_3 y_7) + w_4\eta_1(y_1 + (1-\rho)y_2) + w_5(y_1 + (1-\rho)y_2) + w_7\eta_3(y_1 + (1-\rho)y_2) + w_8\eta_2(y_1 + (1-\rho)y_2)\big] > 0$

Since $a < 0$ and $b > 0$, the model system (3.4) has no backward bifurcation at $R^*_{CVST} = 1$. The absence of backward bifurcation implies that it is possible to eradicate pulmonary TB whenever an index case of an infectious individual infects, on average, less than one person during the infectious period.

4.2.11 Sensitivity analysis on control reproduction numbers

In this section, a sensitivity analysis of the reproduction numbers is presented to determine the relative importance of various parameters responsible for the transmission and prevalence of pulmonary TB in the population. The normalized forward sensitivity index was employed to perform the sensitivity analysis, as used by Makinde and Okosun (2023). The normalized sensitivity index, which measures the relative change in a parameter, say k, with respect to the reproduction number R_C, is given by:

$$\Upsilon_k^{R_C} = \frac{\partial R_C}{\partial k} \cdot \frac{k}{R_C} \tag{4.62}$$

Mathematica software was used to compute expressions for the sensitivity analysis of the control reproduction number relative to selected model parameters, employing equation (4.62). The results are given as follows:

$\Upsilon_\beta^{R_{CVST}} = 1$

$\Upsilon_{\theta_1}^{R_{CVST}} = -\frac{\theta_1}{\mu+\theta_1+\chi_1+\chi_2}$

$\Upsilon_{\chi_1}^{R_{CVST}} = \frac{\chi_1\left[\eta_3 x_6\chi_2(\theta_2(\mu+\delta_1)-x_5(\mu+\theta_2)+\eta_1 x_3 x_5)-\theta_3\chi_2(\eta_2 x_5-\eta_3 x_6\theta_2)+(\mu+\theta_1)(x_3 x_6(x_5+\eta_3\theta_2)+\omega x_5(x_6+\eta_2\theta_3))\right]}{x_1\left[x_2 x_5\chi_2(x_6+\eta_2\theta_3)+\chi_1(x_3 x_6(\eta_1 x_5+\eta_3\theta_2)+\omega x_5(x_6+\eta_2\theta_3))\right]}$

$\Upsilon_{\chi_2}^{R_{CVST}} = \frac{\chi_2\left[\eta_2\theta_3\chi_1 x_5(\mu+\theta_2)-x_3 x_6\chi_1(\eta_1 x_5+\eta_3\theta_2)+\eta_2\theta_3 x_2 x_5(\theta_1+\mu)+x_5 x_6\left((\mu+\chi_1+\chi_2)(\mu+\theta_2)-\omega(\mu+\theta_1)\right)\right]}{x_1\left[x_2 x_5\chi_2(x_6+\eta_2\theta_3)+x_6 x_3\chi_1(\eta_1 x_5+\eta_3\theta_2)+x_5\chi_1\omega(x_6+\eta_2\theta_3)\right]}$

$\Upsilon_{\theta_2}^{R_{CST}} = \frac{\theta_2\left[\eta_3 x_2 x_3 x_6\chi_1+x_2 x_5\chi_2(x_6+\eta_2\theta_3)-\eta_3 x_3 x_6\theta_2\chi_1-\eta_2 x_5\theta_3(\omega\chi_1+\chi_2 x_2)-x_5 x_6\left(x_2\chi_2+\chi_1(\eta_1 x_3+\omega)\right)\right]}{x_2\left[x_2 x_5\chi_2(x_6+\eta_2\theta_3)+\chi_1\left(x_3 x_6(\eta_1 x_5+\eta_3\theta_2)\right)+x_5\omega(x_6+\eta_2\theta_3)\right]}$

$\Upsilon_{\theta_3}^{R_{cVST}} = -\frac{x_5\theta_3(\chi_2\omega+\chi_2 x_2)[x_6-\eta_2(\mu+\delta_1)]}{x_3\left[x_2 x_5\chi_2(x_6+\eta_2\theta_3)+\chi_1\left(x_3 x_6(\eta_1 x_5+\eta_3\theta_2)+h_5\omega(x_6+\eta_2\theta_3)\right)\right]}$

$\Upsilon_\rho^{R_{CVST}} = 1 + \frac{1}{-1+\rho P}$

where:

$x_1 = (\chi_1 + \chi_2 + \theta_1 + \mu), \quad x_2 = (\theta_2 + \omega + \mu), \quad x_3 = (\theta_3 + \delta_1 + \mu), \quad x_5 = (\xi_2 + \mu),$
$x_6 = (\delta_2 + \xi_3 + \mu).$

Expressions for the sensitivity analysis of the other reproduction numbers R_{CST}, R_{CVT_S}, and, R_{CT_S} can also be determined using a similar approach.

The parameter values in Table 4.1 were used to calculate the sensitivity indices of the reproduction numbers for the parameters $\beta, \rho, \chi_1, \chi_2, \theta_1, \theta_2$ and θ_3 using equation (4.62) implemented in Mathematica software. The calculated sensitivity indices of the reproduction numbers are presented in Table 4.2. A positive sensitivity index indicates that the reproduction number is an increasing function of the corresponding parameter, whereas a negative sensitivity index indicates that the reproduction number is a decreasing function of the corresponding parameter. Thus, increasing a parameter with a positive sensitivity index, while holding other parameters constant, increases the reproduction number, whereas increasing a parameter with a negative sensitivity index, while other factors are held constant, decreases the reproduction number (Chowell and Hyman, 2023).

4.3 Numerical Simulations of the Model

Numerical simulations of the system of model equations (3.4) were conducted to predict the epidemic behavior of pulmonary TB. These simulations were performed using MATLAB's built-in ordinary differential equation solver, the ode45 function. The ode45 function utilizes fourth- and fifth-order Runge-Kutta methods with a variable time step to ensure efficient computation (Dormand and Prince, 1980). To estimate the initial conditions of the steady states, the Kenyan population, which is approximately 53,704,243 according to Kenya National Bureau of Statistics (KNBS) and ICF (2023), was used. This population is equivalent to:

$N = S + V + E + I_a + I_S + T_E + T_a + T_S + R.$

The initial state values are as follows:

$S(0) = 1182969, V(0) = 26294166, E(0) = 13442825, I_a(0) = 59557,$
$I_S(0) = 37949, T_E(0) = 300000, T_a(0) = 40000, T_S(0) = 91560, R(0) = 12255217,$

based on the NTLLDP 2022 data. The initial state and parameter values in Table 4.1 were used to perform numerical simulations, and the results are presented as follows.

Table 4.1

Parameter values for the pulmonary TB model

Parameter	Value	Source
π	$1\,514\,825$ year^{-1}	KNBS (2023)
P	0.8 year^{-1}	KNBS (2023)
ρ	0.5	WHO (2023)
μ	0.0147 year^{-1}	KNBS (2023)
θ_1	0.34 year^{-1}	NTLLDP (2022)
χ_1	0.05 year^{-1}	NTLLDP (2019)
χ_2	0.1 year^{-1}	NTLLDP (2019)
ω	0.6 year^{-1}	NTLLDP (2022)
m	0.0003	Estimate
δ_1	0.5 year^{-1}	WHO (2024)
δ_2	0.06 year^{-1}	NTLLDP (2021)
θ_2	0.2 year^{-1}	NTLLDP (2022)
θ_3	0.63 year^{-1}	NTLLDP (2022)
ξ_1	0.85 year^{-1}	NTLLDP (2020)
ξ_2	0.8 year^{-1}	NTLLDP (2021)
ξ_3	0.75 year^{-1}	NTLLDP (2021)
σ	0.08 year^{-1}	NTLLDP (2022)
β	0.15 year^{-1}	NTLLDP (2021)
η_1	0.003	Estimate
η_2	0.002	Estimate
η_3	0.0016	Estimate

Source: Researcher (2024)

Table 4.2

Sensitivity indices of TB model reproduction numbers

Parameter	R_{CVST}	R_{CST}	R_{CVT_S}	R_{CT_S}
θ_1	-0.673668	-0.673668	—	—
θ_2	-0.751639	-0.751362	—	—
θ_3	-0.5690921	-0.0519066	-0.0519052	-0.569053
ρ	-0.666667	—	-0.6666667	—
χ_1	+0.11309	+0.113028	+0.024444	+0.0245257
χ_2	+0.589703	+0.589756	+0.0648092	+0.0647274
β	+1	+1	+1	+1

Source: Researcher (2024)

4.3.1 Change in population over time across different compartments

In this subsection, the changes in population over time across different compartments are predicted and discussed. Additionally, strategies to reduce the transmission of active pulmonary TB infections within the community are suggested.

Figure 4.1

Change in population over time across different compartments

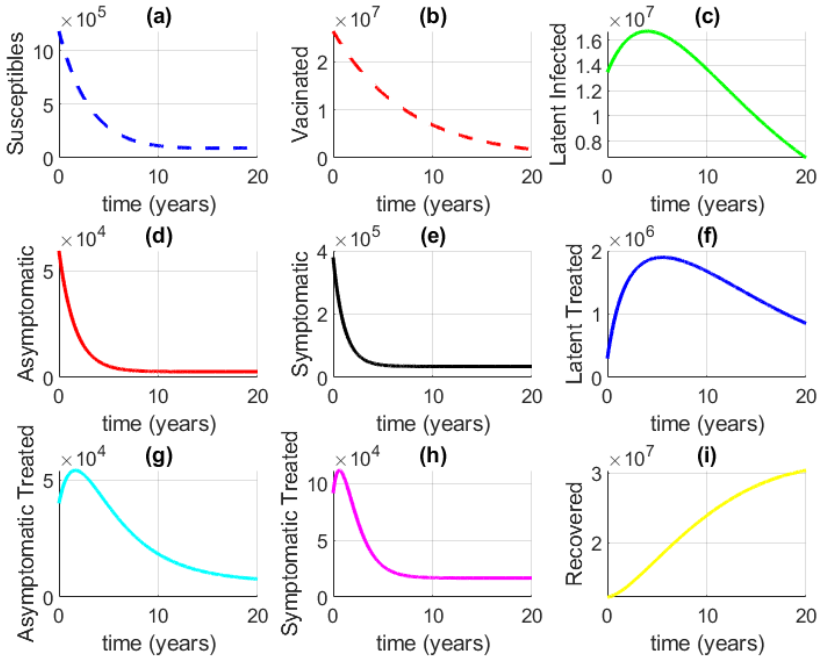

Source: Researcher (2024)

Figure 4.1(a) illustrates the change in the susceptible population over time. The susceptible population is observed to decrease and eventually reach equilibrium. Before the epidemic peaks, more susceptible individuals become infected and transition to the latent class than are replenished through births and waning immunity. This trend is attributed to the high rate of infection transmission. Consequently, the susceptible population declines over time. Equilibrium is achieved as the susceptible population is continuously replenished by new births and individuals whose immunity wanes. To address this, it is crucial for all mothers to deliver in healthcare facilities to ensure that newborns are vaccinated, thereby significantly reducing the size of the susceptible population. The depletion of the susceptible pool implies that each infected individual may eventually be unable to transmit the infection to at least one other person, rendering the epidemic unsustainable and ultimately leading to its resolution.

Figure 4.1(b) illustrates the change in the vaccinated population over time. The vaccinated population is observed to decrease steadily. This decline is attributed to the low efficacy of

the currently used pulmonary tuberculosis vaccine and the waning of its protective effects over time. Consequently, a significant number of vaccinated individuals lose immunity and transition to the latent class after becoming infected. However, the vaccinated population does not drop to zero, as it is continuously replenished by children born in healthcare facilities who receive the vaccine. Given the limited efficacy of the BCG vaccine currently in use, there is an urgent need for researchers to develop a more effective vaccine to provide better protection for the vaccinated population.

Figure 4.1(c) illustrates the change in the latent infected population over time. The latent infected population is observed to increase initially, reach a peak, and then decrease. At the onset, the percentage of the susceptible population is sufficiently high to facilitate the spread of infection, leading to a rise in latent infections. Before the peak is reached, the number of susceptible individuals transitioning to the latent class exceeds those replenished through births and waning immunity, causing the susceptible population to decline. As the susceptible population decreases over the course of the epidemic, the control reproduction number also decreases, leading to a reduction in the rate of infection transmission over time. The peak occurs when the control reproduction number declines to one. As it falls further below one, the epidemic prevalence diminishes. Additionally, the number of latent infected individuals is observed to decrease to zero after 20 years. This decline is attributed to a reduced transmission rate, combined with sustained screening and treatment efforts. These findings underscore that treating latent infections is a critical strategy for controlling pulmonary tuberculosis transmission, as it reduces the reservoir of latent infections that could otherwise reactivate during an individual's lifespan.

Figure 4.1(d) illustrates the change in the asymptomatic infectious population over time. It is observed that the asymptomatic infectious population decreases initially before reaching equilibrium. This decline is attributed to the implementation of control measures, which lead to a stable equilibrium where a small portion of the population remains infected. The asymptomatic infectious population stabilizes at an endemic equilibrium, with the control reproduction number remaining constant, as the pool of susceptible individuals is continuously replenished through new births and waning immunity. These findings highlight the

importance of strategies to trace, screen, and treat infectious contacts as essential efforts to mitigate the persistent spread of pulmonary tuberculosis infections within the population.

Figure 4.1(e) depicts the change in the symptomatic population over time. It is observed that the symptomatic population decreases over time. This decline occurs because the screening of asymptomatic infectious and latently infected individuals reduces the number of people who would otherwise progress to severe disease. Furthermore, the symptomatic population stabilizes at an endemic equilibrium. This stabilization occurs because the pool of susceptible individuals is continuously replenished through new births and waning immunity, resulting in a small portion of the population remaining infected. However, once the susceptible population is replenished to a level where infectious individuals can cause at least one secondary case, the epidemic recurs, leading to cyclical outbreaks. Therefore, there is a critical need to develop a new, more effective vaccine to achieve sufficient herd immunity in the population and ultimately prevent epidemic cycles.

Figure 4.1(f) illustrates the change in the population of latently infected individuals undergoing treatment over time. It is observed that this population initially increases, reaches a peak, and then decreases. At the beginning, the proportion of latently infected individuals is sufficiently high, leading to an increase in the number of individuals screened and initiated into latent treatment. Just before the peak, more latently infected individuals are screened than are added through new infections. The peak occurs when the rate of latent screening matches the rate of latent infection. After the peak, the proportion of infected individuals becomes too low, resulting in a decrease in the number of individuals being screened and, consequently, a decline in the population undergoing latent treatment. Additionally, the treatment of latently infected individuals is effective, causing the treated population to transition to the recovered class, thereby further reducing the population undergoing latent treatment.

Figure 4.1(g) illustrates the change in the asymptomatic infectious population undergoing treatment over time. It is observed that this population initially increases, reaches a peak, decreases, and then attains equilibrium. At the beginning, the proportion of asymptomatic infectious individuals is sufficiently high, leading to more individuals being iden-

tified through screening and initiated into treatment. At the peak, the rate at which asymptomatic individuals are screened matches the rate at which they are added through new infections. After the peak, the decrease in the asymptomatic population results in fewer individuals being identified through screening, causing a subsequent decline in the asymptomatic infectious population undergoing treatment. Eventually, equilibrium is reached as the asymptomatic infectious population undergoing treatment is continuously replenished by new individuals from the infectious population.

Figure 4.1(h) depicts the change in the symptomatic population undergoing treatment over time. This population initially experiences a slight increase, followed by a significant decrease, before ultimately reaching equilibrium. At the onset, the proportion of symptomatic individuals is sufficiently high, leading to an increase in the number of individuals seeking treatment. However, the screening of asymptomatic infectious and latently infected individuals reduces the progression to severe disease, resulting in a decline in the number of symptomatic individuals requiring treatment. Equilibrium is eventually reached as the population seeking treatment is continuously replenished by new individuals from the infectious classes. Since treatment reduces the number of individuals capable of transmitting infections, it serves as an effective strategy for combating pulmonary tuberculosis within the community.

Figure 4.1(i) depicts the change in the recovered population over time. The recovered population increases steadily before eventually reaching equilibrium. This increase occurs due to the availability of effective treatment for all forms of pulmonary tuberculosis, enabling individuals undergoing treatment to transition to the recovered class. However, the growth is not exponential, as the immunity of recovered individuals wanes over time, causing them to transition back to the susceptible class. The recovered population ultimately stabilizes at equilibrium because it is continuously replenished by individuals recovering from various forms of pulmonary tuberculosis.

4.3.2 Effects of varying natural immunity on the pulmonary TB

In this subsection, the predicted effects of varying natural immunity in populations with pulmonary tuberculosis were analyzed to assess its role in preventing the transmission of

infection to the susceptible population.

In the flow chart depicted in Figure 3.1, m represents natural immunity. Figures 4.2 and 4.3 illustrate the predicted impact of varying natural immunity on populations with pulmonary TB. It is observed that an increase in natural immunity decreases the populations with pulmonary tuberculosis. Furthermore, Figures 4.4 and 4.5 show that higher levels of natural immunity reduce the populations with pulmonary tuberculosis seeking treatment. This reduction occurs because increased immunity decreases the reactivation of latent infections, leading to lower transmission rates and, consequently, a smaller number of individuals seeking treatment for pulmonary tuberculosis. These findings indicate that enhancing the immunity of individuals with latent infections is an effective strategy for controlling the spread of infections to the susceptible population.

4.3.3 Effects of varying screening rates on pulmonary TB

This subsection highlights the predicted impact of screening individuals who are latently infected with TB and those within the asymptomatic pulmonary TB population. The results are analyzed and discussed with the aim of suggesting appropriate measures to curb the spread of pulmonary tuberculosis in the community.

Referring to the flow chart depicted in Figure 3.1, θ_1 represents the rate of screening for the latently infected TB population. Figures 4.6 and 4.7 illustrate the effects of screening latently infected individuals on the pulmonary TB population. It is observed that an increase in the screening rate for latently infected individuals significantly decreases the population with pulmonary TB. Additionally, Figures 4.8 and 4.9 demonstrate that increased screening for individuals with latent TB infection reduces the population seeking treatment for pulmonary TB. Screening latently infected individuals and initiating them on treatment reduces the transmission of infections to the susceptible population by decreasing the reactivation of latent infections. The reduction in the population seeking treatment for pulmonary TB not only lowers the rate of infection transmission to healthcare workers but also alleviates the strain on healthcare resources, particularly in developing countries. Therefore, increasing the screening rate for latently infected individuals is an effective strategy for controlling the transmission of tuberculosis within the population.

In the flow chart depicted in Figure 3.1, θ_2 represents the screening rate for asymptomatic infectious individuals. Figures 4.10 and 4.11 illustrate the effects of screening asymptomatic individuals with pulmonary TB on the population with severe pulmonary TB disease and the population undergoing treatment, respectively. It is observed that an increase in the screening rate for asymptomatic infectious individuals decreases both the population with severe pulmonary TB disease and the population undergoing treatment. This reduction is attributed to the decreased progression of the asymptomatic infectious population to severe pulmonary TB disease and, consequently, a smaller number of individuals seeking treatment for the disease.

4.3.4 Effects of varying vaccine efficacy on pulmonary TB

This subsection examines the predictions of varying vaccine efficacy on pulmonary TB disease to evaluate its impact on the transmission of infection to the susceptible population. Referring to the model flow chart depicted in Figure 3.1, ρ represents vaccine efficacy. Figures 4.12 and 4.13 illustrate the effects of varying vaccine efficacy on the symptomatic and asymptomatic infectious populations, respectively. It is observed that an increase in vaccine efficacy reduces the numbers of both symptomatic and asymptomatic infectious individuals. This reduction occurs because a higher-efficacy vaccine enhances individual immunity, thereby decreasing the proportion of the population infected with pulmonary TB.

4.3.5 Effects of various intervention strategies on control reproduction numbers

This subsection discusses the predicted effects of various intervention strategies on the transmission of pulmonary TB. These strategies include screening for both latently infected and asymptomatic infectious populations, as well as vaccination and treatment for all forms of pulmonary TB.

Equations (4.16), (4.17), (4.18), and (4.19) represent the control reproduction numbers for different intervention strategies: R_{CVST} for vaccination, screening, and treatment of all infected cases; R_{CST} for screening and treatment of all infected cases; R_{CVT_S} for vaccination and treatment of the symptomatic population; and R_{CT_S} for treatment of the symptomatic population alone. Figure 4.14 illustrates the effects of varying reproduction numbers with

respect to the transmission rate (β). It is observed that $R_{CVST} < R_{CST} < R_{CVT_S} < R_{CT_S}$. This indicates that a combination of vaccination, screening, and treatment of all infected cases is the most effective control measure in reducing infection transmission within the population. Following this, the combination of screening and treatment of all infected cases is the next most effective strategy, while the combination of vaccination and treatment of symptomatic individuals ranks third. Finally, treating symptomatic cases alone is noted to be the least effective strategy for reducing infection transmission in the population.

4.3.6 Effects of varying screening rates on control reproduction numbers

In the model flow chart depicted in Figure 3.1, θ_1 represents the rate of screening latently infected individuals, with Figure 4.15 illustrating the predicted effects of screening the latently infected population on the control reproduction number. Similarly, θ_2 represents the rate of screening the asymptomatic infectious population, as shown in Figure 4.16, which displays the effects of screening this population on the control reproduction number. It is observed that increasing screening rates for both latently infected and asymptomatic infectious populations reduces the control reproduction number, thereby decreasing the rate of infection transmission. Screening and treating latently infected individuals reduce reactivation and subsequently lowers infection transmission in the population. Screening asymptomatic infectious individuals is crucial because, lacking symptoms, this population continues their daily activities without seeking medical intervention. This behavior leads to frequent interactions with susceptible individuals, significantly contributing to the rate of infection transmission in the population. Therefore, it is essential to screen and treat asymptomatic infectious individuals, as they unknowingly and persistently spread infections.

4.3.7 Effects of varying treatment rates and vaccine efficacy on control reproduction numbers

In the model flow chart depicted in Figure 3.1, θ_3 represents the rate of treating the symptomatic population, while Figure 4.17 illustrates the predicted effects of varying treatment rates on the control reproduction number for this population. It is observed that increasing the treatment rate for the symptomatic population reduces the control reproduction number.

This reduction occurs due to a decrease in the infectious population, which subsequently lowers the rate of infection transmission. Furthermore, it is demonstrated that an increase in vaccine efficacy also reduces the control reproduction number. This effect is attributed to a decrease in the number of individuals who become infectious, as a more effective vaccine enhances immunity, thereby reducing the rate of infection transmission to susceptible populations.

This study was extended to model the co-infection of pulmonary TB and pneumonia to suggest appropriate intervention strategies that could halt the spread of infections globally. Several clinical studies and reports (Chavarría and Laura, 2018; Garcia, 2019; Oliwa et al., 2019; Xiao-Ying et al., 2016) have shown that there is lethal synergism between pulmonary TB and pneumonia due to their overlapping symptoms. The co-infection model is presented in the next section.

Figure 4.2

Effects of varying levels of natural immunity on the symptomatic TB population

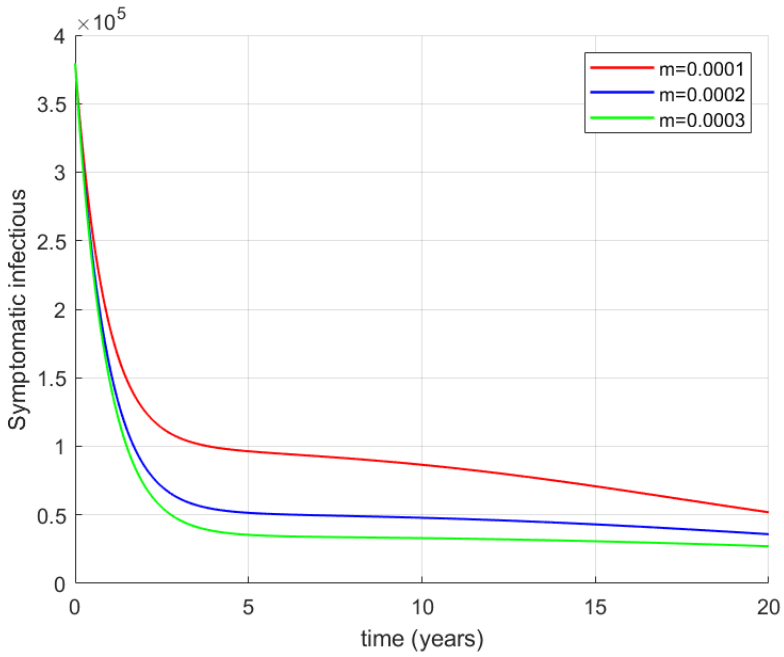

Source: Researcher (2024)

Figure 4.3

Effects of varying levels of natural immunity on the asymptomatic TB population

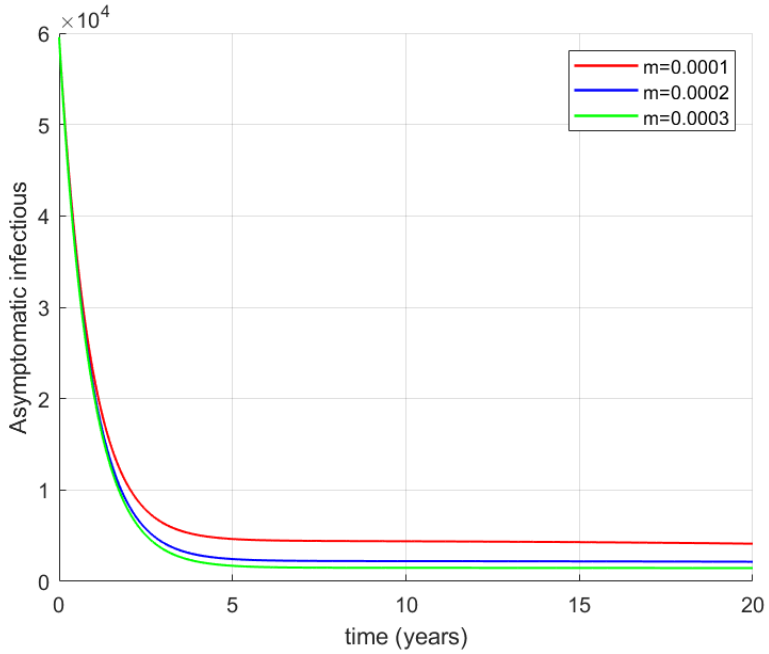

Source: Researcher (2024)

Figure 4.4

Effects of varying levels of natural immunity on the symptomatic TB population undergoing treatment

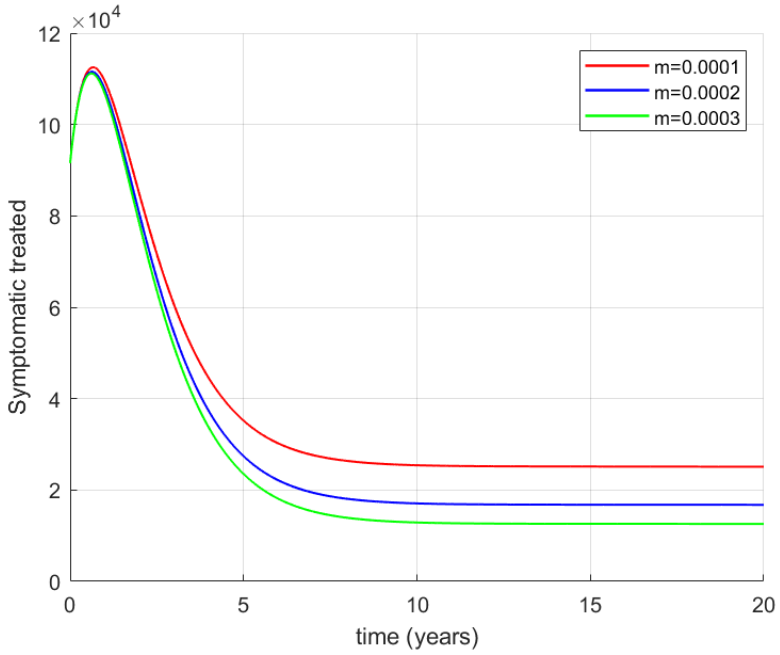

Source: Researcher (2024)

Figure 4.5

Effects of varying levels of natural immunity on the asymptomatic TB population undergoing treatment

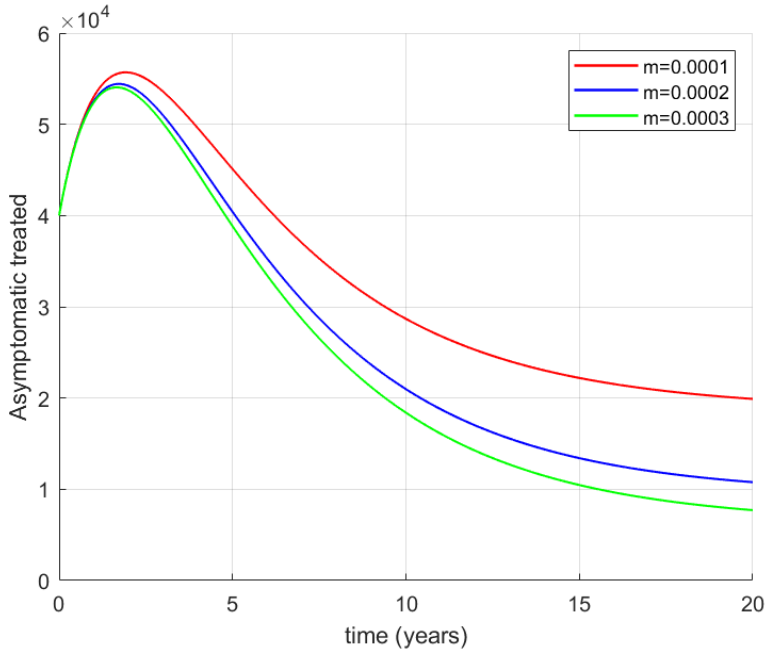

Source: Researcher (2024)

Figure 4.6

Effects of varying the screening rate for latently infected individuals on the symptomatic TB population

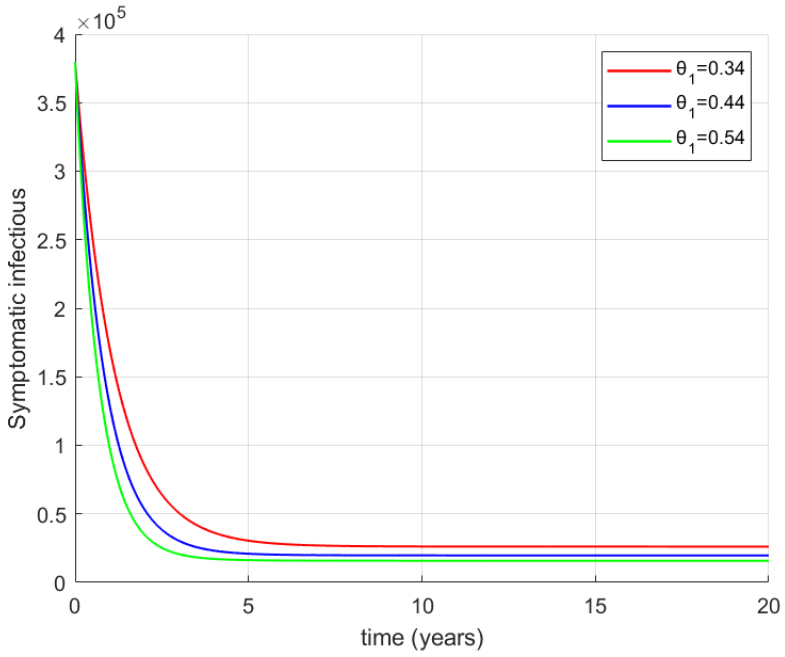

Source: Researcher (2024)

Figure 4.7

Effects of varying the screening rate for latently infected individuals on the asymptomatic TB population

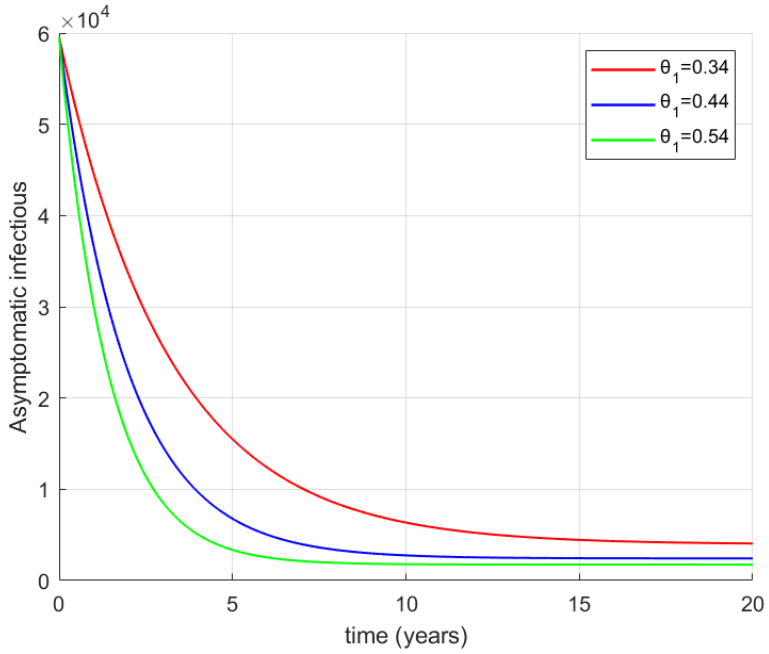

Source: Researcher (2024)

Figure 4.8

Effects of varying the screening rate for latently infected individuals on the symptomatic TB population undergoing treatment

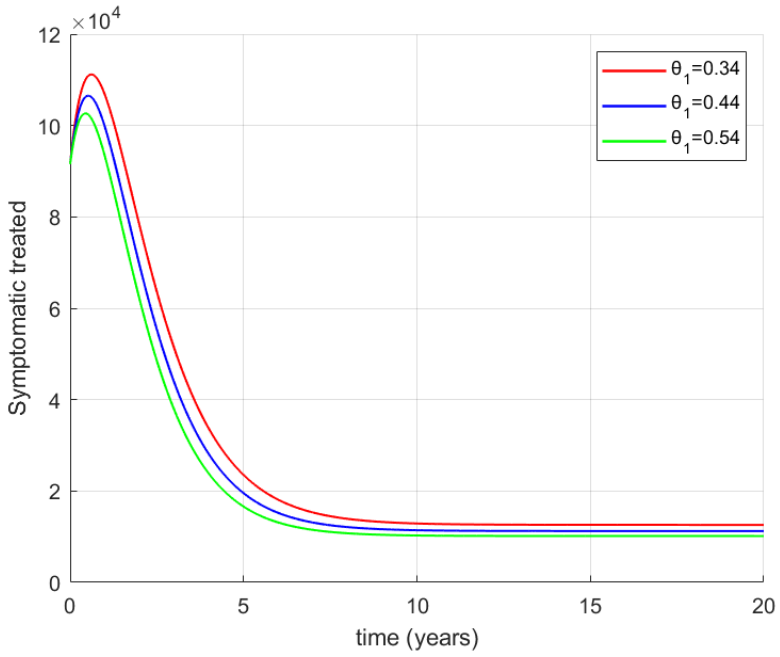

Source: Researcher (2024)

Figure 4.9

Effects of varying the screening rate for latently infected individuals on the asymptomatic infectious TB population undergoing treatment

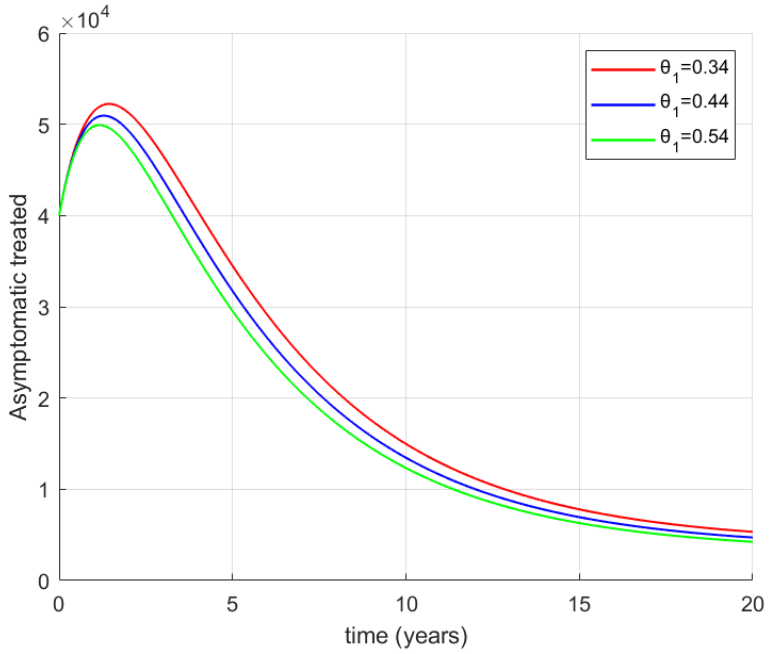

Source: Researcher (2024)

Figure 4.10

Effects of varying the screening rate for asymptomatic infectious individuals on the symptomatic TB population.

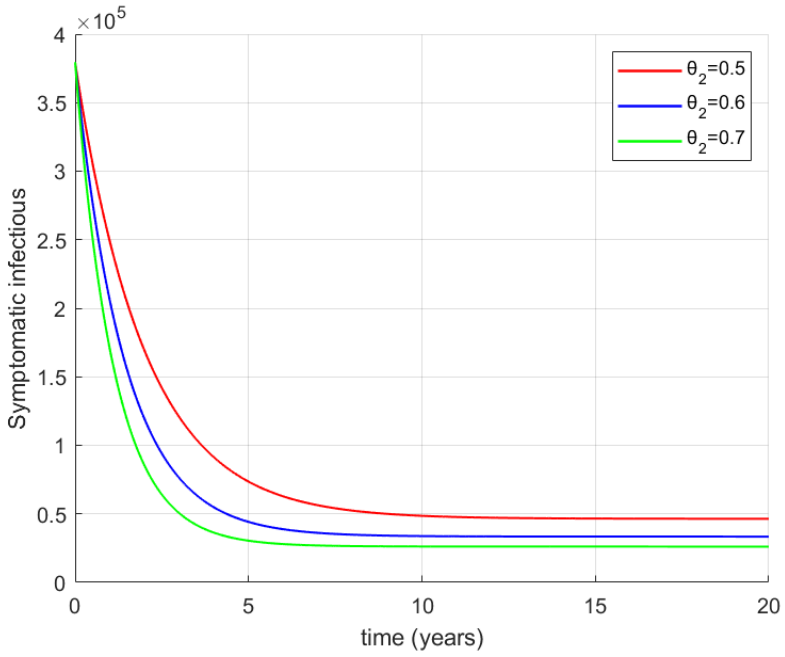

Source: Researcher (2024)

Figure 4.11

Effects of varying the screening rate for asymptomatic infectious individuals on the symptomatic TB population undergoing treatment

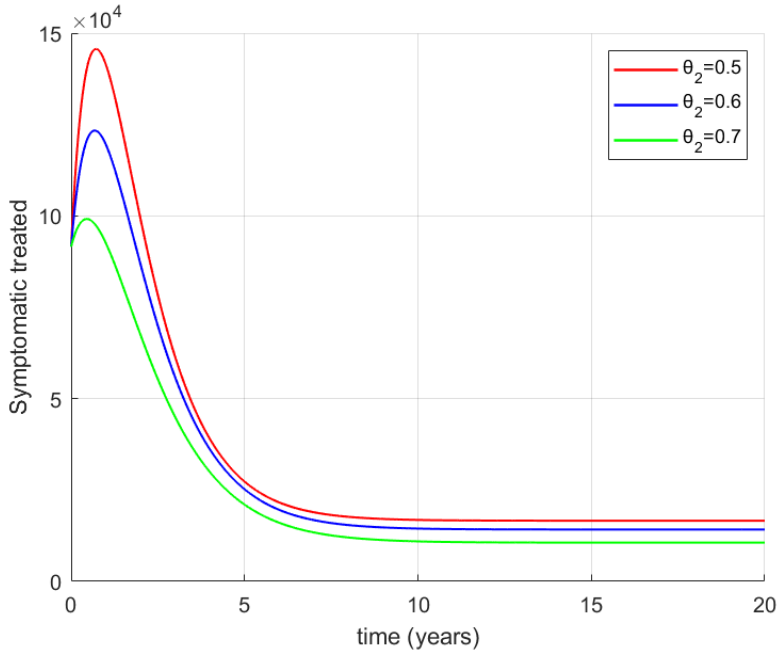

Source: Researcher (2024)

Figure 4.12

Effects of varying vaccine efficacy on the symptomatic TB population

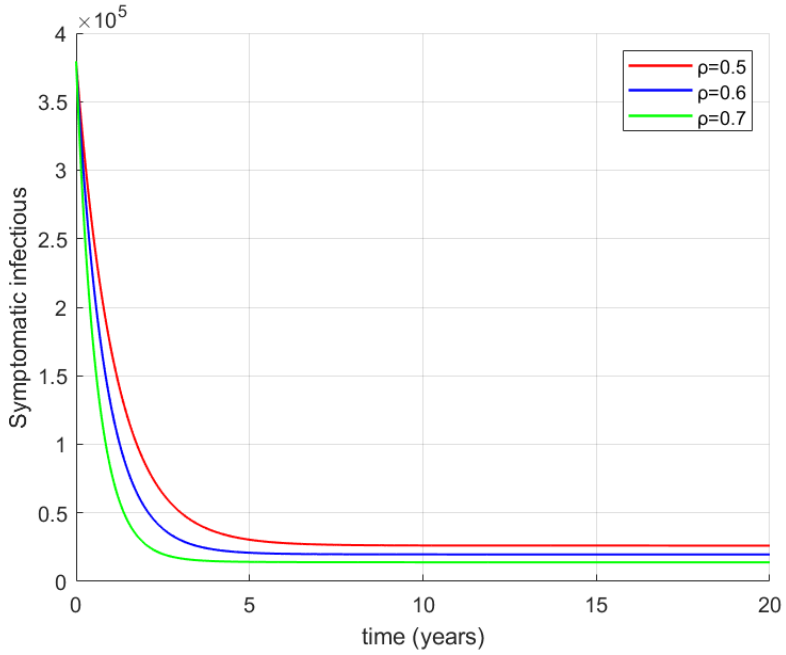

Source: Researcher (2024)

Figure 4.13

Effects of varying vaccine efficacy on the asymptomatic infectious TB population

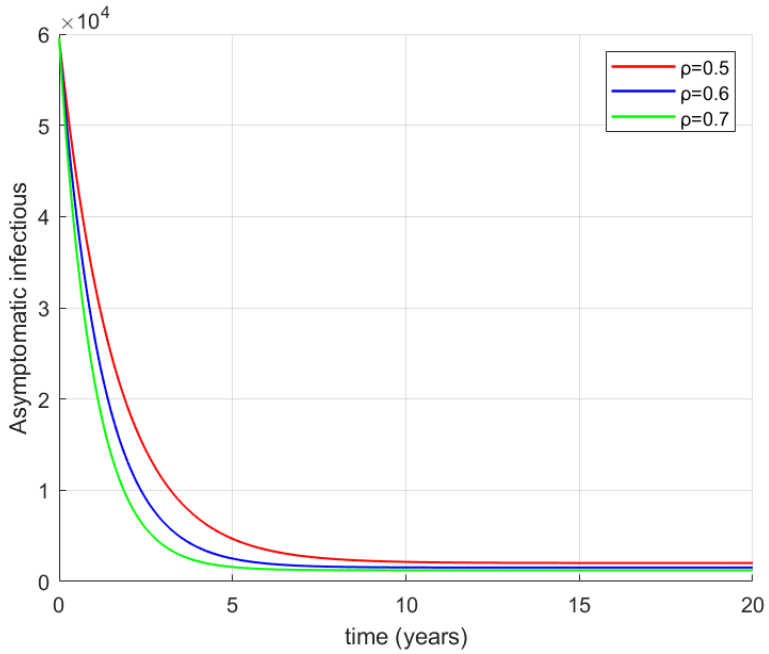

Source: Researcher (2024)

Figure 4.14

Effects of various intervention strategies on the control reproduction number

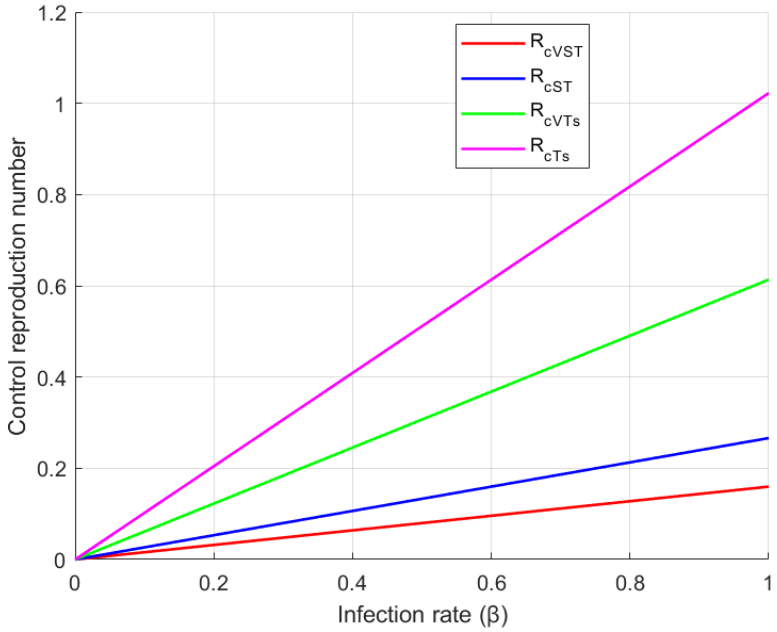

Source: Researcher (2024)

Figure 4.15

Effects of varying the screening rate for latently infected individuals on the control reproduction number

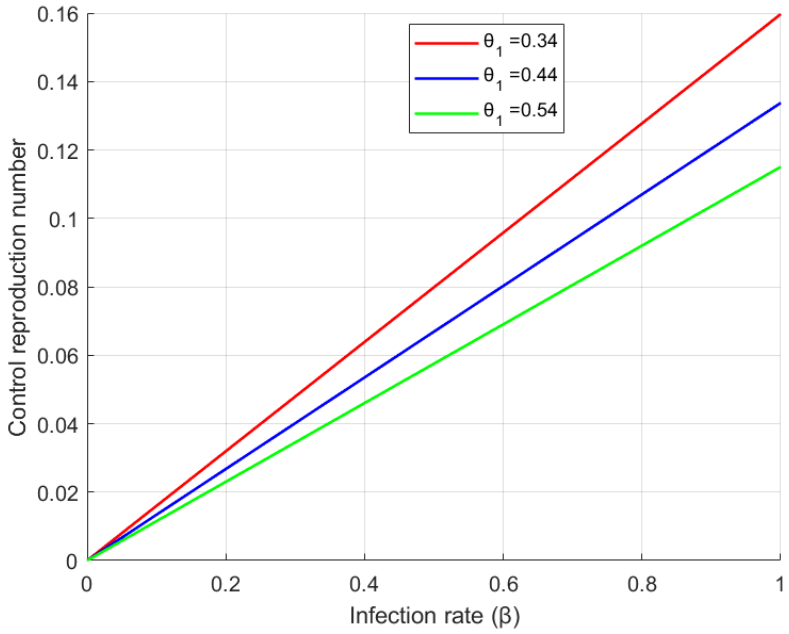

Source: Researcher (2024)

Figure 4.16

Effects of varying the screening rate for asymptomatic infectious individuals on the control reproduction number

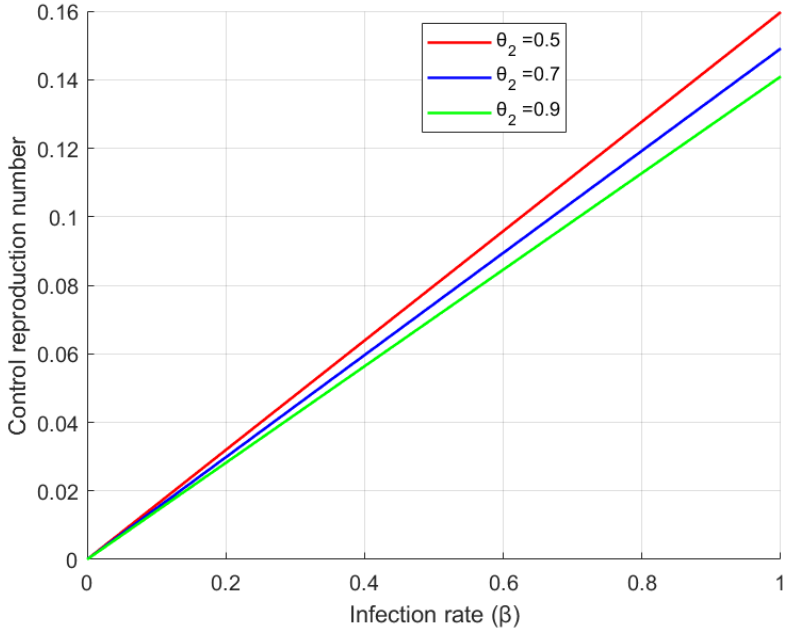

Source: Researcher (2024)

Figure 4.17

Effects of varying the treatment rate for symptomatic individuals on the control reproduction number

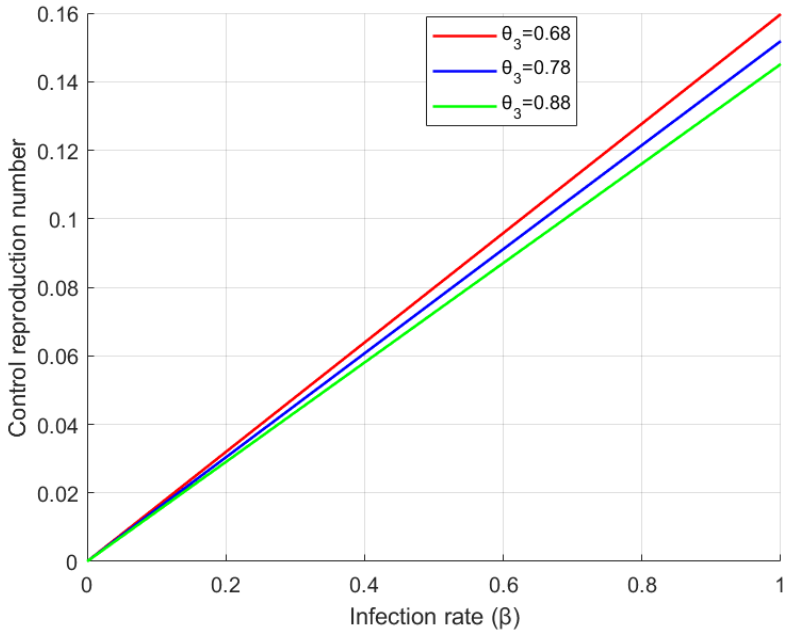

Source: Researcher (2024)

Figure 4.18

Effects of varying vaccine efficacy on the control reproduction number

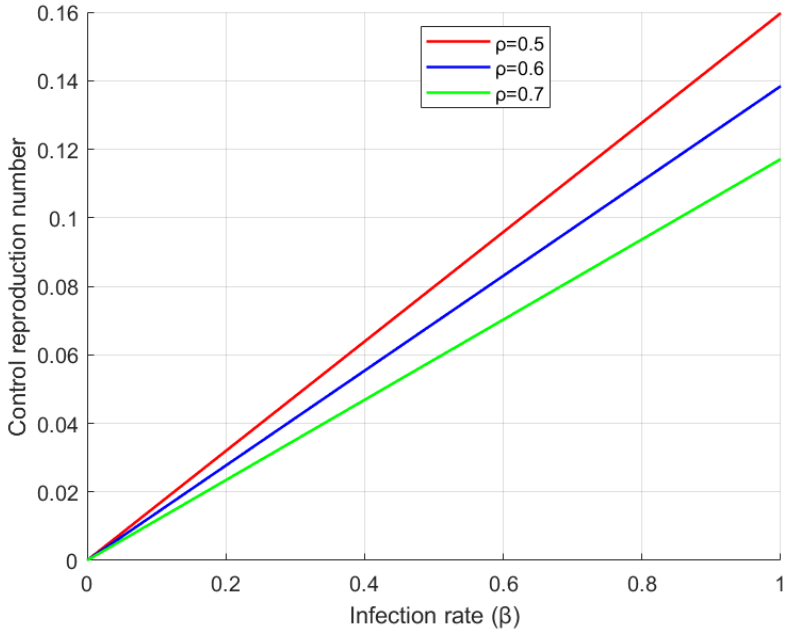

Source: Researcher (2024)

4.4 Pulmonary TB and Pneumonia Co-infection Model Analysis

In this section, a pulmonary TB-pneumonia co-infection model is analyzed, focusing on several aspects: the positivity of model solutions, invariant region, disease-free and endemic equilibrium points, reproduction number of the model, bifurcation analysis, and sensitivity analysis.

4.4.1 Positivity of the solutions

The dynamical system (3.8) illustrates changes in the human population. Therefore, it is necessary to prove that, given non-negative initial conditions, its solutions remain positive for all $t > 0$, as demonstrated by theorem 4.7.

Theorem 4.7. *Given that the initial conditions* $S(0)$, $V(0)$, $E(0)$, $I_a(0)$, $I_S(0)$, $I_{aP}(0)$, $I_{SP}(0)$, $T_E(0)$, $T_a(0)$, $T_S(0)$, $T_{aP}(0)$, $T_{SP}(0)$ *and* $R(0)$ *are non -negative, the solutions* $S(t)$, $V(t)$, $E(t)$, $I_a(t)$, $I_S(t)$, $I_{aP}(t)$, $I_{SP}(t)$, $T_E(t)$, $T_a(t)$, $T_S(t)$, $T_{aP}(t)$, $T_{SP}(t)$, *and* $R(t)$ *remain positive for all* $t > 0$.

Proof. The method of contradiction was used to demonstrate the positivity of solutions for all $0 < t < \infty$, under the condition that the initial values of the state variables are positive, as utilized by Kizito et al. (2024). Suppose, at a given time, there exists a possibility such that:

(i) t_1 is such that $S(t_1) = 0$ and $\dot{S}(t_1) < 0$, whenever $V(t) > 0$, $E(t) > 0$, $I_a(t) > 0$, $I_S(t) > 0$, $I_{aP}(t) > 0$, $I_{SP}(t) > 0$, $T_E(t) > 0$, $T_a(t) > 0$, $T_S(t) > 0$, $T_{aP}(t)$, $T_{SP}(t) > 0$ and $R(t) > 0$ for $0 < t < t_1$.

Applying claim (i) to first equation of the system (3.8), yields:

$$\dot{S}(t_1) = (1 - Q)\Lambda + \kappa R(t_1) > 0 \tag{4.63}$$

Equation (4.63) contradicts claim (i), as when $S(t_1) = 0$ it follows that $\dot{S}(t_1) < 0$. Therefore, for all t in the interval $0 < t < t_1$, $S(t) > 0$, and hence t_1 can be extended to ∞.
Similarly, it can be shown that the solutions:
$V(t), E(t), I_a(t), I_S(t), I_{aP}(t), I_{SP}(t), T_E(t), T_a(t), T_S(t), T_{aP}(t), T_{SP}(t)$, and $R(t)$ are non-negative.

Thus, the solutions set:

$S(t), V(t), E(t), I_a(t), I_S(t), I_{aP}(t), I_{SP}(t), T_E(t), T_a(t), T_S(t), T_{aP}(t), T_{SP}(t), R(t)\,\} \geq 0, \quad \forall\, t > 0.$

This proves that the solutions of the model system (3.8) remain positive for all $t > 0$.

4.4.2 Invariant region

In this subsection, a region in which the solution of the system (3.8) remains bounded is determined, as it deals with the human population. The total human population at any given time t in this model is defined by:

$$N = S + V + E + I_a + I_S + I_{aP} + I_{SP} + T_E + T_a + T_S + T_{aP} + T_{SP} + R \tag{4.64}$$

Differentiating equation (4.64) with respect to time gives:

$$\frac{dN}{dt} = \frac{dS}{dt} + \frac{dV}{dt} + \frac{dE}{dt} + \frac{dI_a}{dt} + \frac{dI_S}{dt} + \frac{dI_{aP}}{dt} + \frac{dI_{SP}}{dt} + \frac{dT_E}{dt} + \frac{dT_a}{dt} + \frac{dT_S}{dt} + \frac{dT_{aP}}{dt} + \frac{dT_{SP}}{dt} + \frac{dR}{dt} \tag{4.65}$$

Substituting the system (3.8) into equation (4.65) yields:

$$\frac{dN}{dt} = \Lambda - \mu N - \gamma_1 I_S - \gamma_2 I_{SP} - \gamma_3 T_{SP} - \gamma_4 T_S - \gamma_5 I_{aP} \tag{4.66}$$

In the absence of mortality due to pulmonary TB and co-infection between pulmonary TB and pneumonia infections (i.e.,$\gamma_1 = \gamma_2 = \gamma_3 = \gamma_4 = \gamma_5 = 0$), equation (4.66) becomes:

$$\frac{dN}{dt} = \Lambda - \mu N \tag{4.67}$$

By separation of variables, equation (4.67) yields:

$$\frac{dN}{\Lambda - \mu N} = dt \tag{4.68}$$

Integrating equation (4.68) gives:

$$-\frac{1}{\mu} \ln(\Lambda - \mu N) = t + k \tag{4.69}$$

Where k is a constant of integration. Simplifying equation (4.69) yields:

$$\Lambda - \mu N(t) = Ae^{-\mu t} \tag{4.70}$$

Where A is a constant. Applying initial condition at $t = 0$, $N(t) = N(0)$, A is given as follows:

$$A = \Lambda - \mu N(0) \tag{4.71}$$

Substituting equation (4.71) into equation (4.70) gives:

$$N(t) = \frac{\Lambda}{\mu} + \left(N(0) - \frac{\Lambda}{\mu}\right) e^{-\mu t} \tag{4.72}$$

As $t \to \infty$ in equation (4.72), the population $N(t) \to \frac{\Lambda}{\mu}$, implying that
$0 \leq N(t) \leq \frac{\Lambda}{\mu}$. Thus, the feasible solution of the system enters and remains in the region:

$$\Omega_1 = \left\{(S(t), V(t), E(t), I_a(t), I_S(t), I_{aP}(t), I_{SP}(t), T_E(t), T_a(t), T_S(t), T_{aP}(t), T_{SP}(t), R(t)) \in \mathbb{R}^{13}_+ : N(t) \leq \tfrac{\Lambda}{\mu}\right\} \tag{4.73}$$

Therefore, the basic model is well-posed both epidemiologically and mathematically, and hence it is sufficient to study its dynamics in Ω_1.

4.4.3 Disease free equilibrium point

The disease-free equilibrium point of the system (3.8) is obtained by setting the latent infected class, all infectious classes, all classes undergoing treatment, and the recovered class to zero, i.e.,

$E = I_a = I_S = I_{aP} = I_{SP} = T_E = T_a = T_S = T_{aP} = T_{SP} = R = 0.$

The following equations are then obtained:

$$\begin{cases} (1-Q)\Lambda - \mu S^0 = 0, \\ \\ Q\Lambda - \mu V^0 = 0 \end{cases} \tag{4.74}$$

Solving the system (4.74), yields:

$S^0 = \frac{(1-Q)\Lambda}{\mu}$, $V^0 = \frac{Q\Lambda}{\mu}$

The disease-free equilibrium is therefore given by:

$$B_1^0 = (\frac{(1-Q)\Lambda}{\mu}, \frac{Q\Lambda}{\mu}, 0, 0, 0, 0, 0, 0, 0, 0, 0, 0, 0) \tag{4.75}$$

4.4.4 The control reproduction number

The Next-Generation Matrix method is used to obtain the control reproduction number, as described by Driessche et al. (2020). According to the principle of the Next-Generation Matrix, the equations for the infected classes are considered as follows:

$$\begin{cases} \frac{dE}{dt} = \lambda_1 S + (1-\rho)\lambda_1 V - \left(\frac{\varepsilon_1}{1+nE} + \frac{\varepsilon_2}{1+nE} + \vartheta_1 + \mu \right) E, \\ \frac{dI_a}{dt} = \frac{\varepsilon_2 E}{1+nE} - (\lambda_2 + \phi_1 + \mu + \vartheta_2) I_a, \\ \frac{dI_S}{dt} = \frac{\varepsilon_1 E}{1+nE} + \phi_1 I_a - (\lambda_2 + \vartheta_3 + \mu + \gamma_1) I_S, \\ \frac{dI_{aP}}{dt} = \lambda_2 I_a - (\mu + \gamma_5 + \phi_2 + \vartheta_4) I_{aP}, \\ \frac{dI_{SP}}{dt} = \lambda_2 I_S + \phi_2 I_{aP} - (\gamma_2 + \vartheta_5 + \mu) I_{SP}, \\ \frac{dT_a}{dt} = \vartheta_2 I_a + \phi_3 T_{aP} - (\mu + \alpha_2) T_a, \\ \frac{dT_S}{dt} = \vartheta_3 I_S + \phi_4 T_{SP} - (\mu + \gamma_4 + \alpha_3) T_S, \\ \frac{dT_{aP}}{dt} = \vartheta_4 I_{aP} - (\mu + \phi_3) T_{aP}, \\ \frac{dT_{SP}}{dt} = \vartheta_5 I_{SP} - (\mu + \phi_4 + \gamma_3) T_{SP}. \end{cases} \tag{4.76}$$

Let

$$X = (E, I_a, I_S, I_{aP}, I_{SP}, T_a, T_S, T_{aP}, T_{SP})^T \tag{4.77}$$

It follows from system (4.76) that:

$$\frac{dX}{dt} = f - v \tag{4.78}$$

where f and v are matrices representing the new infections and transition terms, respectively, given as:

$$f = \begin{bmatrix} \lambda_1 S + (1-\rho)\lambda_1 V \\ 0 \\ 0 \\ \lambda_2 I_a \\ \lambda_2 I_S \\ 0 \\ 0 \\ 0 \\ 0 \end{bmatrix}$$

,

$$v = \begin{bmatrix} \left(\frac{\varepsilon_1}{1+nE} + \frac{\varepsilon_2}{1+nE} + \vartheta_1 + \mu\right) E \\ (\lambda_2 + \phi_1 + \mu + \vartheta_2) I_a - \frac{\varepsilon_2 E}{1+nE} \\ (\lambda_2 + \vartheta_3 + \mu + \gamma_1) I_S - \frac{\varepsilon_1 E}{1+nE} - \phi_1 I_a \\ (\mu + \gamma_5 + \phi_2 + \vartheta_4) I_{aP} \\ (\gamma_2 + \vartheta_5 + \mu) I_{SP} - \phi_2 I_{aP} \\ (\mu + \alpha_2) T_a - \vartheta_2 I_a - \phi_3 T_{aP} \\ (\mu + \gamma_4 + \alpha_3) T_S - \vartheta_3 I_S - \phi_4 T_{SP} \\ (\mu + \phi_3) T_{aP} - \vartheta_4 I_{aP} \\ (\mu + \phi_4 + \gamma_3) T_{SP} - \vartheta_5 I_{SP} \end{bmatrix}$$

The Jacobian matrices of f and v are computed with respect to the state variables of system (4.77) at the disease-free equilibrium B_1^0. These Jacobian matrices are denoted by F and V, respectively, and are given as:

$$F = \begin{bmatrix} 0 & g_1 & g_2 & g_3 & g_4 & g_5 & g_6 & g_7 & g_8 \\ 0 & 0 & 0 & 0 & 0 & 0 & 0 & 0 & 0 \\ 0 & 0 & 0 & 0 & 0 & 0 & 0 & 0 & 0 \\ 0 & 0 & 0 & 0 & 0 & 0 & 0 & 0 & 0 \\ 0 & 0 & 0 & 0 & 0 & 0 & 0 & 0 & 0 \\ 0 & 0 & 0 & 0 & 0 & 0 & 0 & 0 & 0 \\ 0 & 0 & 0 & 0 & 0 & 0 & 0 & 0 & 0 \\ 0 & 0 & 0 & 0 & 0 & 0 & 0 & 0 & 0 \\ 0 & 0 & 0 & 0 & 0 & 0 & 0 & 0 & 0 \end{bmatrix} \tag{4.79}$$

where:

$g_1 = \beta_1\eta_6[S^0 + (1-\rho)V^0]$, $g_2 = \beta_1\eta_4[S^0 + (1-\rho)V^0]$, $g_3 = \beta_1\eta_5[S^0 + (1-\rho)V^0]$, $g_4 = \beta_1[S^0 + (1-\rho)V^0]$, $g_5 = \beta_1\eta_{10}[S^0 + (1-\rho)V^0]$, $g_6 = \beta_1\eta_8[S^0 + (1-\rho)V^0]$, $g_7 = \beta_1\eta_9[S^0 + (1-\rho)V^0]$, and $g_8 = \beta_1\eta_7[S^0 + (1-\rho)V^0]$.

$$V = \begin{bmatrix} h_1 & 0 & 0 & 0 & 0 & 0 & 0 & 0 & 0 \\ -\varepsilon_2 & h_2 & 0 & 0 & 0 & 0 & 0 & 0 & 0 \\ -\varepsilon_1 & -\phi_1 & h_3 & 0 & 0 & 0 & 0 & 0 & 0 \\ 0 & 0 & 0 & h_4 & 0 & 0 & 0 & 0 & 0 \\ 0 & 0 & 0 & -\phi_2 & h_5 & 0 & 0 & 0 & 0 \\ 0 & -\vartheta_2 & 0 & 0 & 0 & h_7 & 0 & -\phi_3 & 0 \\ 0 & 0 & -\vartheta_3 & 0 & 0 & 0 & h_8 & 0 & -\phi_4 \\ 0 & 0 & 0 & -\vartheta_4 & 0 & 0 & 0 & h_9 & 0 \\ 0 & 0 & 0 & 0 & -\vartheta_5 & 0 & 0 & 0 & h_{10} \end{bmatrix} \tag{4.80}$$

where:

$h_1 = (\varepsilon_1 + \varepsilon_2 + \vartheta_1 + \mu)$, $h_2 = (\phi_1 + \vartheta_2 + \mu)$, $h_3 = (\vartheta_3 + \gamma_1 + \mu)$, $h_4 = (\phi_2 + \gamma_5 + \vartheta_4 + \mu)$, $h_5 = (\gamma_2 + \vartheta_5 + \mu)$, $h_7 = (\mu + \alpha_2)$, $h_8 = (\mu + \gamma_4 + \alpha_3)$, $h_9 = (\mu + \phi_3)$, and $h_{10} = (\mu + \phi_4 + \gamma_3)$.

Using Mathematica software, the inverse of V is given as:

$$V^{-1} = \begin{bmatrix} \frac{1}{h_1} & 0 & 0 & 0 & 0 & 0 & 0 & 0 & 0 \\ \frac{\varepsilon_2}{h_1h_2} & \frac{1}{h_2} & 0 & 0 & 0 & 0 & 0 & 0 & 0 \\ \frac{h_2\varepsilon_1+\varepsilon_2\phi_1}{h_1h_2h_3} & \frac{\phi_1}{h_2h_3} & \frac{1}{h_3} & 0 & 0 & 0 & 0 & 0 & 0 \\ 0 & 0 & 0 & \frac{1}{h_4} & 0 & 0 & 0 & 0 & 0 \\ 0 & 0 & 0 & \frac{\phi_2}{h_4h_5} & \frac{1}{h_5} & 0 & 0 & 0 & 0 \\ \frac{\varepsilon_2\vartheta_2}{h_1h_2h_7} & \frac{\vartheta_2}{h_2h_7} & 0 & \frac{\vartheta_4\phi_3}{h_4h_7h_9} & 0 & \frac{1}{h_7} & 0 & \frac{\phi_3}{h_7h_9} & 0 \\ \frac{\vartheta_3(h_2\varepsilon_1+\varepsilon_2\phi_1)}{h_1h_2h_3h_8} & \frac{\vartheta_3\phi_1}{h_2h_3h_8} & \frac{\vartheta_3}{h_3h_8} & \frac{\vartheta_5\phi_2\phi_4}{h_4h_5h_8h_{10}} & \frac{\vartheta_5\phi_4}{h_5h_8h_{10}} & 0 & \frac{1}{h_8} & 0 & \frac{\phi_4}{h_8h_{10}} \\ 0 & 0 & 0 & \frac{\vartheta_4}{h_4h_9} & 0 & 0 & 0 & \frac{1}{h_9} & 0 \\ 0 & 0 & 0 & \frac{\vartheta_5\phi_2}{h_4h_5h_{10}} & \frac{\vartheta_5}{h_5h_{10}} & 0 & 0 & 0 & \frac{1}{h_{10}} \end{bmatrix}$$

The product of F and V^{-1} becomes:

$$FV^{-1} = \begin{bmatrix} R_1 & R_2 & R_3 & R_4 & R_5 & R_6 & R_7 & R_8 & R_9 \\ 0 & 0 & 0 & 0 & 0 & 0 & 0 & 0 & 0 \\ 0 & 0 & 0 & 0 & 0 & 0 & 0 & 0 & 0 \\ 0 & 0 & 0 & 0 & 0 & 0 & 0 & 0 & 0 \\ 0 & 0 & 0 & 0 & 0 & 0 & 0 & 0 & 0 \\ 0 & 0 & 0 & 0 & 0 & 0 & 0 & 0 & 0 \\ 0 & 0 & 0 & 0 & 0 & 0 & 0 & 0 & 0 \\ 0 & 0 & 0 & 0 & 0 & 0 & 0 & 0 & 0 \\ 0 & 0 & 0 & 0 & 0 & 0 & 0 & 0 & 0 \end{bmatrix} \tag{4.81}$$

where:

$$R_1 = \frac{g_1\varepsilon_2}{h_1h_2} + \frac{g_2(\varepsilon_1h_2+\varepsilon_2\phi_1)}{h_1h_2h_3} + \frac{g_5\varepsilon_2\vartheta_2}{h_1h_2h_7} + \frac{g_6\vartheta_3(\varepsilon_1h_2+\varepsilon_2\phi_1)}{h_1h_2h_3h_8},$$
$$R_2 = \frac{g_1}{h_2} + \frac{g_2\phi_1}{h_2h_3} + \frac{g_5\vartheta_2}{h_2h_7} + \frac{g_6\vartheta_3\phi_1}{h_2h_3h_8},$$
$$R_3 = \frac{g_2}{h_3} + \frac{g_6\vartheta_3}{h_3h_8},$$
$$R_4 = \frac{g_3}{h_4} + \frac{g_4\phi_2}{h_4h_5} + \frac{g_5\vartheta_4\phi_3}{h_4h_7h_9} + \frac{g_6\vartheta_5\phi_2\phi_4}{h_4h_5h_8h_{10}} + \frac{g_7\vartheta_4}{h_4h_9} + \frac{g_8\vartheta_5\phi_2}{h_4h_5h_{10}},$$
$$R_5 = \frac{g_4}{h_5} + \frac{g_6\vartheta_5\phi_4}{h_5h_8h_{10}} + \frac{g_8\vartheta_5}{h_5h_{10}}, \quad R_6 = \frac{g_5}{h_7}, \quad R_7 = \frac{g_6}{h_8},$$
$$R_8 = \frac{g_5\phi_3}{h_7h_9} + \frac{g_7}{h_9}, \quad R_9 = \frac{g_6\phi_4}{h_8h_{10}} + \frac{g_8}{h_{10}}.$$

The Eigen values of FV^{-1} are given as:

$\lambda_1 = \lambda_2 = \lambda_3 = \lambda_4 = \lambda_5 = \lambda_6 = \lambda_7 = \lambda_8 = 0, \lambda_9 = R_1.$

From the eigen values, the dominant eigen value is λ_9.Therefore, the control reproduction number for the model is given by:

$$R_C = R_1 = \frac{g_1\varepsilon_2}{h_1h_2} + \frac{g_2(\varepsilon_1h_2 + \varepsilon_2\phi_1)}{h_1h_2h_3} + \frac{g_5\varepsilon_2\vartheta_2}{h_1h_2h_7} + \frac{g_6\vartheta_3(\varepsilon_1h_2 + \varepsilon_2\phi_1)}{h_1h_2h_3h_8} \tag{4.82}$$

Simplifying further:

$$R_C = \frac{g_1\varepsilon_2h_3h_7h_8 + g_2h_7h_8(\varepsilon_1h_2 + \varepsilon_2\phi_1) + g_5\varepsilon_2\vartheta_2h_3h_8 + g_6\vartheta_3h_7(\varepsilon_1h_2 + \varepsilon_2\phi_1)}{h_1h_2h_3h_7h_8} \tag{4.83}$$

4.4.5 Local stability of the disease-free equilibrium

The following theorem establishes the local stability of the endemic equilibrium point for the pulmonary TB and pneumonia co-infection model:

Theorem 4.8. *The disease-free equilibrium point is locally asymptotically stable if* $R_C < 1$ *and unstable if* $R_C > 1$.

Proof. To prove the local stability of the disease-free equilibrium, the Jacobian matrix of system (3.8) is evaluated at the disease-free equilibrium B_1^0, given as:

$$J(B_1^0) = \begin{bmatrix}
-\mu & 0 & 0 & -r_1 & -r_2 & -r_3 & -\beta_1S^0 & 0 & -r_4 & -r_5 & -r_6 & -r_7 & \kappa \\
0 & -\mu & 0 & -r_8 & -r_9 & -r_{10} & -r_{11} & 0 & -r_{12} & -r_{13} & -r_{14} & -r_{15} & 0 \\
0 & 0 & -h_1 & g_1 & g_2 & g_3 & g_4 & 0 & g_5 & g_6 & g_7 & g_8 & 0 \\
0 & 0 & \varepsilon_2 & -h_2 & 0 & 0 & 0 & 0 & 0 & 0 & 0 & 0 & 0 \\
0 & 0 & \varepsilon_1 & \phi_1 & -h_3 & 0 & 0 & 0 & 0 & 0 & 0 & 0 & 0 \\
0 & 0 & 0 & 0 & 0 & -h_4 & 0 & 0 & 0 & 0 & 0 & 0 & 0 \\
0 & 0 & 0 & 0 & 0 & \phi_2 & -h_5 & 0 & 0 & 0 & 0 & 0 & 0 \\
0 & 0 & \vartheta_1 & 0 & 0 & 0 & 0 & -h_6 & 0 & 0 & 0 & 0 & 0 \\
0 & 0 & 0 & \vartheta_2 & 0 & 0 & 0 & 0 & -h_7 & 0 & \phi_3 & 0 & 0 \\
0 & 0 & 0 & 0 & \vartheta_3 & 0 & 0 & 0 & 0 & -h_8 & 0 & \phi_4 & 0 \\
0 & 0 & 0 & 0 & 0 & \vartheta_4 & 0 & 0 & 0 & 0 & -h_9 & 0 & 0 \\
0 & 0 & 0 & 0 & 0 & 0 & \vartheta_5 & 0 & 0 & 0 & 0 & -h_{10} & 0 \\
0 & 0 & 0 & 0 & 0 & 0 & 0 & \alpha_1 & \alpha_2 & \alpha_3 & 0 & 0 & -h_{11}
\end{bmatrix} \tag{4.84}$$

where:

$r_1 = \beta_1\eta_6 S^0$, $r_2 = \beta_1\eta_4 S^0$, $r_3 = \beta_1\eta_5 S^0$, $r_4 = \beta_1\eta_{10} S^0$, $r_5 = \beta_1\eta_8 S^0$, $r_6 = \beta_1\eta_9 S^0$, $r_7 = \beta_1\eta_7 S^0$, $r_8 = \beta_1(1-\rho)\eta_6 V^0$, $r_9 = \beta_1(1-\rho)\eta_4 V^0$, $r_{10} = \beta_1(1-\rho)\eta_5 V^0$, $r_{11} = \beta_1(1-\rho)V^0$, $r_{12} = \beta_1(1-\rho)\eta_{10} V^0$, $r_{13} = \beta_1(1-\rho)\eta_8 V^0$, $r_{14} = \beta_1(1-\rho)\eta_9 V^0$, $r_{15} = \beta_1(1-\rho)\eta_7 V^0$, $h_6 = \mu + \alpha_1$, and $h_{11} = \mu + \kappa$.

The eigenvalues of equation (4.84) are obtained as follows:

Either,

$$(\mu+\lambda)(\mu+\lambda)(h_4+\lambda)(h_5+\lambda)(h_9+\lambda)(h_{10}+\lambda)(h_{11}+\lambda) = 0 \tag{4.85}$$

Or

$$\begin{vmatrix} -h_1-\lambda & g_1 & g_2 & 0 & g_5 & g_6 \\ \varepsilon_2 & -h_2-\lambda & 0 & 0 & 0 & 0 \\ \varepsilon_1 & \phi_1 & -h_3-\lambda & 0 & 0 & 0 \\ \vartheta_1 & 0 & 0 & -h_6-\lambda & 0 & 0 \\ 0 & \vartheta_2 & 0 & 0 & -h_7-\lambda & 0 \\ 0 & 0 & \vartheta_3 & 0 & 0 & -h_8-\lambda \end{vmatrix} = 0 \tag{4.86}$$

Then, by the Routh-Hurwitz criterion, equation (4.85) has strictly negative roots, given as follows:

$\lambda_1 = \lambda_2 = -\mu, \lambda_3 = -h_4, \lambda_4 = -h_5, \lambda_5 = -h_9, \lambda_6 = -h_{10}, \lambda_7 = -h_{11}$.

The characteristic polynomial of equation (4.86) is given by:

$$N_1\lambda^6 + N_2\lambda^5 + N_3\lambda^4 + N_4\lambda^3 + N_5\lambda^2 + N_6\lambda + N_7 = 0 \tag{4.87}$$

where $N_1, N_2, N_3, N_4, N_5, N_6$, and N_7 are determined as follows:

$N_1 = 1 > 0$,

$N_2 = h_1 + h_2 + h_3 + h_6 + h_7 + h_8$,

$N_3 = h_8(h_1+h_2+h_3+h_6+h_7) + h_7(h_1+h_2+h_6) + h_6(h_1+h_2+h_3) +$

$h_3(h_1+h_2) + h_1h_2 - g_1\varepsilon_2 - g_2\varepsilon_1$,

$N_4 = h_8\big[h_7(h_1+h_2+h_3+h_6) + h_6(h_1+h_2+h_3) + h_3(h_1+h_2) + h_1h_2 -$

$(g_1\varepsilon_2 + g_2\varepsilon_1)\big] + h_7\big[h_6(h_1 + h_2 + h_3) + h_3(h_1 + h_2) + h_1h_2 - (g_1\varepsilon_2 + g_2\varepsilon_1)\big] +$
$h_6\big[h_3(h_1 + h_2) + h_1h_2 - (g_1\varepsilon_2 + g_2\varepsilon_1)\big] + h_3(h_1h_2 - g_1\varepsilon_2) - h_2g_2\varepsilon_1 - \phi_1g_2\varepsilon_2 -$
$\vartheta_2g_5\varepsilon_2 - \vartheta_3g_6\varepsilon_1,$
$N_5 = h_8\big[h_6h_7(h_1 + h_2 + h_3) + h_3h_7(h_1 + h_2) + h_2h_7h_1 + h_3h_6(h_1 + h_2) +$
$h_1h_2(h_3 + h_6) - g_1\varepsilon_2(h_3 + h_6 + h_7) \quad - g_2\phi_1\varepsilon_2 - g_2\varepsilon_1(h_2 + h_6 + h_7) - g_5\vartheta_2\varepsilon_2\big] +$
$h_7\big[h_1h_2(h_3 + h_6) + h_3h_6(h_1 + h_2) - g_1\varepsilon_2(h_3 + h_6) - g_2\phi_1\varepsilon_2 - g_2\varepsilon_1(h_2 + h_6) - g_6\vartheta_3\varepsilon_1\big] +$
$h_6\big[h_3h_2h_1 - g_1\varepsilon_2h_3 - g_2\phi_1\varepsilon_2 - g_2\varepsilon_1h_2 - g_5\vartheta_2\varepsilon_2 - g_6\vartheta_3\varepsilon_1\big] - g_5\vartheta_2\varepsilon_2h_3 - g_6\vartheta_3\varepsilon_1h_2 -$
$g_6\vartheta_3\phi_1\varepsilon_2,$
$N_6 = h_4\big[h_1h_2(h_3h_6 + h_3h_7 + h_6h_7) + h_3h_6h_7(h_1 + h_2) - g_1\varepsilon_2(h_3h_6 + h_3h_7 + h_6h_7) -$
$g_2\phi_1\varepsilon_2(h_6 + h_7) - g_2\varepsilon_1(h_2h_6 + h_2h_7 + h_6h_7) - g_5\vartheta_2\varepsilon_2(h_3 + h_6)\big] +$
$h_7\big[h_1h_2h_3h_6 - g_1\varepsilon_2h_3h_6 - g_2\varepsilon_1h_6h_7 - g_2\phi_1\varepsilon_2h_6 - g_6\vartheta_3\varepsilon_1(h_2 + h_6) - g_6\phi_1\vartheta_3\varepsilon_2\big] +$
$h_6\big[- g_5\vartheta_2\varepsilon_2h_3 - g_6\vartheta_3(h_2\varepsilon_1 + \varepsilon_2\phi_1)\big],$
$N_7 = h_1h_2h_3h_7h_8 - \big[g_1\varepsilon_2h_3h_7h_8 + g_2h_7h_8(\varepsilon_1h_2 + \varepsilon_2\phi_1) + g_5\varepsilon_2\vartheta_2h_3h_8 + g_6\vartheta_3h_7(\varepsilon_1h_2 +$
$\varepsilon_2\phi_1)\big].$

By the Routh-Hurwitz criterion:

$N_1 > 0, N_2 > 0, N_3 > 0, N_4 > 0, N_5 > 0, N_6 > 0$ and $N_7 > 0$

From $N_7 > 0$, it follows that:

$h_1h_2h_3h_7h_8 - \Big[g_1\varepsilon_2h_3h_7h_8 + g_2h_7h_8(\varepsilon_1h_2 + \varepsilon_2\phi_1) + g_5\varepsilon_2\vartheta_2h_3h_8 + g_6\vartheta_3h_7(\varepsilon_1h_2 + \varepsilon_2\phi_1)\Big] >$
$0.$

$$\Rightarrow g_1\varepsilon_2h_3h_7h_8 + g_2h_7h_8(\varepsilon_1h_2 + \varepsilon_2\phi_1) + g_5\varepsilon_2\vartheta_2h_3h_8 + g_6\vartheta_3h_7(\varepsilon_1h_2 + \varepsilon_2\phi_1) < h_1h_2h_3h_7h_8$$

$$\Rightarrow \frac{g_1\varepsilon_2h_3h_7h_8 + g_2h_7h_8(\varepsilon_1h_2 + \varepsilon_2\phi_1) + g_5\varepsilon_2\vartheta_2h_3h_8 + g_6\vartheta_3h_7(\varepsilon_1h_2 + \varepsilon_2\phi_1)}{h_1h_2h_3h_7h_8} < 1 \quad (4.88)$$

Comparing Equation (4.83) and inequality (4.88) gives:

$$R_C < 1 \quad (4.89)$$

Thus, the disease-free equilibrium for this model is locally asymptotically stable if $R_C < 1$.

4.4.6 Global stability of disease-free equilibrium

The Castillo-Chavez method was used to investigate the global stability of the disease-free equilibrium, as illustrated by Castillo-Chavez and Song (2004). The model system (3.8) is first written as:

$$\begin{cases} \dfrac{dX}{dt} = F(X, Z), \\ \dfrac{dZ}{dt} = G(X, Z). \end{cases} \tag{4.90}$$

where:

$X = (S, V, R)^T$ represents the uninfected population.

$Z = (E, I_a, I_S, I_{aP}, I_{SP}, T_E, T_a, T_S, T_{aP}, T_{SP})^T$ represents the infected population.

The fixed point of system (3.8) is denoted by:

$U = (X^*, 0) = (\frac{(1-Q)}{\mu}, \frac{Q}{\mu}, 0, 0, 0, 0, 0, 0, 0, 0, 0, 0, 0)$

Theorem 4.9 establishes the global stability of the endemic equilibrium point for the pulmonary TB and pneumonia co-infection model.

Theorem 4.9. *The equilibrium point $U = (X^*, 0)$ is globally asymptotically stable if $R_C < 1$ and satisfies conditions (K_1) and (K_2); otherwise, it is unstable.*

$(K_1) : \frac{dX}{dt} = F(X, 0)$*, X^* is globally asymptotically stable*

$(K_2) : (G, Z) = AZ - \hat{G}(X, Z), \quad \hat{G}(X, Z) \geq 0 \quad$ *for* $\quad (X, Z) \in \mathbb{R}^{13}_+$.

Here, $A = D_Z G(X, Z)$ is a Metzler matrix.

Proof. From system (3.8), $F(X, Z)$ and $G(X, Z)$ are given as:

$$F(X, Z) = \begin{bmatrix} (1-Q)\Lambda + \kappa R - (\lambda_1 + \mu)S \\ Q\Lambda - \big[(1-\rho)\lambda_1 + \mu\big]V \\ \alpha_1 T_E + \alpha_2 T_a + \alpha_3 T_S - (\kappa + \mu)R \end{bmatrix}, \tag{4.91}$$

$$G(X,Z)=\begin{bmatrix} \lambda_1 S+(1-\rho)\lambda_1 V-\dfrac{\varepsilon_1}{1+nE}+\dfrac{\varepsilon_2}{1+nE}+\vartheta_1+\mu E\dfrac{\varepsilon_2 E}{1+nE} \\ -(\lambda_2+\varphi_1+\vartheta_2+\mu)I_a\dfrac{\varepsilon_2 E}{1+nE}+\varphi_1 I_a \\ -(\lambda_2+\vartheta_3+\gamma_1+\mu)I_S\lambda_2 I_a \\ -(\mu+\gamma_5+\varphi_2+\vartheta_4)I_a P\lambda_2 I_S+\varphi_2 I_a P \\ -(\gamma_2+\vartheta_5+\mu)I_S P\vartheta_1 E-(\mu+\alpha_1)T_E\vartheta_2 I_a+\varphi_3 T_a P \\ -(\mu+\alpha_2)T_a\vartheta_3 I_S+\varphi_4 T_S P-\mu+\gamma_4+\alpha_3 T_S\vartheta_4 I_a P-\mu+\varphi_3 T_a P \\ \vartheta_5 I_S P-\mu+\varphi_4+\gamma_3 T_S P \end{bmatrix}. \quad (4.92)$$

Condition (K_1) examines the global asymptotic stability of X^* as follows:

From the first, second, and twelfth equations of system (3.8), when there is no infection (i.e., $\lambda_1=0, T_E=T_a=T_S=R=0$), they yield:

$$\frac{dX}{dt}\Big|_{Z=0}=\begin{bmatrix}(1-Q)\Lambda-\mu S\\ Q\Lambda-\mu V\\ 0\end{bmatrix} \quad (4.93)$$

The first equation of system (4.93) is given by:

$$\frac{dS}{dt}=(1-Q)\Lambda-\mu S \quad (4.94)$$

Solving equation (4.94) yields:

$$S(t)=\frac{(1-Q)\Lambda}{\mu}+\Big(S(0)-\frac{(1-Q)\Lambda}{\mu}\Big)e^{-\mu t}$$

As $t\to\infty$, the solution $S(t)\to\frac{(1-Q)\Lambda}{\mu}$.

Similarly, solving the second equation of system (4.93) and taking the limit as t approaches infinity gives $V(t)\to\frac{Q\Lambda}{\mu}$

$S(t)\to\frac{(1-Q)\Lambda}{\mu}$ and $V(t)\to\frac{Q\Lambda}{\mu}$ imply the global convergence of Equation (4.30) in Ω_1. Hence,

$$X^*=\left(\frac{(1-Q)\Lambda}{\mu},\frac{Q\Lambda}{\mu},0\right)$$

is globally asymptotically stable, satisfying condition (K_1). Global stability under Condition (K_2) is examined as follows:

The matrix A is given as:

$$A = \begin{bmatrix} -t_1 & H_1 & H_2 & H_3 & H_4 & 0 & H_5 & H_6 & H_7 & H_8 \\ H_9 & -t_2 & 0 & 0 & 0 & 0 & 0 & 0 & 0 & 0 \\ H_{10} & \phi_1 & -t_3 & 0 & 0 & 0 & 0 & 0 & 0 & 0 \\ 0 & \lambda_2 & 0 & -t_4 & 0 & 0 & 0 & 0 & 0 & 0 \\ 0 & 0 & \lambda_2 & \phi_2 & -t_5 & 0 & 0 & 0 & 0 & 0 \\ \vartheta_1 & 0 & 0 & 0 & 0 & -t_6 & 0 & 0 & 0 & 0 \\ 0 & \vartheta_2 & 0 & 0 & 0 & 0 & -t_7 & 0 & \phi_3 & 0 \\ 0 & 0 & \vartheta_3 & 0 & 0 & 0 & 0 & -t_8 & 0 & \phi_4 \\ 0 & 0 & 0 & \vartheta_4 & 0 & 0 & 0 & 0 & -t_9 & 0 \\ 0 & 0 & 0 & 0 & \vartheta_5 & 0 & 0 & 0 & 0 & -t_{10} \end{bmatrix} \tag{4.95}$$

here:

$$t_1 = \frac{\varepsilon_1}{1+nE} + \frac{\varepsilon_2}{1+nE} + \vartheta_1 + \mu,$$

$$H_1 = \beta_1\eta_6[S + (1-\rho)V], \quad H_2 = \beta_1\eta_4[S + (1-\rho)V], \quad H_3 = \beta_1\eta_5[S + (1-\rho)V],$$

$$H_4 = \beta_1[S + (1-\rho)V], \quad H_5 = \beta_1\eta_{10}[S + (1-\rho)V], \quad H_6 = \beta_1\eta_8[S + (1-\rho)V],$$

$$H_7 = \beta_1\eta_9[S + (1-\rho)V], \quad H_8 = \beta_1\eta_7[S + (1-\rho)V], \quad H_9 = \frac{\varepsilon_2}{1+nE}, \quad H_{10} = \frac{\varepsilon_1}{1+nE},$$

$$t_2 = \lambda_2 + \phi_1 + \vartheta_2 + \mu, \quad t_3 = \lambda_2 + \vartheta_3 + \gamma_1 + \mu, \quad t_4 = \mu + \gamma_5 + \phi_2 + \vartheta_4,$$

$$t_5 = \gamma_2 + \vartheta_5 + \mu, \quad t_6 = \mu + \alpha_1, \quad t_7 = \mu + \alpha_2, \quad t_8 = \mu + \gamma_4 + \alpha_3,$$

$$t_9 = \mu + \phi_3, \quad t_{10} = \mu + \phi_4 + \gamma_3.$$

Computing AZ gives:

$$AZ = \begin{bmatrix} -t_1E + H_1I_a + H_2I_S + H_3I_{aP} + H_4I_{SP} + H_5T_a + H_6T_S + H_7T_{aP} + H_8T_{SP} \\ H_9E - t_2I_a \\ H_{10}E + \phi_1I_a - t_3I_S \\ \lambda_2I_a - t_4I_{aP} \\ \lambda_2I_S + \phi_2I_{aP} - t_5I_{SP} \\ \vartheta_1E - t_6T_E \\ \vartheta_2I_a - t_7T_a + \phi_3T_{aP} \\ \vartheta_3I_S - t_8T_S + \phi_4T_{SP} \\ \vartheta_4I_{aP} - t_9T_{aP} \\ \vartheta_5I_{SP} - t_{10}T_{SP} \end{bmatrix} \tag{4.96}$$

Then,

$$\hat{G}(X,Z) = AZ - G(X,Z),$$

which, upon computation, gives:

$$\hat{G}(X,Z) = \begin{bmatrix} \hat{G}_1(X,Z) \\ \hat{G}_2(X,Z) \\ \hat{G}_3(X,Z) \\ \hat{G}_4(X,Z) \\ \hat{G}_5(X,Z) \\ \hat{G}_6(X,Z) \\ \hat{G}_7(X,Z) \\ \hat{G}_8(X,Z) \\ \hat{G}_9(X,Z) \\ \hat{G}_{10}(X,Z) \end{bmatrix} = \begin{bmatrix} \beta_1(\eta_6I_a + \eta_4I_S + \eta_5I_{aP} + I_{SP} + \eta_{10}T_a + \eta_8T_S + \eta_9T_aP + \eta_7T_{SP})\big[(S^0 - S) + (V^0 - V)(1-\rho)\big] \\ 0 \\ 0 \\ 0 \\ 0 \\ 0 \\ 0 \\ 0 \\ 0 \\ 0 \end{bmatrix} \tag{4.97}$$

Since both the susceptible and vaccinated populations are bounded by $S \leq S^0$ and $V \leq V^0$, and $0 \leq \rho \leq 1$, we have $\hat{G}_1(X,Z) \geq 0$ and $\hat{G}_i(X,Z) = 0$ for $i = 2,3,\ldots,9$. Thus, $\hat{G}(X,Z) \geq 0$, and Condition (K_2) is satisfied. Since both Conditions (K_1) and (K_2) hold, the equilibrium point $U = (X^*, 0)$ is globally asymptotically stable whenever $R_c < 1$.

4.4.7 The endemic equilibrium

The steady state, in which pulmonary TB persists in the presence of opportunistic pneumonia within the community, is referred to as the endemic equilibrium of the system (3.8). At

this equilibrium, the rate of change of the population in each class is zero. In the endemic equilibrium, the natural immunity parameter n is assumed to approach zero. Hence, the model system (3.8) can be represented as:

$$\begin{cases} 0 = (1-Q)\Lambda + \kappa R^* - (\lambda_1 + \mu)S^*, \\ 0 = Q\Lambda - [(1-\rho)\lambda_1 + \mu]V^*, \\ 0 = \lambda_1 S^* + (1-\rho)\lambda_1 V^* - (\varepsilon_2 + \varepsilon_1 + \vartheta_1 + \mu)E^*, \\ 0 = \varepsilon_2 E^* - (\lambda_2 + \phi_1 + \mu + \vartheta_2)I_a^*, \\ 0 = \varepsilon_1 E^* + \phi_1 I_a^* - (\lambda_2 + \vartheta_3 + \mu + \gamma_1)I_S^*, \\ 0 = \lambda_2 I_a^* - (\mu + \gamma_5 + \phi_2 + \vartheta_4)I_{aP}^*, \\ 0 = \lambda_2 I_S^* + \phi_2 I_{aP}^* - (\gamma_2 + \vartheta_5 + \mu)I_{SP}^*, \\ 0 = \vartheta_1 E^* - (\mu + \alpha_1)T_E^*, \\ 0 = \vartheta_2 I_a^* + \phi_3 T_{aP}^* - (\mu + \alpha_2)T_a^*, \\ 0 = \vartheta_3 I_S^* + \phi_4 T_{SP}^* - (\mu + \gamma_4 + \alpha_3)T_S^*, \\ 0 = \vartheta_4 I_{aP}^* - (\mu + \phi_3)T_{aP}^*, \\ 0 = \vartheta_5 I_{SP}^* - (\mu + \phi_4 + \gamma_3)T_{SP}^*, \\ 0 = \alpha_1 T_E^* + \alpha_2 T_a^* + \alpha_3 T_S^* - (\mu + \kappa)R^*. \end{cases} \tag{4.98}$$

The steady-state solution for system (4.98) is given by:

$B_1^* = \left(S^*, V^*, E^*, I_a^*, I_S^*, I_{aP}^*, I_{SP}^*, T_E^*, T_a^*, T_S^*, T_{aP}^*, T_{SP}^*, R^*\right)$,
where:

$$S^* = \frac{(1-Q)\Lambda + \kappa R^*}{\lambda_1^{**} + \mu},$$

$$V^* = \frac{Q\Lambda}{(1-\rho)\lambda_1^{**} + \mu},$$

$$E^* = \frac{\lambda_1^{**}\left[((1-\rho)\lambda_1^{**} + \mu)((1-Q)\Lambda + \kappa R^*) + (\lambda_1^{**} + \mu)(1-\rho)Q\Lambda\right]}{(\lambda_1^{**} + \mu)(\epsilon_1 + \epsilon_2 + \vartheta_1 + \mu)((1-\rho)\lambda_1^{**} + \mu)},$$

$$I_a^* = \frac{\epsilon_2\lambda_1^{**}\left[((1-\rho)\lambda_1^{**} + \mu)((1-Q)\Lambda + \kappa R^*) + (\lambda_1^{**} + \mu)(1-\rho)Q\Lambda\right]}{(\lambda_2^{**} + \phi_1 + \mu + \vartheta_2)(\lambda_1^{**} + \mu)(\epsilon_1 + \epsilon_2 + \vartheta_1 + \mu)((1-\rho)\lambda_1^{**} + \mu)},$$

$$I_S^* = \frac{\lambda_1^{**}\left[((1-\rho)\lambda_1^{**} + \mu)((1-Q)\Lambda + \kappa R^*) + (\lambda_1^{**} + \mu)(1-\rho)Q\Lambda\right]\left[(\lambda_2^{**} + \vartheta_2 + \phi_1 + \mu)\epsilon_1 + \phi_1\epsilon_2\right]}{(\lambda_2^{**} + \vartheta_3 + \mu + \gamma_1)(\lambda_2^{**} + \phi_1 + \mu + \vartheta_2)(\lambda_1^{**} + \mu)(\epsilon_1 + \epsilon_2 + \vartheta_1 + \mu)((1-\rho)\lambda_1^{**} + \mu)},$$

$$I_{aP}^* = \frac{\lambda_2^{**}\epsilon_2\lambda_1^{**}\left[((1-\rho)\lambda_1^{**} + \mu)((1-Q)\Lambda + \kappa R^*) + (\lambda_1^{**} + \mu)(1-\rho)Q\Lambda\right]}{(\mu + \gamma_5 + \phi_2 + \vartheta_4)(\lambda_2^{**} + \phi_1 + \mu + \vartheta_2)(\lambda_1^{**} + \mu)(\epsilon_1 + \epsilon_2 + \vartheta_1 + \mu)((1-\rho)\lambda_1^{**} + \mu)},$$

$$I_{SP}^* = \frac{D_4\lambda_2^{**}\left[(\mu + \gamma_5 + \phi_2 + \vartheta_4)((\lambda_2^{**} + \vartheta_2 + \phi_1 + \mu)\epsilon_1 + \phi_1\epsilon_2) + (\lambda_2^{**} + \vartheta_3 + \mu + \gamma_1)\phi_2\epsilon_2\right]}{(\gamma_2 + \vartheta_5 + \mu)(\lambda_2^{**} + \vartheta_3 + \mu + \gamma_1)(\mu + \gamma_5 + \phi_2 + \vartheta_4)(\lambda_2^{**} + \phi_1 + \mu + \vartheta_2)(\lambda_1^{**} + \mu)(\epsilon_1 + \epsilon_2 + \vartheta_1 + \mu)((1-\rho)\lambda_1^{**} + \mu)},$$

$$T_E^* = \frac{\vartheta_1\lambda_1^{**}\left[((1-\rho)\lambda_1^{**} + \mu)((1-Q)\Lambda + \kappa R^*) + (\lambda_1^{**} + \mu)(1-\rho)Q\Lambda\right]}{(\mu + \alpha_1)(\lambda_1^{**} + \mu)(\epsilon_1 + \epsilon_2 + \vartheta_1 + \mu)},$$

$$T_a^* = \frac{\epsilon_2\lambda_1^{**}\left[((1-\rho)\lambda_1^{**} + \mu)((1-Q)\Lambda + \kappa R^*) + (\lambda_1^{**} + \mu)(1-\rho)Q\Lambda\right]\left[\vartheta_2(\mu + \phi_3)(\mu + \gamma_5 + \phi_2 + \vartheta_4) + \lambda_2^{**}\phi_3\vartheta_4\right]}{(\alpha_2 + \mu)(\mu + \phi_3)(\mu + \gamma_5 + \phi_2 + \vartheta_4)(\lambda_2^{**} + \phi_1 + \mu + \vartheta_2)(\lambda_1^{**} + \mu)(\epsilon_1 + \epsilon_2 + \vartheta_1 + \mu)((1-\rho)\lambda_1^{**} + \mu)},$$

$$T_S^* = \frac{D_4(\mu + \gamma_5 + \phi_2 + \vartheta_4)\left[(\lambda_2^{**} + \vartheta_2 + \phi_1 + \mu)\epsilon_1 + \phi_1\epsilon_2\right]\left[\vartheta_3(\mu + \phi_4 + \gamma_3)(\gamma_2 + \vartheta_5 + \mu) + \phi_4(\lambda_2^{**} + \vartheta_3 + \mu + \gamma_1)\phi_2\epsilon_2\vartheta_5\right]}{(\mu + \gamma_4 + \alpha_3)(\mu + \phi_4 + \gamma_3)(\gamma_2 + \vartheta_5 + \mu)(\lambda_2^{**} + \vartheta_3 + \mu + \gamma_1)(\mu + \gamma_5 + \phi_2 + \vartheta_4)(\lambda_2^{**} + \phi_1 + \mu + \vartheta_2)D_5},$$

$$T_{aP}^* = \frac{\vartheta_4\lambda_2^{**}\epsilon_2\lambda_1^{**}\left[((1-\rho)\lambda_1^{**} + \mu)((1-Q)\Lambda + \kappa R^*) + (\lambda_1^{**} + \mu)(1-\rho)Q\Lambda\right]}{(\mu + \phi_3)(\mu + \gamma_5 + \phi_2 + \vartheta_4)(\lambda_2^{**} + \phi_1 + \mu + \vartheta_2)(\lambda_1^{**} + \mu)(\epsilon_1 + \epsilon_2 + \vartheta_1 + \mu)((1-\rho)\lambda_1^{**} + \mu)},$$

$$T_{SP}^* = \frac{\vartheta_5 D_4\lambda_2^{**}\left[(\mu + \gamma_5 + \phi_2 + \vartheta_4)((\lambda_2^{**} + \vartheta_2 + \phi_1 + \mu)\epsilon_1 + \phi_1\epsilon_2) + (\lambda_2^{**} + \vartheta_3 + \mu + \gamma_1)\phi_2\epsilon_2\right]}{(\mu + \phi_4 + \gamma_3)(\gamma_2 + \vartheta_5 + \mu)(\lambda_2^{**} + \vartheta_3 + \mu + \gamma_1)(\mu + \gamma_5 + \phi_2 + \vartheta_4)(\lambda_2^{**} + \phi_1 + \mu + \vartheta_2)D_5},$$

$$R^* = \frac{\lambda_1^{**}\left[((1-\rho)\lambda_1^{**} + \mu)S^* + (\lambda_1^{**} + \mu)(1-\rho)Q\Lambda\right](D_6 + D_7 + D_8)}{D_9(\mu + \phi_3)(\mu + \gamma_5 + \phi_2 + \vartheta_4)(\mu + \phi_4 + \gamma_3)(\gamma_2 + \vartheta_5 + \mu)(\lambda_2^{**} + \vartheta_3 + \mu + \gamma_1)(\lambda_2^{**} + \phi_1 + \mu + \vartheta_2)A_5A_6A_7A_8}.$$

here,

$$D_4 = \lambda_1^{**}\left[((1-\rho)\lambda_1^{**} + \mu)((1-Q)\Lambda + \kappa R^*) + (\lambda_1^{**} + \mu)(1-\rho)Q\Lambda\right],$$

$$D_5 = (\lambda_1^{**} + \mu)(\varepsilon_1 + \varepsilon_2 + \vartheta_1 + \mu)((1-\rho)\lambda_1^{**} + \mu),$$

$$D_6 = \vartheta_1\alpha_1(\mu + \phi_3)(\mu + \gamma_5 + \phi_2 + \vartheta_4)(\mu + \phi_4 + \gamma_3)(\gamma_2 + \vartheta_5 + \mu)(\lambda_2^{**} + \vartheta_3 + \mu + \gamma_1)(\lambda_2^{**} + \phi_1 + \mu + \vartheta_2)A_2A_3,$$

$$D_7 = \varepsilon_2\alpha_2(\mu + \phi_4 + \gamma_3)(\gamma_2 + \vartheta_5 + \mu)(\lambda_2^{**} + \vartheta_3 + \mu + \gamma_1)\left[\vartheta_2(\mu + \phi_3)(\mu + \gamma_5 + \phi_2 + \vartheta_4) + \lambda_2^{**}\phi_3\vartheta_4\right]A_1A_3,$$

$$D_8 = (\mu + \phi_3)\left[(\mu + \gamma_5 + \phi_2 + \vartheta_4)((\lambda_2^{**} + \vartheta_2 + \phi_1 + \mu)\varepsilon_1 + \phi_1\varepsilon_2)\right]\left[\vartheta_3(\mu + \phi_4 + \gamma_3)(\gamma_2 + \vartheta_5 + \mu) + \phi_4(\lambda_2^{**} + \vartheta_3 + \mu + \gamma_1)\phi_2\varepsilon_2\vartheta_5\right]A_1A_2,$$

$$D_9 = (\varepsilon_1 + \varepsilon_2 + \vartheta_1 + \mu)((1-\rho)\lambda_1^{**} + \mu),$$

$$A_5 = (\alpha_1 + \mu),\ A_6 = (\alpha_2 + \mu),\ A_7 = (\mu + \gamma_4 + \alpha_3),\ A_8 = (\kappa + \mu).$$

4.4.8 Local stability of the endemic equilibrium

The local stability of the endemic equilibrium in the mathematical model of pulmonary TB and pneumonia co-infection is determined using Theorem 4.10.

Theorem 4.10. *A positive endemic equilibrium exists and is locally asymptotically stable whenever* $R_c > 1$.

Proof. The disease is endemic if:

$\frac{dE}{dt} > 0, \quad \frac{dI_a}{dt} > 0, \quad \frac{dI_S}{dt} > 0, \quad \frac{dI_{aP}}{dt} > 0, \quad \frac{dI_{SP}}{dt} > 0, \quad \frac{dT_E}{dt} > 0, \quad \frac{dT_a}{dt} > 0,$
$\frac{dT_S}{dt} > 0, \quad \frac{dT_{aP}}{dt} > 0, \quad \frac{dT_{SP}}{dt} > 0.$

Considering $\frac{dE}{dt} > 0$, it follows that:

$$\frac{dE}{dt} = \lambda_1 S + (1-\rho)\lambda_1 V - (\varepsilon_1 + \varepsilon_2 + \vartheta_1 + \mu)E > 0 \tag{4.99}$$

Inequality (4.99) simplifies to:

$$E < \frac{\lambda_1 S + (1-\rho)\lambda_1 V}{\varepsilon_1 + \varepsilon_2 + \vartheta_1 + \mu} \tag{4.100}$$

The endemicity of the coexistence of the two diseases is primarily driven by the spread of pulmonary tuberculosis, with pneumonia acting as an opportunistic disease. Hence, the force of infection for pulmonary TB is:

$$\lambda_1 = \beta_1\big(\eta_4 I_S + \eta_6 I_a + \eta_8 T_S + \eta_{10} T_a\big) \tag{4.101}$$

Substituting equation (4.101) into inequality (4.100), yields:

$$E < \frac{\beta_1\big(\eta_4 I_S + \eta_6 I_a + \eta_8 T_S + \eta_{10} T_a\big)[S + (1-\rho)V]}{\varepsilon_1 + \varepsilon_2 + \vartheta_1 + \mu} \tag{4.102}$$

From the steady-state system (4.98), the equilibrium values of the infectious and treated compartments for the spread of pulmonary TB are given by:

$$\begin{cases} I_a^* = \dfrac{\varepsilon_2 E^*}{\phi_1 + \mu + \vartheta_2}, \\ I_S^* = \dfrac{\varepsilon_1 E^* + \phi_1 I_a^*}{\vartheta_3 + \mu + \gamma_1}, \\ T_a^* = \dfrac{\vartheta_2 I_a^*}{\mu + \alpha_2}, \\ T_S^* = \dfrac{\vartheta_3 I_S^*}{\mu + \gamma_4 + \alpha_3}. \end{cases} \tag{4.103}$$

Substituting system (4.103) into inequality (4.102) yields:

$$E^* < \frac{\beta_1 \left[\dfrac{\eta_4\left(\varepsilon_1 E^* + \phi_1 I_a^*\right)}{\vartheta_3 + \mu + \gamma_1} + \dfrac{\eta_6 \varepsilon_2 E^*}{\phi_1 + \mu + \vartheta_2} + \dfrac{\eta_8 \vartheta_2 I_S^*}{\mu + \gamma_4 + \alpha_3} + \dfrac{\eta_{10} \vartheta_2 I_a^*}{\mu + \alpha_2} \right] \left(S + (1-\rho)V\right)}{\varepsilon_2 + \varepsilon_1 + \vartheta_1 + \mu} \tag{4.104}$$

Simplifying and factoring E^* leads to:

$$E^* < \frac{\left[g_1 \varepsilon_2 h_3 h_7 h_8 + g_2 h_7 h_8 \left(\varepsilon_1 h_2 + \varepsilon_2 \phi_1\right) + g_5 \varepsilon_2 \vartheta_2 h_3 h_8 + g_6 \vartheta_3 h_7 \left(h_2 \varepsilon_1 + \varepsilon_2 \phi_1\right) \right] E^*}{h_1 h_2 h_3 h_7 h_8} \tag{4.105}$$

Simplifying inequality (4.105) further yields:

$$1 < \frac{g_1 \varepsilon_2 h_3 h_7 h_8 + g_2 h_7 h_8 \left(\varepsilon_1 h_2 + \varepsilon_2 \phi_1\right) + g_5 \varepsilon_2 \vartheta_2 h_3 h_8 + g_6 \vartheta_3 h_7 \left(h_2 \varepsilon_1 + \varepsilon_2 \phi_1\right)}{h_1 h_2 h_3 h_7 h_8} \tag{4.106}$$

However,

$$\frac{g_1 \varepsilon_2 h_3 h_7 h_8 + g_2 h_7 h_8 \left(\varepsilon_1 h_2 + \varepsilon_2 \phi_1\right) + g_5 \varepsilon_2 \vartheta_2 h_3 h_8 + g_6 \vartheta_3 h_7 \left(h_2 \varepsilon_1 + \varepsilon_2 \phi_1\right)}{h_1 h_2 h_3 h_7 h_8} = R_c$$

Therefore, inequality (4.106) is rewritten as:

$$R_C > 1 \tag{4.107}$$

Thus, there is an endemic equilibrium for co -infection model when $R_C > 1$.

4.4.9 Global stability of the endemic equilibrium

The endemicity of the pulmonary tuberculosis and pneumonia co-infection model is established by considering the following theorem:

Theorem 4.11. *If $R_C > 1$, the endemic equilibrium of the system* (3.8) *is globally asymptotically stable.*

Proof. The method of Lyapunov functions is used to prove the global asymptotic stability of the endemic equilibrium. A Lyapunov function is proposed and defined as follows:

$$\begin{aligned} L = {} & (S - S^* + S^* \ln \tfrac{S^*}{S}) + (V - V^* + V^* \ln \tfrac{V^*}{V}) + (E - E^* + E^* \ln \tfrac{E^*}{E}) \\ & + (I_a - I_a^* + I_a^* \ln \tfrac{I_a^*}{I_a}) + (I_S - I_S^* + I_S^* \ln \tfrac{I_S^*}{I_S}) + (I_{aP} - I_{aP}^* + I_{aP}^* \ln \tfrac{I_{aP}^*}{I_{aP}}) \\ & + (I_{SP} - I_{SP}^* + I_{SP}^* \ln \tfrac{I_{SP}^*}{I_{SP}}) + (I_{SP} - I_{SP}^* + I_{SP}^* \ln \tfrac{I_{SP}^*}{I_{SP}}) \\ & + (T_E - T_E^* + T_E^* \ln \tfrac{T_E^*}{T_E}) + (T_a - T_a^* + T_a^* \ln \tfrac{T_a^*}{T_a}) + (T_S - T_S^* + T_S^* \ln \tfrac{T_S^*}{T_S}) \\ & + (T_{aP} - T_{aP}^* + T_{aP}^* \ln \tfrac{T_{aP}^*}{T_{aP}}) + (T_{SP} - T_{SP}^* + T_{SP}^* \ln \tfrac{T_{SP}^*}{T_{SP}}) \\ & + (R - R^* + R^* \ln \tfrac{R^*}{R}) \end{aligned} \tag{4.108}$$

Taking the derivative of equation (4.108) with respect to t gives:

$$\begin{aligned} \frac{dL}{dt} = {} & \frac{(S - S^*)}{S}\frac{dS}{dt} + \frac{(V - V^*)}{V}\frac{dV}{dt} + \frac{(E - E^*)}{E}\frac{dE}{dt} + \frac{(I_a - I_a^*)}{I_a}\frac{dI_a}{dt} \\ & + \frac{(I_S - I_S^*)}{I_S}\frac{dI_S}{dt} + \frac{(I_{aP} - I_{aP}^*)}{I_{aP}}\frac{dI_{aP}}{dt} + \frac{(I_{SP} - I_{SP}^*)}{I_{SP}}\frac{dI_{SP}}{dt} \\ & + \frac{(T_E - T_E^*)}{T_E}\frac{dT_E}{dt} + \frac{(T_a - T_a^*)}{T_a}\frac{dT_a}{dt} + \frac{(T_S - T_S^*)}{T_S}\frac{dT_S}{dt} \\ & + \frac{(T_{aP} - T_{aP}^*)}{T_{aP}}\frac{dT_{aP}}{dt} + \frac{(T_{SP} - T_{SP}^*)}{T_{SP}}\frac{dT_{SP}}{dt} + \frac{(R - R^*)}{R}\frac{dR}{dt} \end{aligned} \tag{4.109}$$

Substituting system (3.8) into equation (4.109) yields:

$$\frac{dL}{dt} = K_1 - Y_1 \tag{4.110}$$

If $K_1 \leq Y_1$, then $\dfrac{dL}{dt} \leq 0$, and $\dfrac{dL}{dt} = 0$ if and only if

$S = S^*, \quad V = V^*, \quad E = E^*, \quad I_a = I_a^*, \quad I_S = I_S^*, \quad I_{aP} = I_{aP}^*, \quad I_{SP} = I_{SP}^*,$

$T_E = T_E^*, \quad T_a = T_a^*, \quad T_S = T_S^*, \quad T_{aP} = T_{aP}^*, \quad T_{SP} = T_{SP}^*, \quad R = R^*.$

This implies that the largest compact invariant set in:

$$\{(S^*, V^*, E^*, I_a^*, I_S^*, I_{aP}^*, I_{SP}^*, T_E^*, T_a^*, T_S^*, T_{aP}^*, T_{SP}^*, R^*) \in \Omega_1 : \tfrac{dL}{dt} = 0\}$$

is the singleton endemic equilibrium point B_1^*. Thus, from LaSalle's invariance principle (La Salle, 1976), it is concluded that as $t \to \infty$, the solution of the model system (3.8) approaches the endemic equilibrium B_1^* when the control reproduction number $R_c > 1$. Therefore, the endemic equilibrium point B_1^* is globally asymptotically stable in the in-

variant set Ω_1 if $K_1 < Y_1$. K_1 and Y_1 are given as follows:

$$\begin{aligned}
K_1 = \Lambda + \kappa R + \frac{\kappa R^* S^*}{S} + \frac{\lambda_1 S^* E^*}{E} + (1-\rho)\lambda_1 V + \frac{(1-\rho)\lambda_1 V^* E^*}{E} \\
+ \varepsilon_2 E + \frac{\varepsilon_2 I_a^* E^*}{I_a} + \varepsilon_1 E + \frac{\varepsilon_1 I_S^* E^*}{I_S} + \phi_1 I_a + \frac{\phi_1 I_S^* I_a^*}{I_S} \\
+ \lambda_2 I_a + \frac{\lambda_2 I_{aP}^* I_a^*}{I_{aP}} + \lambda_2 I_s + \frac{\lambda_2 I_{SP}^* I_s^*}{I_{SP}} + \phi_2 I_{aP} + \frac{\phi_2 I_{SP}^* I_{aP}^*}{I_{SP}} \\
+ \vartheta_1 E + \frac{\vartheta_1 T_E^* E^*}{T_E} + \vartheta_2 I_a + \frac{\vartheta_2 I_a^* T_a^*}{T_a} + \phi_3 T_{aP} + \frac{\phi_3 T_a^* T_{aP}^*}{T_a} \\
+ \vartheta_3 I_S + \frac{\vartheta_3 I_S^* T_S^*}{T_S} + \phi_4 T_{aP} + \frac{\phi_4 T_S^* T_{aP}^*}{T_S} + \vartheta_4 I_{aP} + \frac{\vartheta_4 T_{aP}^* I_{aP}^*}{T_{aP}} \\
+ \vartheta_5 I_{SP} + \frac{\vartheta_5 T_{SP}^* I_{SP}^*}{T_{SP}} + \alpha_1 T_E + \frac{\alpha_1 T_E^* R^*}{R} + \alpha_2 T_a + \frac{\alpha_2 T_a^* R^*}{R} \\
+ \alpha_3 T_S + \frac{\alpha_3 T_S^* R^*}{R} + \frac{\Lambda Q V^*}{V} + \lambda_1 S.
\end{aligned}$$

$$\begin{aligned}
Y_1 = \frac{\Lambda S^*}{S} + \frac{\Lambda Q S^*}{S} + \frac{\kappa R S^*}{S} + \frac{\lambda_1 S E^*}{E} + (1-\rho)\lambda_1 V^* + \frac{(1-\rho)\lambda_1 E^*}{E^*} \\
+ \varepsilon_2 E^* + \frac{\varepsilon_2 E I_a^*}{I_a} + \varepsilon_1 E^* + \frac{\varepsilon_1 E I_S^*}{I_S} + \phi_1 I_a^* + \frac{\phi_1 I_a I_S^*}{I_S} \\
+ \lambda_2 I_a^* + \frac{\lambda_2 I_{aP}^* I_a}{I_{aP}} + \lambda_2 I_S^* + \frac{\lambda_2 I_{SP}^* I_S}{I_{SP}} + \phi_2 I_{aP}^* + \frac{\phi_2 I_{SP}^* I_{aP}}{I_{SP}} \\
+ \vartheta_1 E^* + \frac{\vartheta_1 E T_E^*}{T_E} + \vartheta_2 I_a^* + \frac{\vartheta_2 I_a T_a^*}{T_a} + \phi_3 T_{aP}^* + \frac{\phi_3 T_a^* T_{aP}}{T_a} \\
+ \vartheta_3 I_S^* + \frac{\vartheta_3 I_S T_S^*}{T_S} + \phi_4 T_{aP}^* + \frac{\phi_4 T_S^* T_{aP}}{T_S} + \alpha_1 T_E^* + \frac{\alpha_1 T_E R^*}{R} \\
+ \alpha_2 T_a^* + \frac{\alpha_2 T_a R^*}{R} + \alpha_3 T_S^* + \frac{\alpha_3 T_S R^*}{R} + \lambda_1 S^* + \frac{(S-S^*)^2}{S}(\lambda_1 + \mu) \\
+ \frac{(V-V^*)^2}{V}((1-\rho)\lambda_1 + \mu) + \frac{(E-E^*)^2}{E}(\varepsilon_2 + \varepsilon_1 + \vartheta_1 + \mu) \\
+ \frac{(I_a - I_a^*)^2}{I_a}(\vartheta_2 + \phi_1 + \lambda_2 + \mu) + \frac{(I_S - I_S^*)^2}{I_S}(\vartheta_3 + \gamma_1 + \lambda_2 + \mu) \\
+ \frac{(I_{aP} - I_{aP}^*)^2}{I_{aP}}(\phi_2 + \gamma_5 + \vartheta_4 + \mu) + \frac{(I_{SP} - I_{SP}^*)^2}{I_{SP}}(\gamma_2 + \vartheta_5 + \mu) \\
+ \frac{(T_E - T_E^*)^2}{T_E}(\alpha_1 + \mu) + \frac{(T_a - T_a^*)^2}{T_a}(\alpha_2 + \mu) + \frac{(T_S - T_S^*)^2}{T_S}(\gamma_4 + \alpha_3 + \mu) \\
+ \frac{(T_{aP} - T_{aP}^*)^2}{T_{aP}}(\mu + \phi_3) + \frac{(T_{SP} - T_{SP}^*)^2}{T_{SP}}(\mu + \phi_4 + \gamma_3) + \frac{(R-R^*)^2}{R}(\kappa + \mu).
\end{aligned}$$

4.4.10 Bifurcation analysis

The nature of the model's bifurcation is investigated using the center manifold theory as outlined by Castillo-Chavez and Song (2004). The analysis of the model's bifurcation considers two quantities: the coefficients a and b of the normal form representing the dynamics of the system on the center manifold. If $a < 0$ and $b > 0$, the bifurcation is forward. Conversely, if $a > 0$ and $b > 0$, the bifurcation is backward. The coefficients a and b are defined by the Castillo-Chavez theorem as follows:

$$\begin{cases} a = \sum_{k,j,i=1}^{n} v_k u_i u_j \frac{\partial^2 f_k}{\partial z_i \partial z_j}, \\ b = \sum_{k,i=1}^{n} v_k u_i \frac{\partial^2 f_k}{\partial z_i \partial \beta}. \end{cases} \tag{4.111}$$

Here, u is a right eigenvector of the Jacobian $J(B_1^*)$ for the system (3.8) at the disease-free equilibrium associated with the zero eigenvalue, while v is a left eigenvector of the Jacobian $J(B_1^*)$ associated with the zero eigenvalue. The derivation of z_i and f_k follows. To determine the bifurcation of the model system (3.8), the following changes of variables are made:

$$S = z_1,\ V = z_2,\ E = z_3,\ I_a = z_4,\ I_S = z_5,\ I_{aP} = z_6,\ I_{SP} = z_7,$$
$$T_E = z_8,\ T_a = z_9,\ T_S = z_{10},\ T_{aP} = z_{11},\ T_{SP} = z_{12},\ R = z_{13}.$$

Using vector notation, let

$$z = (z_1, z_2, z_3, z_4, z_5, z_6, z_7, z_8, z_9, z_{10}, z_{11}, z_{12}, z_{13})^T.$$

The model system (3.8) can then be written in the form:

$$\frac{dz}{dt} = F(t),$$

with

$$F = \big(f_1, f_2, f_3, f_4, f_5, f_6, f_7, f_8, f_9, f_{10}, f_{11}, f_{12}, f_{13}\big)^T$$

given by:

$$
\begin{cases}
\dfrac{dz_1}{dt} = f_1 = (1-Q)\Lambda + \kappa z_{13} - (\lambda_1 + \mu)z_1, \\
\dfrac{dz_2}{dt} = f_2 = Q\Lambda - \big[(1-\rho)\lambda_1 + \mu\big]z_2, \\
\dfrac{dz_3}{dt} = f_3 = \lambda_1 z_1 + (1-\rho)\lambda_1 z_2 - \Big(\frac{\varepsilon_1}{1+nz_3} + \frac{\varepsilon_2}{1+nz_3} + \vartheta_1 + \mu\Big)z_3, \\
\dfrac{dz_4}{dt} = f_4 = \dfrac{\varepsilon_2 z_3}{1+nz_3} - (\lambda_2 + \phi_1 + \mu + \vartheta_2)z_4, \\
\dfrac{dz_5}{dt} = f_5 = \dfrac{\varepsilon_1 z_3}{1+nz_3} + z_4 - (\lambda_2 + \vartheta_3 + \mu + \gamma_1)z_5, \\
\dfrac{dz_6}{dt} = f_6 = \lambda_2 z_4 - (\mu + \gamma_5 + \phi_2 + \vartheta_4)z_6, \\
\dfrac{dz_7}{dt} = f_7 = \lambda_2 z_5 + \phi_2 z_6 - (\gamma_2 + \vartheta_5 + \mu)z_7, \\
\dfrac{dz_8}{dt} = f_8 = \vartheta_1 z_3 - (\mu + \alpha_1)z_8, \\
\dfrac{dz_9}{dt} = f_9 = \vartheta_2 z_4 + \phi_3 z_{11} - (\mu + \alpha_2)z_9, \\
\dfrac{dz_{10}}{dt} = f_{10} = \vartheta_3 z_5 + \phi_4 z_{12} - (\mu + \gamma_4 + \alpha_3)z_{10}, \\
\dfrac{dz_{11}}{dt} = f_{11} = \vartheta_4 z_6 - (\mu + \phi_3)z_{11}, \\
\dfrac{dz_{12}}{dt} = f_{12} = \vartheta_5 z_7 - (\mu + \phi_4 + \gamma_3)z_{12}, \\
\dfrac{dz_{13}}{dt} = f_{13} = \alpha_1 z_8 + \alpha_2 z_9 + \alpha_3 z_{10} - (\mu + \kappa)z_{13}.
\end{cases}
\tag{4.112}
$$

Here,

$$\lambda_1 = \beta_1\big(z_7 + \eta_4 z_5 + \eta_5 z_6 + \eta_6 z_4 + \eta_7 z_{12} + \eta_8 z_{10} + \eta_9 z_{11} + \eta_{10} z_9\big),$$

and

$$\lambda_2 = \beta_2\big(z_7 + \epsilon_1 z_6 + \epsilon_2 z_{12} + \epsilon_3 z_{11}\big).$$

This method involves evaluating the Jacobian for the system (4.112) at the disease-free equilibrium, given by:

$$J(B_1^0) = \begin{bmatrix} -\mu & 0 & 0 & -r_1 & -r_2 & -r_3 & -\beta_1 S^0 & 0 & -r_4 & -r_5 & -r_6 & -r_7 & \kappa \\ 0 & -\mu & 0 & -r_8 & -r_9 & -r_{10} & -r_{11} & 0 & -r_{12} & -r_{13} & -r_{14} & -r_{15} & 0 \\ 0 & 0 & -h_1 & g_1 & g_2 & g_3 & g_4 & 0 & g_5 & g_6 & g_7 & g_8 & 0 \\ 0 & 0 & \varepsilon_2 & -h_2 & 0 & 0 & 0 & 0 & 0 & 0 & 0 & 0 & 0 \\ 0 & 0 & \varepsilon_1 & \phi_1 & -h_3 & 0 & 0 & 0 & 0 & 0 & 0 & 0 & 0 \\ 0 & 0 & 0 & 0 & 0 & -h_4 & 0 & 0 & 0 & 0 & 0 & 0 & 0 \\ 0 & 0 & 0 & 0 & 0 & \phi_2 & -h_5 & 0 & 0 & 0 & 0 & 0 & 0 \\ 0 & 0 & \vartheta_1 & 0 & 0 & 0 & 0 & -h_6 & 0 & 0 & 0 & 0 & 0 \\ 0 & 0 & 0 & \vartheta_2 & 0 & 0 & 0 & 0 & -h_7 & 0 & \phi_3 & 0 & 0 \\ 0 & 0 & 0 & 0 & \vartheta_3 & 0 & 0 & 0 & 0 & -h_8 & 0 & \phi_4 & 0 \\ 0 & 0 & 0 & 0 & 0 & \vartheta_4 & 0 & 0 & 0 & 0 & -h_9 & 0 & 0 \\ 0 & 0 & 0 & 0 & 0 & 0 & \vartheta_5 & 0 & 0 & 0 & 0 & -h_{10} & 0 \\ 0 & 0 & 0 & 0 & 0 & 0 & 0 & \alpha_1 & \alpha_2 & \alpha_3 & 0 & 0 & -h_{11} \end{bmatrix} \tag{4.113}$$

To implement the method, $R_c^* = 1$ was considered, and $\beta_1 = \beta_1^*$ was chosen as the bifurcation parameter. By using Mathematica software, the Jacobian of $\dfrac{dz}{dt} = F(z)$ at the disease-free equilibrium point with $\beta_1 = \beta_1^*$ has one of the eigenvalues as a simple zero. Hence, the Center Manifold theory is applied to analyze the dynamics of the system near $\beta_1 = \beta_1^*$.

The Jacobian $J(B_1^*)$ of the model near $\beta_1 = \beta_1^*$ has a right eigenvector associated with the zero eigenvalue, given by:

$$u = (u_1, u_2, u_3, u_4, u_5, u_6, u_7, u_8, u_9, u_{10}, u_{11}, u_{12}, u_{13})^T$$

which satisfies the system:

$$J(B_1^0)=\begin{bmatrix}
-\mu & 0 & 0 & -r_1 & -r_2 & -r_3 & -\beta_1 & 0 & -r_4 & -r_5 & -r_6 & -r_7 & \kappa \\
0 & -\mu & 0 & -r_8 & -r_9 & -r_{10} & -r_{11} & 0 & -r_{12} & -r_{13} & -r_{14} & -r_{15} & 0 \\
0 & 0 & -h_1 & g_1 & g_2 & g_3 & g_4 & 0 & g_5 & g_6 & g_7 & g_8 & 0 \\
0 & 0 & \varepsilon_2 & -h_2 & 0 & 0 & 0 & 0 & 0 & 0 & 0 & 0 & 0 \\
0 & 0 & \varepsilon_1 & \phi_1 & -h_3 & 0 & 0 & 0 & 0 & 0 & 0 & 0 & 0 \\
0 & 0 & 0 & 0 & 0 & -h_4 & 0 & 0 & 0 & 0 & 0 & 0 & 0 \\
0 & 0 & 0 & 0 & 0 & \phi_2 & -h_5 & 0 & 0 & 0 & 0 & 0 & 0 \\
0 & 0 & \vartheta_1 & 0 & 0 & 0 & 0 & -h_6 & 0 & 0 & 0 & 0 & 0 \\
0 & 0 & 0 & \vartheta_2 & 0 & 0 & 0 & 0 & -h_7 & 0 & \phi_3 & 0 & 0 \\
0 & 0 & 0 & 0 & \vartheta_3 & 0 & 0 & 0 & 0 & -h_8 & 0 & \phi_4 & 0 \\
0 & 0 & 0 & 0 & 0 & \vartheta_4 & 0 & 0 & 0 & 0 & -h_9 & 0 & 0 \\
0 & 0 & 0 & 0 & 0 & 0 & \vartheta_5 & 0 & 0 & 0 & 0 & -h_{10} & 0 \\
0 & 0 & 0 & 0 & 0 & 0 & 0 & \alpha_1 & \alpha_2 & \alpha_3 & 0 & 0 & -h_{11}
\end{bmatrix}\begin{bmatrix}u_1\\u_2\\u_3\\u_4\\u_5\\u_6\\u_7\\u_8\\u_9\\u_{10}\\u_{11}\\u_{12}\\u_{13}\end{bmatrix}=\begin{bmatrix}0\\0\\0\\0\\0\\0\\0\\0\\0\\0\\0\\0\\0\end{bmatrix} \tag{4.114}$$

Equation (4.114) can be expressed as:

$$\begin{cases}
-\mu u_1 - r_1 u_4 - r_2 u_5 - r_3 u_6 - \beta_1 u_7 - r_4 u_9 - r_5 u_{10} - r_6 u_{11} - r_7 u_{12} + \kappa u_{13} = 0, \\
-\mu u_2 - r_8 u_4 - r_9 u_5 - r_{10} u_6 - r_{11} u_7 - r_{12} u_9 - r_{13} u_{10} - r_{14} u_{11} - r_{15} u_{12} = 0, \\
-h_1 u_3 + g_1 u_4 + g_2 u_5 + g_3 u_6 + g_4 u_7 + g_5 u_9 + g_6 u_{10} + g_7 u_{11} + g_8 u_{12} = 0, \\
\varepsilon_2 u_3 - h_2 u_4 = 0, \\
\varepsilon_1 u_3 + \phi_1 u_4 - h_3 u_5 = 0, \\
-h_4 u_6 = 0, \\
\phi_2 u_6 - h_5 u_7 = 0, \\
\vartheta_1 u_3 - h_6 u_8 = 0, \\
\vartheta_2 u_4 - h_7 u_9 + \phi_3 u_{11} = 0, \\
\vartheta_3 u_5 - h_8 u_{10} + \phi_4 u_{12} = 0, \\
\vartheta_4 u_6 - h_9 u_{11} = 0, \\
\vartheta_5 u_7 - h_{10} u_{12} = 0, \\
\alpha_1 u_8 + \alpha_2 u_9 + \alpha_3 u_{10} - h_{11} u_{13} = 0.
\end{cases} \tag{4.115}$$

Solving the system of equations (4.115) gives:

$$
\begin{aligned}
u_1 &= \frac{-(r_1u_4 + r_2u_5 + r_4u_9 + r_5u_{10}) + \kappa u_{13}}{\mu} < 0,\\
u_2 &= \frac{-(r_8u_4 + r_9u_5 + r_{12}u_9 + r_{13}u_{10})}{\mu} < 0,\\
u_3 &= u_3 > 0, \quad u_4 = \frac{\varepsilon_2 u_3}{h_2} > 0, \quad u_5 = \frac{\varepsilon_1 u_3 + \phi_1 u_4}{h_3} > 0, \quad u_6 = 0, \quad u_7 = 0,\\
u_8 &= \frac{\vartheta_1 u_3}{h_6} > 0, \quad u_9 = \frac{\vartheta_2 u_4}{h_7}, \quad u_{10} = \frac{\vartheta_3 u_5}{h_8}, \quad u_{11} = 0, \quad u_{12} = 0,\\
u_{13} &= \frac{\alpha_1 u_8 + \alpha_2 u_9 + \alpha_3 u_{10}}{h_{11}} > 0.
\end{aligned}
$$

Furthermore, the Jacobian $[J(B_1^0)]$ of the model near $\beta_1 = \beta_1^*$ has a left eigenvector associated with the zero-eigenvalue given by:

$$v = (v_1, v_2, v_3, v_4, v_5, v_6, v_7, v_8, v_9, v_{10}, v_{11}, v_{12}, v_{13})^T$$

which satisfies the system:

$$
J(B_1^0) = \begin{bmatrix}
-\mu & 0 & 0 & -r_1 & -r_2 & -r_3 & -\beta_1 & 0 & -r_4 & -r_5 & -r_6 & -r_7 & \kappa \\
0 & -\mu & 0 & -r_8 & -r_9 & -r_{10} & -r_{11} & 0 & -r_{12} & -r_{13} & -r_{14} & -r_{15} & 0 \\
0 & 0 & -h_1 & g_1 & g_2 & g_3 & g_4 & 0 & g_5 & g_6 & g_7 & g_8 & 0 \\
0 & 0 & \varepsilon_2 & -h_2 & 0 & 0 & 0 & 0 & 0 & 0 & 0 & 0 & 0 \\
0 & 0 & \varepsilon_1 & \phi_1 & -h_3 & 0 & 0 & 0 & 0 & 0 & 0 & 0 & 0 \\
0 & 0 & 0 & 0 & 0 & -h_4 & 0 & 0 & 0 & 0 & 0 & 0 & 0 \\
0 & 0 & 0 & 0 & 0 & \phi_2 & -h_5 & 0 & 0 & 0 & 0 & 0 & 0 \\
0 & 0 & \vartheta_1 & 0 & 0 & 0 & 0 & -h_6 & 0 & 0 & 0 & 0 & 0 \\
0 & 0 & 0 & \vartheta_2 & 0 & 0 & 0 & 0 & -h_7 & 0 & \phi_3 & 0 & 0 \\
0 & 0 & 0 & 0 & \vartheta_3 & 0 & 0 & 0 & 0 & -h_8 & 0 & \phi_4 & 0 \\
0 & 0 & 0 & 0 & 0 & \vartheta_4 & 0 & 0 & 0 & 0 & -h_9 & 0 & 0 \\
0 & 0 & 0 & 0 & 0 & 0 & \vartheta_5 & 0 & 0 & 0 & 0 & -h_{10} & 0 \\
0 & 0 & 0 & 0 & 0 & 0 & 0 & \alpha_1 & \alpha_2 & \alpha_3 & 0 & 0 & -h_{11}
\end{bmatrix}
\begin{bmatrix} v_1 \\ v_2 \\ v_3 \\ v_4 \\ v_5 \\ v_6 \\ v_7 \\ v_8 \\ v_9 \\ v_{10} \\ v_{11} \\ v_{12} \\ v_{13} \end{bmatrix}
= \begin{bmatrix} 0 \\ 0 \\ 0 \\ 0 \\ 0 \\ 0 \\ 0 \\ 0 \\ 0 \\ 0 \\ 0 \\ 0 \\ 0 \end{bmatrix}
\tag{4.116}
$$

Equation (4.116) can be expressed as:

$$\begin{cases} -\mu v_1 = 0, \\ -\mu v_2 = 0, \\ -h_1 v_3 + \varepsilon_2 v_4 + \varepsilon_1 v_5 + \vartheta_1 v_8 = 0, \\ -r_1 v_1 - r_8 v_2 + g_1 v_3 - h_2 v_4 + \phi_1 v_5 + \vartheta_2 v_9 = 0, \\ -r_2 v_1 - r_9 v_2 + g_2 v_3 - h_3 v_5 + \vartheta_3 v_{10} = 0, \\ -r_3 v_1 - r_{10} v_2 + g_3 v_3 - h_4 v_6 + \phi_2 v_7 + \vartheta_4 v_{11} = 0, \\ -\beta_1 v_1 - r_{11} v_2 + g_4 v_3 - h_5 v_7 + \vartheta_5 v_{12} = 0, \\ -h_6 v_8 + \alpha_1 v_{13} = 0, \\ -r_4 v_1 - r_{12} v_2 + g_5 v_3 - h_7 v_9 + \alpha_2 v_{13} = 0, \\ -r_5 v_1 - r_{13} v_2 + g_6 v_3 - h_8 v_{10} + \alpha_3 v_{13} = 0, \\ -r_6 v_1 - r_{14} v_2 + g_7 v_3 + \phi_3 v_9 - h_9 v_{11} = 0, \\ -r_7 v_1 - r_{15} v_2 + g_8 v_3 + \phi_4 v_{10} - h_{10} v_{12} = 0, \\ \kappa v_1 - h_{11} v_{13} = 0. \end{cases} \tag{4.117}$$

Solving the system of equations (4.117) yields:

$v_1 = 0$, $v_2 = 0$, $v_3 = v_3 > 0$, $v_4 = \frac{g_1 v_3 + \phi_1 v_5 + \vartheta_2 v_9}{h_4} > 0$, $v_5 = \frac{g_2 v_3 + \vartheta_3 v_{10}}{h_3} > 0$,

$v_6 = \frac{g_3 v_3 + \phi_2 v_7 + \vartheta_4 v_{11}}{h_4} > 0$, $v_7 = \frac{g_4 v_3 + \vartheta_5 v_{12}}{h_5} > 0$, $v_8 = 0$, $v_9 = \frac{g_5 v_3 + \alpha_2 v_{13}}{h_7} > 0$,

$v_{10} = \frac{g_6 v_3 + \alpha_3 v_{13}}{h_8} > 0$, $v_{11} = \frac{g_7 v_3 + \phi_3 v_9}{h_9} > 0$, $v_{12} = \frac{g_8 v_3 + \phi_4 v_{10}}{h_{10}} > 0$, $v_{13} = 0$.

To compute a, $\frac{\partial^2 f_k}{\partial z_i \, \partial z_j}$ was determined as follows:

$\frac{\partial^2 f_3}{\partial z_1 \, \partial z_4} = \frac{\partial^2 f_3}{\partial z_4 \, \partial z_1} = \beta_1 \eta_6$, $\quad \frac{\partial^2 f_3}{\partial z_1 \, \partial z_5} = \frac{\partial^2 f_3}{\partial z_5 \, \partial z_1} = \beta_1 \eta_4$, $\quad \frac{\partial^2 f_3}{\partial z_1 \, \partial z_6} = \frac{\partial^2 f_3}{\partial z_6 \, \partial z_1} = \beta_1 \eta_5$,

$\frac{\partial^2 f_3}{\partial z_1 \, \partial z_7} = \frac{\partial^2 f_3}{\partial z_7 \, \partial z_1} = \beta_1$, $\quad \frac{\partial^2 f_3}{\partial z_1 \, \partial z_9} = \frac{\partial^2 f_3}{\partial z_9 \, \partial z_1} = \beta_1 \eta_{10}$, $\quad \frac{\partial^2 f_3}{\partial z_1 \, \partial z_{10}} = \frac{\partial^2 f_3}{\partial z_{10} \, \partial z_1} = \beta_1 \eta_8$,

$\frac{\partial^2 f_3}{\partial z_1 \, \partial z_{11}} = \frac{\partial^2 f_3}{\partial z_{11} \, \partial z_1} = \beta_1 \eta_9$, $\quad \frac{\partial^2 f_3}{\partial z_1 \, \partial z_{12}} = \frac{\partial^2 f_3}{\partial z_{12} \, \partial z_1} = \beta_1 \eta_7$.

Therefore, using equation (4.111), a is given as follows:

$$a = 2\, v_3\, u_1\, \beta_1 \left(u_4 \eta_6 + u_5 \eta_4 + u_6 \eta_5 + u_7 + u_9 \eta_{10} + u_{10} \eta_8 + u_{11} \eta_9 + u_{12} \eta_7\right) < 0.$$

To compute b, $\frac{\partial^2 f_k}{\partial z_i \, \partial \beta}$ was determined as follows:

$\frac{\partial^2 f_3}{\partial z_1 \, \partial \beta_1} = z_7 + \eta_4 z_5 + \eta_5 z_6 + \eta_6 z_4 + \eta_7 z_{12} + \eta_8 z_{10} + \eta_9 z_{11} + \eta_{10} z_9,$

$\frac{\partial^2 f_3}{\partial z_2 \, \partial \beta_1} = (1-\rho)(z_7 + \eta_4 z_5 + \eta_5 z_6 + \eta_6 z_4 + \eta_7 z_{12} + \eta_8 z_{10} + \eta_9 z_{11} + \eta_{10} z_9),$

$\frac{\partial^2 f_3}{\partial z_4 \, \partial \beta_1} = \eta_6(z_1 + (1-\rho)z_2)$, $\frac{\partial^2 f_3}{\partial z_5 \, \partial \beta_1} = \eta_4(z_1 + (1-\rho)z_2),$

$\frac{\partial^2 f_3}{\partial z_9 \, \partial \beta_1} = \eta_{10}(z_1 + (1-\rho)z_2)$, $\frac{\partial^2 f_3}{\partial z_{10} \, \partial \beta_1} = \eta_8(z_1 + (1-\rho)z_2).$

Therefore, using equation (4.111), b is given as follows:

$$
\begin{aligned}
b = v_3 \Big\{ & u_1 \big(z_7 + \eta_4 z_5 + \eta_5 z_6 + \eta_6 z_4 + \eta_7 z_{12} + \eta_8 z_{10} + \eta_9 z_{11} + \eta_{10} z_9\big) \\
& + u_2(1-\rho)\big(z_7 + \eta_4 z_5 + \eta_5 z_6 + \eta_6 z_4 + \eta_7 z_{12} + \eta_8 z_{10} + \eta_9 z_{11} + \eta_{10} z_9\big) \\
& + u_4 \eta_6 \big(z_1 + (1-\rho)z_2\big) + u_5 \eta_4 \big(z_1 + (1-\rho)z_2\big) + u_9 \eta_{10} \big(z_1 + (1-\rho)z_2\big) \\
& + u_{10} \eta_8 \big(z_1 + (1-\rho)z_2\big) \Big\} > 0
\end{aligned}
$$

Since $a < 0$ and $b > 0$, the model system (3.8) does not exhibit a backward bifurcation at $R_C^* = 1$. Consequently, the co-infection of pulmonary TB and pneumonia can be eradicated whenever an index case of an infectious individual infects, on average, fewer than one person during the infectious period.

4.4.11 Parameter estimation

The pulmonary tuberculosis–pneumonia co-infection model was fitted to the NTLLDP Kenyan data on pulmonary TB and pneumonia co-infection, as shown in Figure 4.19. The parameters β_2, η_4, η_5, η_6, η_7, η_8, η_9, η_{10}, ε_1, ε_2, ε_3, ϑ_4, ϑ_5, ϕ_2, ϕ_3, ϕ_4, γ_2, γ_3, γ_5, and n, listed in Table 4.3, were estimated from model fitting.

4.4.12 Sensitivity analysis of the control reproduction number

In this section, the sensitivity indices of the control reproduction number due to the co-infection of pulmonary TB and pneumonia are computed to determine the relative importance of various parameters responsible for disease transmission and prevalence in the population. The normalized forward sensitivity approach, as employed by Khajanchi et al. (2018), is used.

The parameter values in Table 4.3 are utilized to calculate the sensitivity indices of the reproduction number for the parameters β_1, Q, ρ, ϑ_1, ϑ_2, ϑ_3, ε_1, ε_2, ϕ_1, α_1, α_2, and α_3, using equation (4.62) implemented in Mathematica software.

Figure 4.19

Prevalence of TB and pneumonia co-infection model: Model fit to NTLLDP data

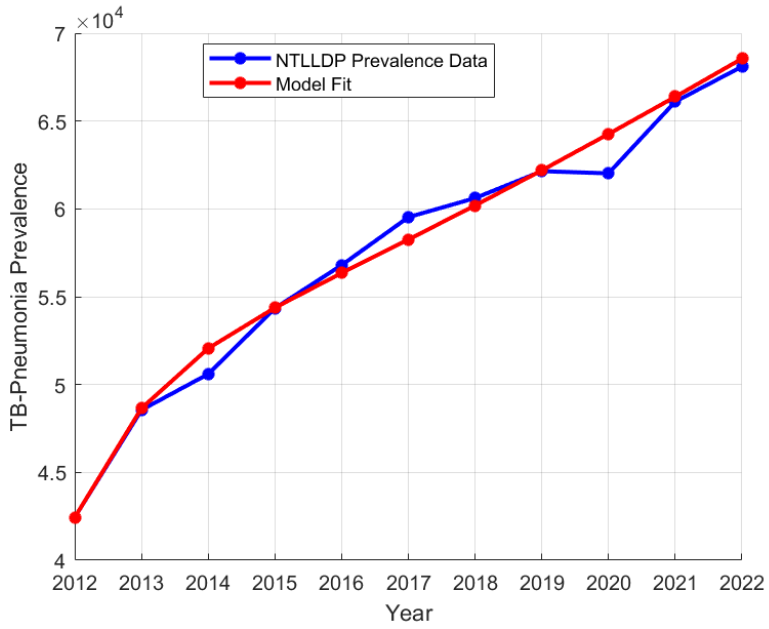

Source: Researcher (2024)

The calculated sensitivity indices of the reproduction numbers are presented in Table 4.4. A positive sensitivity index indicates that the reproduction number increases as the corresponding parameter increases, while a negative sensitivity index indicates that the reproduction number decreases as the corresponding parameter increases. Therefore, increasing a parameter with a positive sensitivity index, while keeping other parameters constant, raises the reproduction number. Conversely, increasing a parameter with a negative sensitivity index, while holding other factors constant, reduces the reproduction number.

From Table 4.4, it is observed that β, ε_1, and ε_2 have positive sensitivity index values, indicating that an increase in these parameters leads to a corresponding rise in the infected population. Conversely, ϑ_1, ϑ_2, ϑ_3, ϕ_1, α_1, α_2, ρ, and Q have negative sensitivity index values, meaning an increase in these parameters reduces the infected population. For example, a 10% increase in the transmission rate, β_1, results in a 10% increase in the reproduction number. In contrast, a 10% increase in the screening rate of latent TB infection, ϑ_1, reduces R_C by 6.673668%, while a 10% increase in the screening rate of asymptomatic TB infections, ϑ_2, decreases R_C by 5.32231%.

Table 4.3

Parameter values used in the TB and pneumonia co-infection model

Parameter	Value	Source
Λ	$1\,514\,825$ year^{-1}	KNBS (2023)
Q	0.8 year^{-1}	KNBS (2023)
ρ	0.5	WHO (2023)
μ	0.0147 year^{-1}	KNBS (2023)
$\varepsilon_1, \varepsilon_2$	$0.1, 0.05$ year^{-1}	NTLLDP (2019)
ϑ_1	0.34 year^{-1}	NTLLDP (2022)
ϑ_2	0.2 year^{-1}	NTLLDP (2022)
ϑ_3	0.63 year^{-1}	NTLLDP (2021)
ϑ_4, ϑ_5	$0.023, 0.175$ year^{-1}	Data fitted
ϕ_1	0.6 year^{-1}	NTLLDP (2022)
ϕ_2, ϕ_3, ϕ_4	$0.5, 0.6, 0.3$ year^{-1}	Data fitted
γ_1	0.5 year^{-1}	WHO (2023)
$\gamma_2, \gamma_3, \gamma_5$	$0.7, 0.21, 0.6$ year^{-1}	Data fitted
γ_4	0.06 year^{-1}	NTLLDP (2021)
α_1	0.85 year^{-1}	NTLLDP (2020)
α_2	0.8 year^{-1}	NTLLDP (2021)
α_3	0.75 year^{-1}	NTLLDP (2022)
κ	0.08 year^{-1}	Data fitted
n	0.0003	Data fitted
$\epsilon_1, \epsilon_2, \epsilon_3$	$0.014, 0.065, 0.008$	Data fitted
β_1	0.15 year^{-1}	NTLLDP (2021)
β_2	0.21 year^{-1}	Data fitted
$\eta_4, \eta_5, \eta_6, \eta_7, \eta_8, \eta_9$	$0.21, 0.03, 0.02, 0.0016, 0.0042, 0.0031, 0.002, 0.0014$	Data fitted

Source: Researcher (2024)

Table 4.4

Sensitivity indices of the control reproduction number with respect to selected co-infection model parameters

Parameter	Sensitivity index
β_1	$+1$
ε_1	$+0.877516$
ε_2	$+0.174723$
ϑ_1	-0.673668
ϑ_2	-0.532231
ϑ_3	-0.169135
ϕ_1	-0.519356
α_2	-0.952773
α_3	-0.440299
Q	-0.666667
ρ	-0.666667

Source: Researcher (2024)

4.5 Numerical Simulation of the Co-infection Model

This section presents the numerical results for modeling pulmonary TB in the presence of opportunistic pneumonia, along with their discussion. The following subsections are included: the predicted effects of varying natural immunity, screening rates, treatment rates for pulmonary TB, and vaccine efficacy on co-infected populations.

4.5.1 Effects of varying natural immunity on the co-infected populations

This subsection examines the predicted effects of varying natural immunity on preventing co-infections of pulmonary TB and pneumonia.

In the model flow chart shown in Figures 3.2, n represents natural immunity. Figures 4.20 and 4.21 illustrate the effects of varying natural immunity on TB-pneumonia co-infections. An increase in natural immunity is predicted to reduce cases of TB–pneumonia co-infection, potentially eliminating the co-infection altogether. Additionally, Figures 4.22 and 4.23 demonstrate that an increase in natural immunity decreases the population of TB-pneumonia co-infected individuals undergoing treatment. This reduction occurs because enhanced natural immunity diminishes infection transmission by slowing the progression of latent TB infections to pulmonary TB disease, thereby significantly lowering the number of individuals requiring treatment for co-infection.

4.5.2 Effects of varying screening rates on co-infected populations

This subsection examines the predicted effects of varying screening rates for latent infections and asymptomatic infectious pulmonary TB on co-infected populations to illustrate their impact on infection transmission to susceptible individuals.

In the flow chart depicted in Figures 3.2, ϑ_1 represents the screening rate for latent TB infections. Figures 4.24 and 4.25 depict the effects of screening the latent infected population on TB-pneumonia co-infections. It is observed that increasing the screening rate for latent infected individuals reduces TB-pneumonia co-infections. Furthermore, Figures 4.26 and 4.27 illustrate that an increase in the screening rate for latent infected individuals decreases the population of TB-pneumonia co-infected individuals undergoing treatment. This reduction is attributed to a decrease in the transmission rate of infections,

driven by the reduced reactivation of latent infections. Consequently, this reduction not only decreases the risk of infection transmission to healthcare workers but also alleviates the strain on resources required for treatment, particularly in sub-Saharan African countries.

In the flow chart depicted in Figures 3.2, ϑ_2 represents the screening rate for individuals with asymptomatic infectious TB. Figure 4.28 illustrates the effects of screening individuals with asymptomatic infectious TB on the population with TB-pneumonia co-infections, while Figure 4.29 shows the effects of screening these individuals on TB-pneumonia co-infected individuals undergoing treatment. An increase in the screening rate for individuals with asymptomatic infectious TB is observed to decrease both the number of individuals with tuberculosis-pneumonia co-infections and those undergoing treatment for co-infection. This decrease is attributed to the reduction in the continuous transmission of pulmonary TB from asymptomatic individuals, which subsequently lowers the rate of infection transmission and results in fewer people becoming co-infected with TB and pneumonia.

4.5.3 Effects of varying screening rates for the co-infected population on pulmonary TB

This subsection examines the predicted effects of screening co-infected individuals on the population infected with pulmonary TB, to assess the impact of co-infections on disease transmission.

In the model flow chart shown in Figures 3.2, ϑ_5 represents the screening rate for symptomatic TB-pneumonia co-infections. Figures 4.30 and 4.31 illustrate the effects of screening these co-infections on the population infected with pulmonary TB only. An increase in the screening rate for TB-pneumonia co-infections is observed to reduce the population infected with pulmonary TB. This reduction is attributed to the decreased transmission of pulmonary TB. Co-infection with pneumonia complicates the diagnosis of pulmonary tuberculosis due to overlapping symptoms, which contributes to a higher transmission rate.

4.5.4 Effects of varying the treatment rate of pulmonary TB disease on the co-infected population

This subsection highlights the predicted effects of treating pulmonary tuberculosis on the co-infected population, aiming to determine its contribution to reducing infection transmis-

sion within the population.

Figures 4.32 and 4.33 illustrate the effects of varying the treatment rate for pulmonary TB on co-infections. An increase in the treatment of pulmonary TB is observed to decrease TB-pneumonia co-infections. Additionally, Figures 4.34 and 4.35 illustrate the effects of varying the treatment rate for pulmonary TB on the population undergoing treatment for co-infections. An increase in the treatment rate for pulmonary TB decreases the population undergoing treatment for TB-pneumonia co-infections. This decrease is attributed to the reduced transmission of infections resulting from pulmonary TB treatment, which subsequently lowers the number of people co-infected with pulmonary TB and pneumonia, leading to a reduction in the number of individuals seeking treatment.

4.5.5 Effects of varying vaccine efficacy on co-infected populations

Considering the model flow chart in Figures 3.2, ρ represents the vaccine efficacy for the pulmonary TB vaccine. Figures 4.36 and 4.37 illustrate the effects of varying vaccine efficacy on the populations co-infected with pulmonary TB and pneumonia. It is predicted that an increase in vaccine efficacy reduces the number of individuals co-infected with TB and pneumonia. Additionally, a prediction is made regarding the effects of increasing vaccine efficacy on the co-infected population undergoing treatment. An increase in vaccine efficacy reduces the number of co-infected individuals seeking treatment. This reduction occurs because a higher-efficacy vaccine enhances individuals' immunity, thereby decreasing the proportion of the population infected with pulmonary tuberculosis and, consequently, significantly reducing the population co-infected with both pulmonary TB and pneumonia.

Figure 4.20

Population of individuals with symptomatic TB-pneumonia co-infections at varying levels of natural immunity

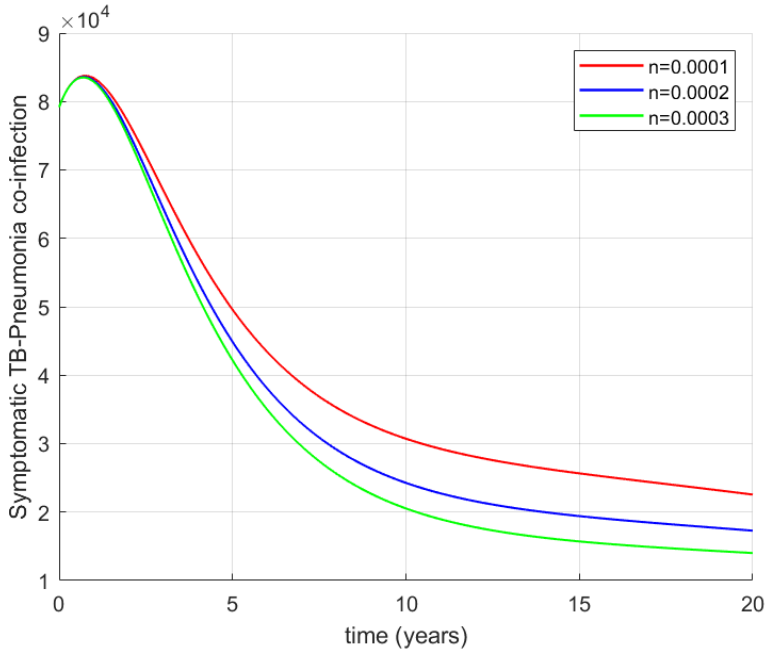

Source: Researcher (2024)

Figure 4.21

Population of individuals with asymptomatic TB-pneumonia co-infections at varying levels of natural immunity

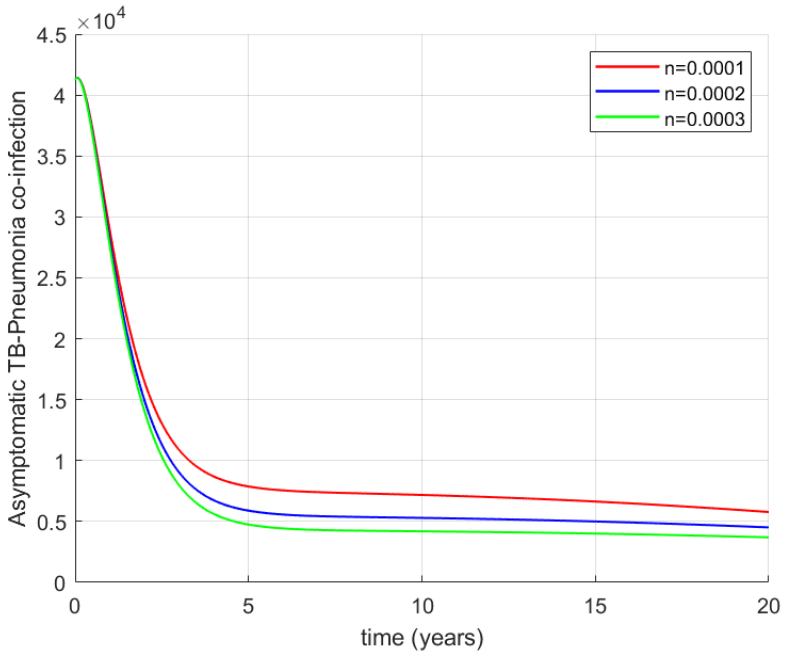

Source: Researcher (2024)

Figure 4.22

Population of symptomatic TB-pneumonia cases receiving treatment at varying levels of natural immunity.

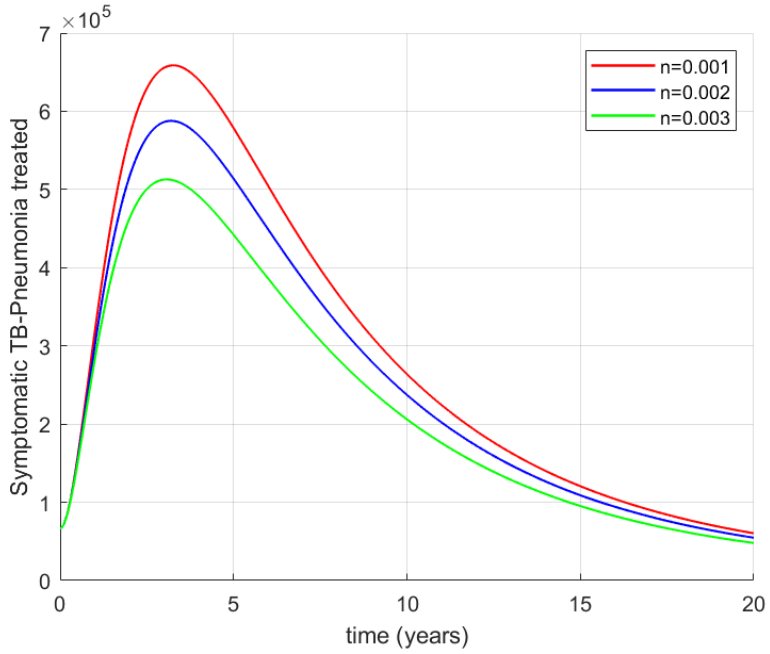

Source: Researcher (2024)

Figure 4.23

Population of asymptomatic TB-pneumonia cases receiving treatment at varying levels of natural immunity.

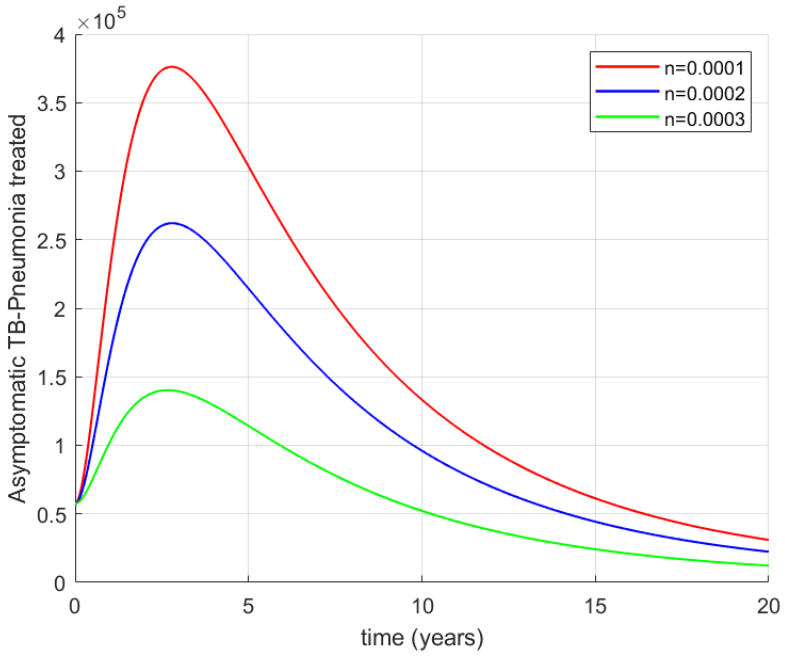

Source: Researcher (2024)

Figure 4.24

Effects of varying the screening rate for latent infections on the symptomatic TB-pneumonia co-infected population

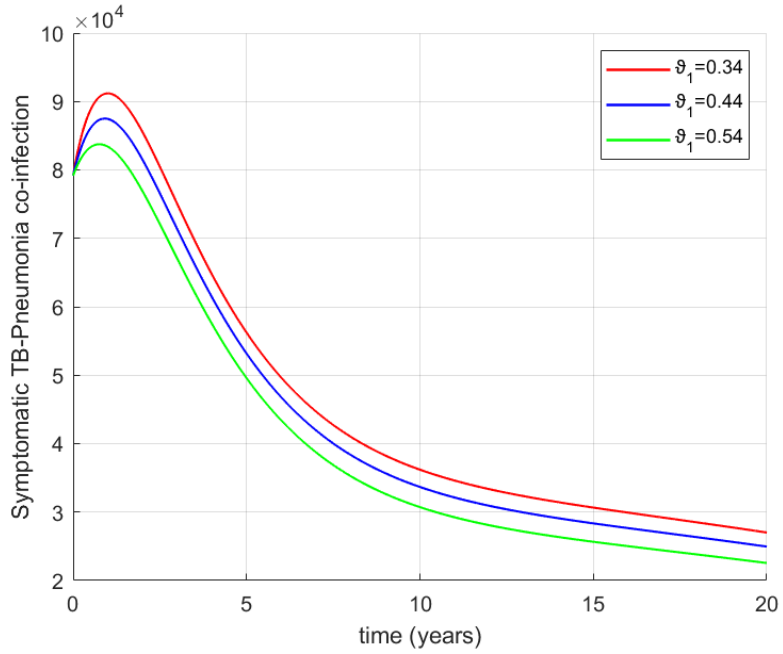

Source: Researcher (2024)

Figure 4.25

Effects of varying the screening rate for latent infections on the asymptomatic TB-pneumonia co-infected population

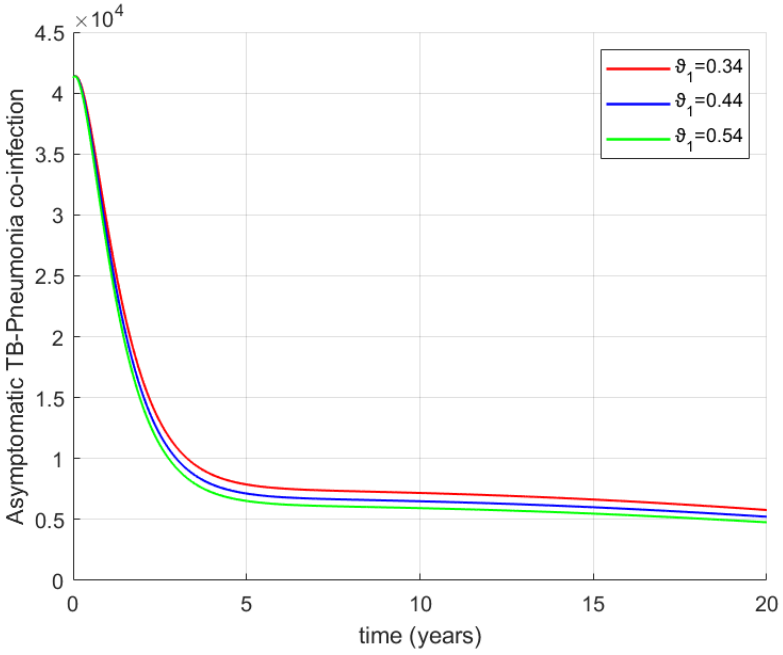

Source: Researcher (2024)

Figure 4.26

Effects of varying the screening rate for individuals with latent TB infections on symptomatic TB-pneumonia cases undergoing treatment.

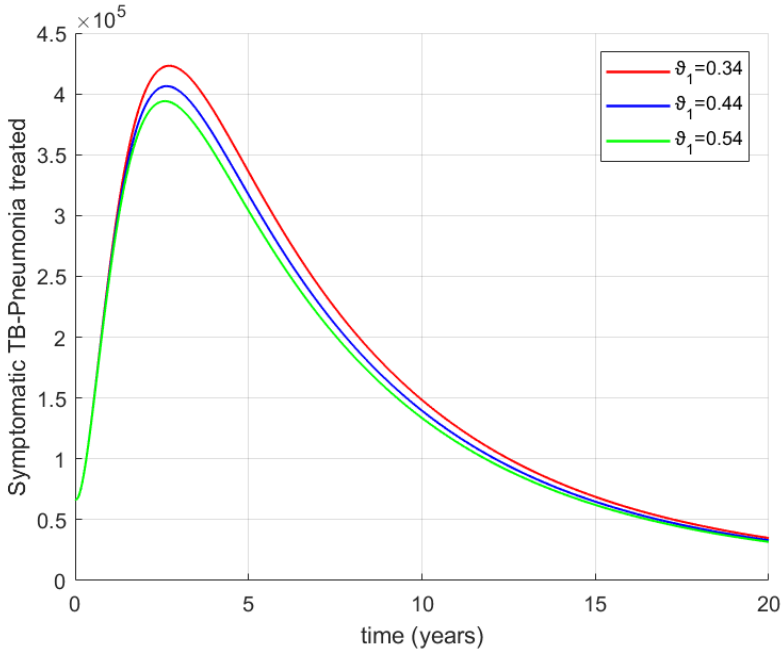

Source: Researcher (2024)

Figure 4.27

Effects of varying the screening rate for individuals with latent tuberculosis infections on asymptomatic tuberculosis-pneumonia cases undergoing treatment.

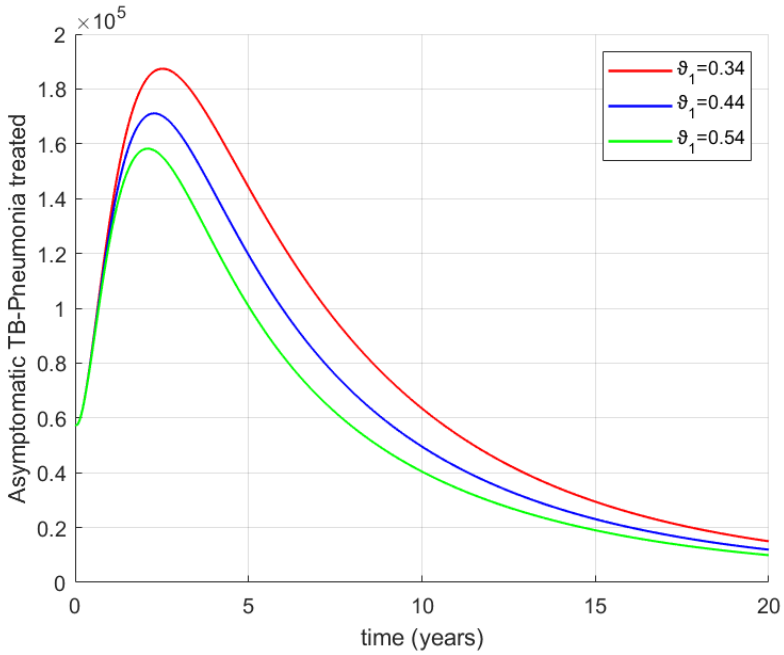

Source: Researcher (2024)

Figure 4.28

Effects of varying the screening rate for individuals with asymptomatic TB on the TB-pneumonia co-infected population.

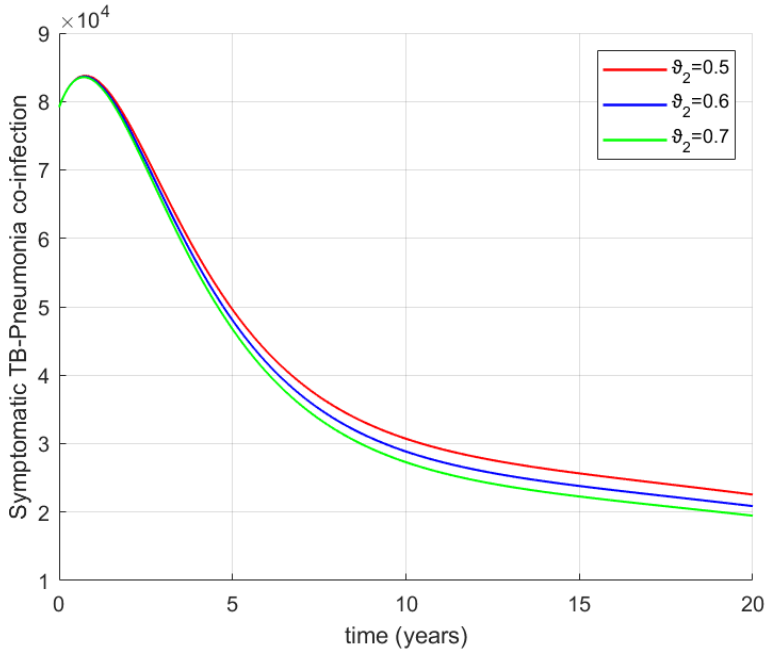

Source: Researcher (2024)

Figure 4.29

Effects of varying the screening rate for individuals with asymptomatic TB on the TB-pneumonia co-infected population undergoing treatment.

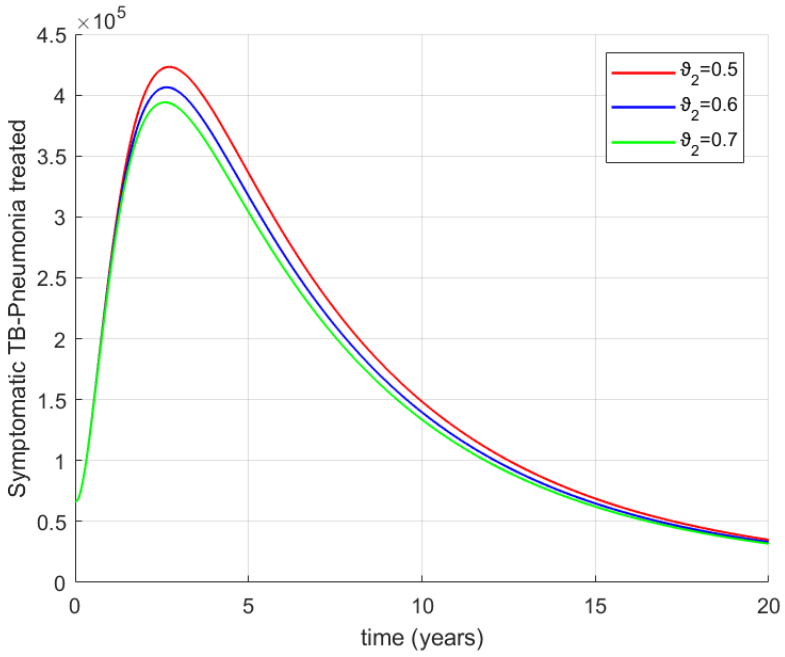

Source: Researcher (2024)

Figure 4.30

Effects of varying the screening rate for TB-pneumonia co-infected individuals on the population with symptomatic TB.

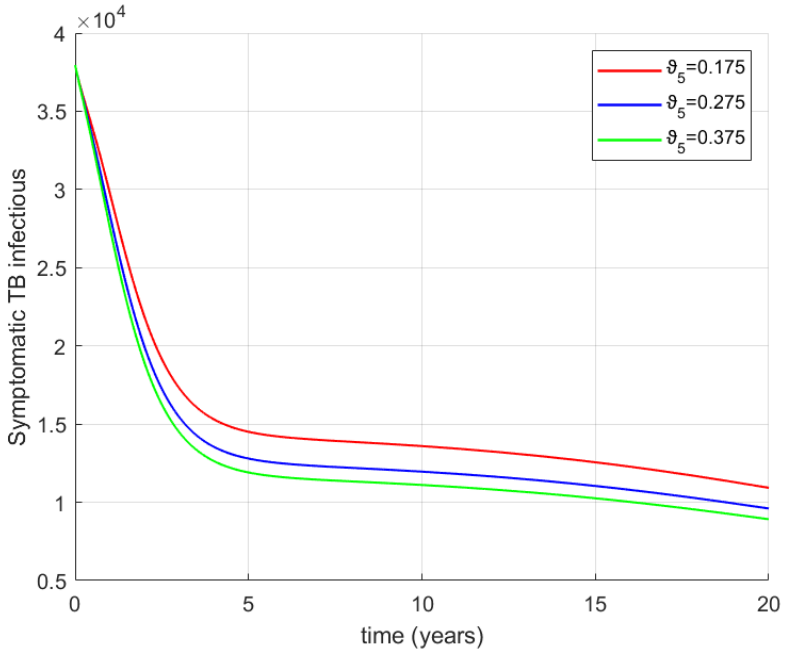

Source: Researcher (2024)

Figure 4.31

Effects of varying the screening rate for TB-pneumonia co-infected individuals on the population with asymptomatic TB.

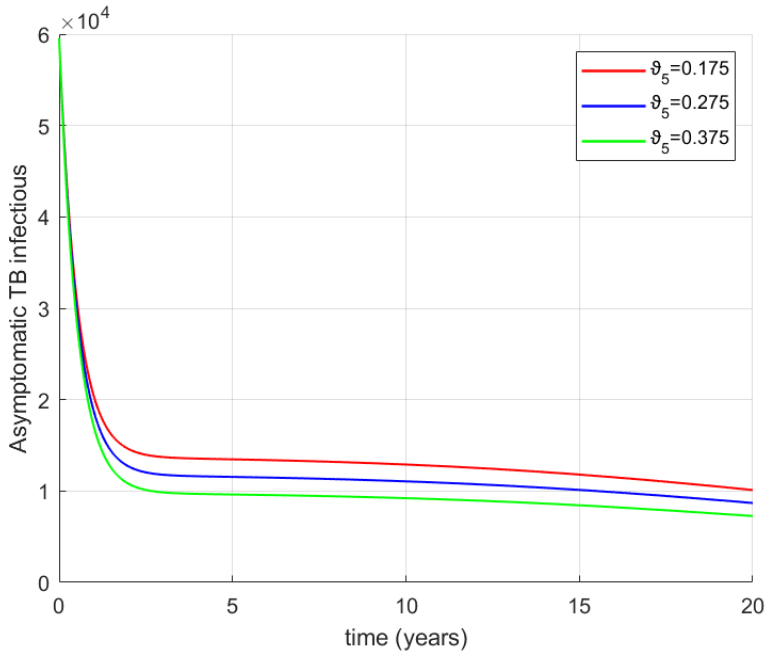

Source: Researcher (2024)

Figure 4.32

Effects of varying the treatment rate for individuals with TB on the population co-infected with symptomatic TB and pneumonia.

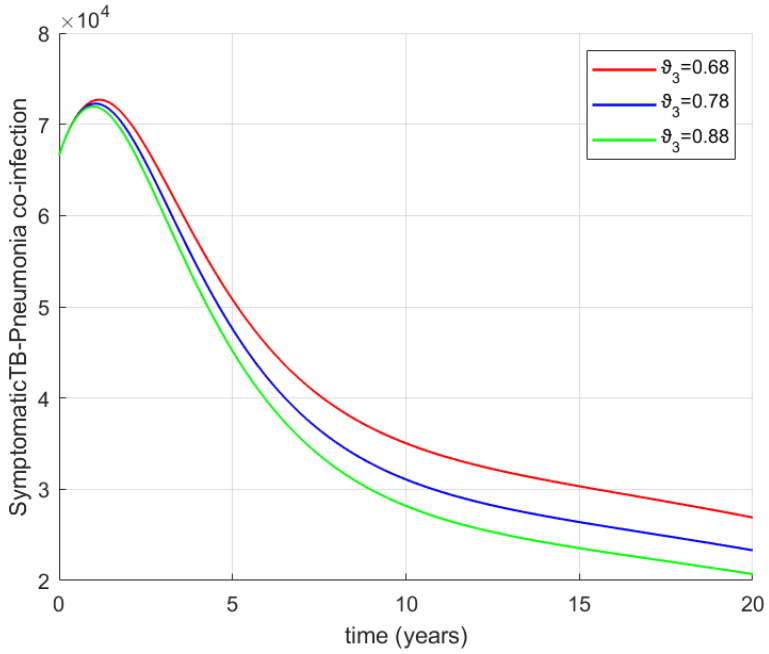

Source: Researcher (2024)

Figure 4.33

Effects of varying the treatment rate for individuals with TB on the population co-infected with asymptomatic TB and pneumonia

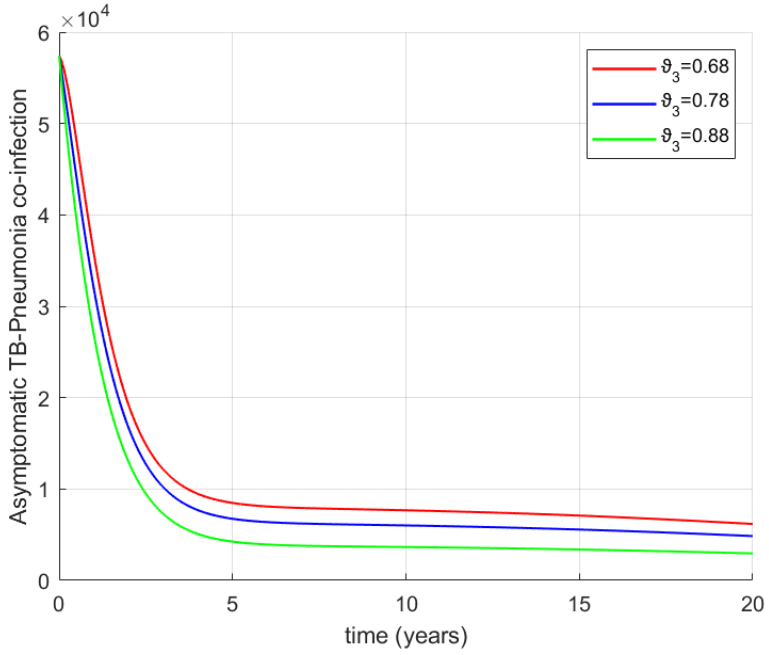

Source: Researcher (2024)

Figure 4.34

Effects of varying the treatment rate for individuals with TB on the population co-infected with symptomatic TB and pneumonia undergoing treatment

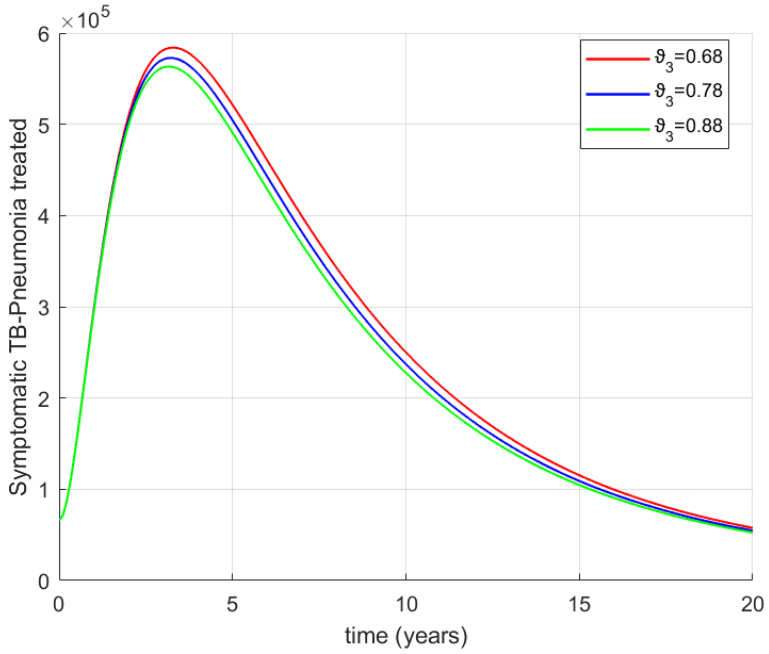

Source: Researcher (2024)

Figure 4.35

Effects of varying the treatment rate for individuals with TB on the population co-infected with asymptomatic TB and pneumonia undergoing treatment

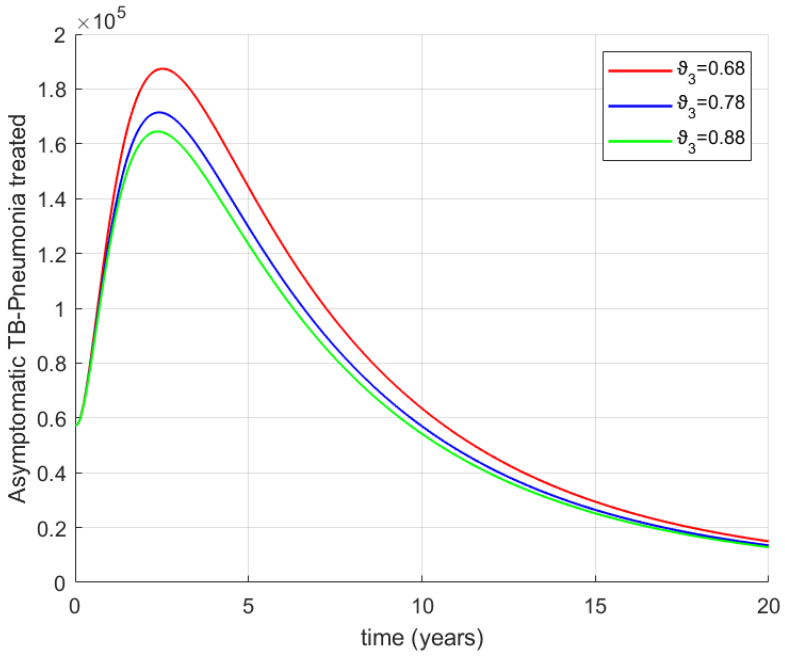

Source: Researcher (2024)

Figure 4.36

Effects of varying vaccine efficacy on individuals co-infected with symptomatic TB and pneumonia

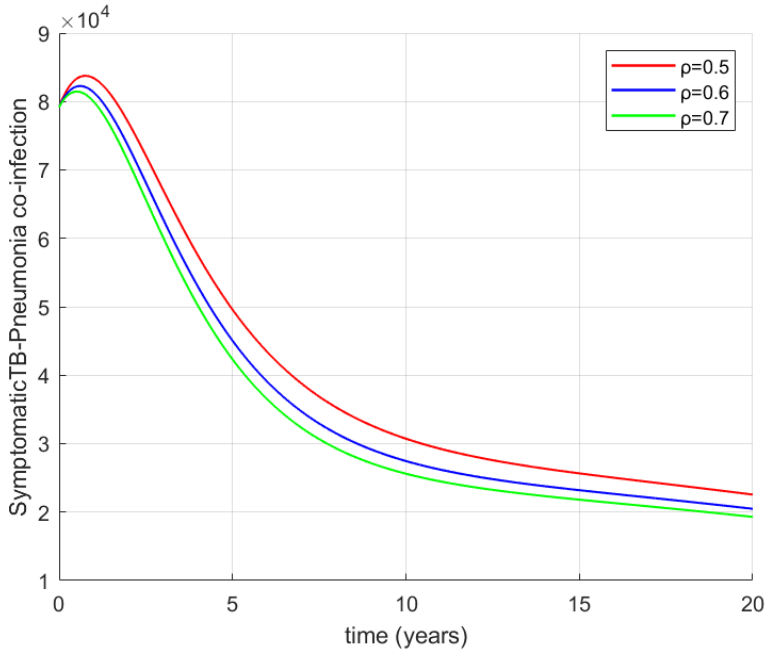

Source: Researcher (2024)

Figure 4.37

Effects of varying vaccine efficacy on individuals co-infected with asymptomatic TB and pneumonia

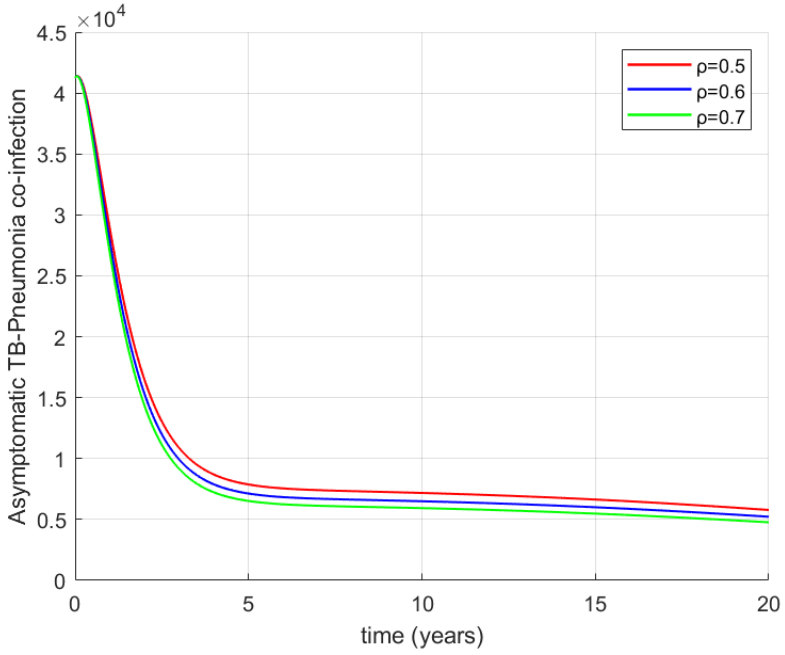

Source: Researcher (2024)

CHAPTER FIVE: CONCLUSION AND RECOMMENDATIONS

5.1 Introduction

In this chapter, conclusions are drawn based on the results obtained in Chapter Four. Additionally, recommendations for further research and published works are provided.

5.2 Conclusion

This study focused on modeling pulmonary TB in the presence of opportunistic pneumonia by incorporating the screening of asymptomatic infectious individuals and accounting for the role of natural immunity. Two mathematical models were formulated: one to describe the dynamics of pulmonary TB, and another to describe the co-dynamics of pulmonary TB and pneumonia. The conclusions derived from the study's findings are presented as follows.

The first objective of this study was to formulate a pulmonary TB model that incorporates an asymptomatic infectious component and natural immunity. This was achieved in Section 3.3 through the derivation of a system of nonlinear differential equations describing the dynamics of pulmonary TB under these conditions.

The second objective was to formulate a pulmonary TB and pneumonia co-infection model that also incorporates an asymptomatic infectious component and natural immunity. This was accomplished in Section 3.4 through the derivation of a system of nonlinear differential equations characterizing the transmission dynamics of TB–pneumonia co-infection under these conditions.

The conclusions for the third objective, which involved determining the reproduction numbers for analyzing the formulated models, are presented as follows.

The control reproduction numbers for the models were determined using the Next Generation Matrix method, as described in Subsections 4.2.4 and 4.4.4 for the TB model and the co-infection model, respectively. For the pulmonary TB model, control reproduction numbers were computed under various intervention strategies. These are as follows: R_{CVST} for vaccination, screening, and treatment of all infected cases; R_{CST} for screening and treatment of all infected cases; R_{CVT_S} for vaccination and treatment of the symptomatic infectious population; and R_{CT_S} for treatment of the symptomatic infectious population alone.

Numerical simulations predicted the relationship $R_{CVST} < R_{CST} < R_{CVT_S} < R_{CT_S}$, as presented in Section 4.3.5. This ordering indicates that the combination of vaccination, screening, and treatment of all forms of pulmonary TB is the most effective intervention for reducing transmission. The next most effective strategy is screening and treatment of all infected cases, followed by vaccination and treatment of symptomatic individuals. Treating symptomatic cases alone is the least effective strategy.

Analysis of the disease-free equilibria of the two models indicates that the necessary and sufficient condition for both local and global stability is that the control reproduction numbers are less than one, as shown in Subsections 4.2.5, 4.2.6, 4.4.5, and 4.4.6. These results demonstrates that control strategies should aim to ensure that an index case does not, on average, infect more than one individual during the infectious period. Conversely, analysis of the endemic equilibrium points shows that pulmonary TB and its coexistence with pneumonia persist in the community if the control reproduction numbers exceed one, as presented in Subsections 4.2.8, 4.2.9, 4.4.8, and 4.4.9.

The bifurcation analysis of the two models showed that the systems did not exhibit backward bifurcation, as presented in Subsections 4.2.10 and 4.4.10 for the TB and co-infection models, respectively. Therefore, it is possible to eradicate tuberculosis and its coexistence with pneumonia whenever the control reproduction numbers are less than one.

The fourth objective was to investigate the effects of various model parameters on the control of pulmonary TB and pneumonia. The conclusions related to this objective are summarized as follows.

The sensitivity analysis results, presented in Subsections 4.2.11 and 4.4.12, demonstrated that the control reproduction numbers are inversely proportional to vaccine efficacy, screening rates for latently infected and asymptomatic infectious individuals, and the treatment rate. Consequently, higher vaccine efficacy and increased screening rates for latently infected and asymptomatic infectious individuals significantly reduce infection transmission. Increasing the treatment rate for the symptomatic infectious population also decreases the spread of infections to susceptible individuals.

Numerical simulations presented in Sections 4.3 and 4.5 further predicted that increases

in natural immunity, screening rates for latently infected individuals, and vaccine efficacy each contribute to reducing both the co-infected population and those undergoing treatment for co-infections. This indicates that enhancing the immunity of latently infected individuals, increasing screening rates, and improving vaccine efficacy are effective strategies for lowering infection transmission to susceptible individuals.

The simulations also showed that increasing the screening rate for individuals with asymptomatic infectious TB reduces the populations with severe pulmonary tuberculosis, severe co-infections, and those undergoing treatment for severe disease. This demonstrates that screening and treating the asymptomatic infectious population can effectively curb the persistent spread of infections to susceptible individuals, thereby lowering transmission rates. Finally, the simulations predicted that increasing the screening rate for co-infected individuals leads to a reduction in the population infected with pulmonary TB. This finding suggests that targeting individuals co-infected with pulmonary tuberculosis and pneumonia is an effective strategy for containing TB. Conversely, increasing the treatment rate for pulmonary TB was predicted to reduce both the co-infected population and the number of individuals undergoing treatment for co-infections.

5.3 Recommendations for Future Research

This study has contributed significantly to the understanding of pulmonary TB transmission within the population and provides a foundation for further research. Future work may focus on developing optimal and cost-effective control strategies to design interventions with minimal expenditure, applying stochastic approaches to assess the effects of randomness on disease dynamics, employing fractional-order models to enhance the accuracy of results, and integrating artificial intelligence techniques to improve the identification of asymptomatic infectious individuals in the population.

5.4 List of Publications

Kirimi, E. M., Muthuri, G. G., Ngari, C. G., Karanja, S. (2024). A Model for the Propagation and Control of Pulmonary Tuberculosis Disease in Kenya. Hindawi: *Discrete Dynamics in Nature and Society*, 2024(1), 5883142.

Kirimi, E. M., Muthuri, G. G., Ngari, C. G., Karanja, S. (2024). Modeling the effects of vaccine efficacy and rate of vaccination on the transmission of pulmonary tuberculosis. Elsevier: *Informatics in Medicine Unlocked*, 46, 101470.

REFERENCES

Anazawa, K. (2025). Evaluating a novel reproduction number estimation method: a comparative analysis. *Scientific Reports*, 15(1):5423.

Aparicio, J. P. and Castillo-Chavez, C. (2021). Mathematical modelling of tuberculosis epidemics. *Mathematical Biosciences and Engineering*, 6(2):209–237.

Attia, E. F., Pho, Y., Nhem, S., Sok, C., By, B., Phann, D., Nob, H., Thann, S., Yin, S., Noce, R., et al. (2023). Tuberculosis and other bacterial co-infection in cambodia: a single center retrospective cross-sectional study. *BMC pulmonary medicine*, 19(1):60.

Avram, F., Adenane, R., and Basnarkov, L. (2024). Some probabilistic interpretations related to the next-generation matrix theory: A review with examples. *Mathematics (2227-7390)*, 12(15).

Avram, F., Adenane, R., Basnarkov, L., and Johnston, M. D. (2023). Algorithmic approach for a unique definition of the next-generation matrix. *Mathematics*, 12(1):27.

Bajaj, S., Thompson, R., and Lambert, B. (2025). A renewal-equation approach to estimating rt and infectious disease case counts in the presence of reporting delays. *Philosophical Transactions A*, 383(2292):20240357.

Banerjee, S. (2021). *Mathematical modeling: models, analysis and applications*. Chapman and Hall/CRC.

Barry, C. E., Boshoff, H. I., Dartois, V., Dick, T., Ehrt, S., Flynn, J., and Young, D. (2019). The spectrum of latent tuberculosis: rethinking the biology and intervention strategies. *Nature Reviews Microbiology*, 7(12):845–855.

Biswas, M. H. A., Paiva, L. T., de Pinho, M. D. R., et al. (2018). A seir model for control of infectious diseases with constraints. *Mathematical Biosciences and Engineering*, 11(4):761–784.

Boccia, D., Rudgard, W., Shrestha, S., Lönnroth, K., Eckhoff, P., Golub, J., Sanchez, M., Maciel, E., Rasella, D., Shete, P., et al. (2023). Modelling the impact of social protection on tuberculosis: the s-protect project. *BMC Public Health*, 18(1):786.

Cao, H., Li, J., and Yu, P. (2025). Study of immune response in a latent tuberculosis infection model. *Communications in Nonlinear Science and Numerical Simulation*, 140:108404.

Castillo-Chavez, C. and Song, B. (2004). Dynamical models of tuberculosis and their applications. *Math. Biosci. Eng*, 1(2):361–404.

Chandra, P., Grigsby, S. J., and Philips, J. A. (2022). Immune evasion and provocation by mycobacterium tuberculosis. *Nature Reviews Microbiology*, 20(12):750–766.

Chavarría, A. G. and Laura, I. B. (2018). Co-infection with bacterial community-acquired pneumonia and mycobacterium tuberculosis: A case report. *International Physical Medicine and Rehabilitation Journal*, 3(3):262–263.

Chong, K. C., Leung, C. C., Yew, W. W., Zee, B. C. Y., Tam, G. C. H., Wang, M. H., Jia, K. M., Chung, P. H., Lau, S. Y. F., Han, X., et al. (2019). Mathematical modelling of the impact of treating latent tuberculosis infection in the elderly in a city with intermediate tuberculosis burden. *Scientific reports*, 9(1):4869.

Chowell, G. and Hyman, J. M. (2023). *Mathematical and statistical modeling for emerging and re-emerging infectious diseases*. Springer.

Civil Registration Services (2023). Kenya vital statistics report, 2022.

Darboe, F., Reijneveld, J. F., Maison, D. P., Martinez, L., and Suliman, S. (2024). Unmasking the hidden impact of viruses on tuberculosis risk. *Trends in immunology*, 45(9):649–661.

Diekmann, O., Heesterbeek, J. A. P., and Roberts, M. G. (2020). The construction of next-generation matrices for compartmental epidemic models. *Journal of the Royal Society Interface*, 7(47):873–885.

Dormand, J. R. and Prince, P. J. (1980). A family of embedded runge–kutta formulae. *Journal of Computational and Applied Mathematics*, 6(1):19–26.

Dowdy, D. W., Basu, S., and Andrews, J. R. (2017). Is passive diagnosis enough? the impact of subclinical disease on diagnostic strategies for tuberculosis. *American Journal of Respiratory and Critical Care Medicine*, 187(5):543–551.

Driessche, K., Khajanchi, S., and Kar, T. K. (2020). Transmission dynamics of tuberculosis with multiple re-infections. *Chaos, Solitons & Fractals*, 130:109450.

Egonmwan, A. and Okuonghae, D. (2019). Analysis of a mathematical model for tuberculosis with diagnosis. *Journal of applied mathematics and computing*, 59(1):129–162.

Eguda, F. Y., Andrawus, J., Usman, I. G., Maiwa, S. I., and Dibal, I. M. (2020). A mathematical model of a tuberculosis transmission dynamics incorporating first and second line treatment. *J. Appl. Sci. Environ. Manage*, 24(5):917–922.

Fatima, S., Abdullah, F. A., and Mohd, M. H. (2020). Deterministic model of tuberculosis infection in the presence of educational counselling, treatment and vaccination. In *AIP Conference Proceedings*, volume 2266, page 050012. AIP Publishing LLC.

Feng, Z., Chavez, C. C., and Capurro, A. F. (2020). A model for tuberculosis with exogenous re-infection. *Theoretical Population Biology*, 57:235–249.

Flores-Garza, E., Zetter, M. A., Hernández-Pando, R., and Domínguez-Hüttinger, E. (2022). Mathematical model of the immunopathological progression of tuberculosis. *Frontiers in Systems Biology*, 2:912974.

Fröberg, G., Borgström, E. W., Chryssanthou, E., Correia-Neves, M., Källenius, G., and Bruchfeld, J. (2022). A new mathematical model to identify contacts with recent and remote latent tuberculosis. *ERJ Open Research*, 5(2).

Garcia, R. (2019). Community acquired pneumonia due to streptococcus pneumoniae: When to consider co-infection with active pulmonary tuberculosis. *Case Reports in Infectious Diseases*. Available at `https://doi.org/10.1155/2019/4618413`.

Government of Kenya (2008). Kenya vision 2030.

Gweryina, R. I., Madubueze, C. E., Bajiya, V. P., and Esla, F. E. (2023). Modeling and analysis of tuberculosis and pneumonia co-infection dynamics with cost-effective strategies. *Results in Control and Optimization*, 10:100210.

Halabitska, I., Petakh, P., Oksenych, V., and Kamyshnyi, O. (2025). Reactivation of latent tuberculosis following covid-19 and epstein-barr virus coinfection: A case report. *Pathogens*, 14(5):488.

Hethcote, H. W. (2004). The mathematics of infectious diseases. *SIAM Review*, 42(4):599–653.

Hethcote, H. W. (2009). The basic epidemiology models: models, expressions for r0, parameter estimation, and applications. In *Mathematical understanding of infectious disease dynamics*, pages 1–61. World Scientific.

Hill, D. T., Zhu, Y., Dunham, C., Moran, E. J., Zhou, Y., Collins, M. B., Kmush, B. L., and Larsen, D. A. (2025). Estimating the effective reproduction number from wastewater (rt): A methods comparison. *Epidemics*, 52:100839.

Hu, Z., Shi, L., Xie, J., and Fan, X.-Y. (2024). Innate and adaptive immunity against tuberculosis infection: diagnostics, vaccines, and therapeutics.

Imran, R. S., Resmawan, Achmad, N., and Nuha, A. R. (2022). Mathematical model of the pneumonia spreading in toddlers with immunization and treatment effects. *Journal of Mathematics, Statistics and Computer*, 17(2):202–218.

Jang, G., Kim, J., Lee, Y., Son, C., Ko, K. T., and Lee, H. (2024). Analysis of the impact of covid-19 variants and vaccination on the time-varying reproduction number: statistical methods. *Frontiers in Public Health*, 12:1353441.

Kalu, A. U. and Inyama, S. (2020). Mathematical model of the role of vaccination and treatment on the transmission dynamics of tuberculosis. *Gen. Maths. Notes*, 11(1):10–23.

Kenya National Bureau of Statistics (KNBS) and ICF (2023). Kenya demographic and health survey 2022: Key indicators report. Technical report, KNBS and ICF, Nairobi, Kenya, and Rockville, Maryland, USA.

Khajanchi, S., Das, D. K., and Kar, T. K. (2018). Dynamics of tuberculosis transmission with exogenous reinfections and endogenous reactivation. *Physica A: Statistical Mechanics and its Applications*, 497:52–71.

Khan, A., Naveed, M., Dur-e Ahmad, M., and Imran, M. (2015). Estimating the basic reproductive ratio for the ebola outbreak in liberia and sierra leone. *Infectious diseases of poverty*, 4(1):13.

Kim, S., de Los Reyes V, A. A., and Jung, E. (2020). Country-specific intervention strategies for top three tb burden countries using mathematical model. *PloS one*, 15(4):e0230964.

Kizito, M., Nampala, H., and Ariho, P. (2024). Mathematical modelling of tuberculosis and hepatitis c coinfection dynamics with no intervention. *Journal of Mathematics*, 2024(1):5521979.

Kizito, M. and Tumwiine, J. (2018). A mathematical model of treatment and vaccination interventions of pneumococcal pneumonia infection dynamics. *Journal of Applied Mathematics*, 2018(1):2539465.

Kuddus, M. A., Tithi, S. K., and Theparod, T. (2024). Implications of asymptomatic carriers for tuberculosis transmission and control in thailand: A modelling approach. *Symmetry*, 16(11):1538.

Kudryavtsev, I., Starshinova, A., Rubinstein, A., Kulpina, A., Ling, H., Zhuang, M., and Kudlay, D. (2024). The role of the immune response in developing tuberculosis infection: from latent infection to active tuberculosis. *Frontiers in Tuberculosis*, 2:1438406.

La Salle, J. P. (1976). *The stability of dynamical systems*. SIAM.

Liu, L. and Wang, Y. (2017). A mathematical study of a tb model with treatment interruptions and two latent periods. *Computational and mathematical methods in medicine*, 2017(1):932186.

MacPherson, P., Shanaube, K., Phiri, M. D., Rickman, H. M., Horton, K. C., Feasey, H. R., Corbett, E. L., Burke, R. M., and Rangaka, M. X. (2024). Community-based active-case finding for tuberculosis: navigating a complex minefield. *BMC global and public health*, 2(1):1–14.

Madhukar, P., Marcel, A. B., and Dowdy, D. W. (2016). Tuberculosis. *Nature Reviews Disease Primers*, 2:1–23.

Mahmoudi, S., Hamidi, M., and Drain, P. K. (2024). Present outlooks on the prevalence of minimal and subclinical tuberculosis and current diagnostic tests: a systematic review and meta-analysis. *Journal of Infection and Public Health*, 17(9):102517.

Makinde, O. D. and Okosun, K. O. (2023). Impact of chemo-therapy on optimal control of malaria disease with infected immigrants. *BioSystems*, 104(1):32–41.

Mandal, S., Satyanarayana, S., McQuaid, F., Dodd, P. J., Menzies, N. A., White, R. G., Arinaminpathy, N., Houben, R. M., Dowdy, D. W., Smit, M., et al. (2025). The global tb portfolio model: a tool for projecting the epidemiological impact of tb policy options. *medRxiv*, pages 2025–05.

Mathur, K. S. and Narayan, P. (2018). Dynamics of an sveirs epidemic model with vaccination and saturated incidence rate. *International Journal of Applied and Computational Mathematics*, 4(5):1–22.

Mishra, B. K. and Srivastava, J. (2019). Mathematical model on pulmonary and multidrug-resistant tuberculosis patients with vaccination. *Journal of the Egyptian Mathematical Society*, 22:311–316.

National Tuberculosis, Leprosy and Lung Disease Program (2016). Kenya tuberculosis prevalence survey 2016.

National Tuberculosis, Leprosy and Lung Disease Program (2019). National strategic plan for tuberculosis, leprosy and lung health 2019–2023.

National Tuberculosis, Leprosy and Lung Disease Program (2020). *Kenya Latent Tuberculosis Infection Policy 2020*. Ministry of Health, Kenya, Nairobi, Kenya.

National Tuberculosis, Leprosy and Lung Disease Program (2021). *2021 Annual Report*. Ministry of Health, Kenya, Nairobi, Kenya.

National Tuberculosis, Leprosy and Lung Disease Program (2022). *2022 Annual Report*. Ministry of Health, Kenya, Nairobi, Kenya.

Ndelwa, E. J., Kgosimore, M., Massawe, E. S., and Namkinga, L. (2015). Mathematical modeling and analysis of treatment and screening of pneumonia. *Mathematical Theory and Modeling*, 5(10):21–40.

Nieto Ramirez, L. M., Mehaffy, C., and Dobos, K. M. (2025). Systematic review of innate immune responses against mycobacterium tuberculosis complex infection in animal models. *Frontiers in Immunology*, 15:1467016.

Nyerere, N., Luboobi, L. S., and Nkansah-Gyekye, Y. (2016). Modeling the effect of screening and treatment on the transmission of tuberculosis infections. *Mathematical Theory and Modeling*, 4(7):51–62.

Okuonghae, D. and Ikhimwin, B. O. (2019). Dynamics of a mathematical model for tuberculosis with variability in susceptibility and disease progression due to difference in awareness level. *Frontiers in Microbiology*, 6:1530. Available at `https://doi.org/10.3389/fmicb.2015.01530`.

Oliwa, J. N., Karumbi, J. M., Marais, B. J., and Madhi, S. A. (2019). Tuberculosis as a cause of or comorbidity of childhood pneumonia in tuberculosis endemic areas: A systematic review. *Lancet Respiratory Medicine*. Available at `http://dx.doi.org/10.1016/`.

Otieno, M. J. O. J. and Paul, O. (2018). Mathematical model for pneumonia dynamics with carriers.

Otoo, D., Opoku, P., Charles, S., and Asekiya, P. K. (2020). Deterministic epidemic model for pneumonia dynamics with vaccination and temporal immunity. *Infectious Disease Modeling*, 5:42–60.

Ryckman, T. S., Dowdy, D. W., and Kendall, E. A. (2022). Infectious and clinical tuberculosis trajectories: Bayesian modeling with case finding implications. *Proceedings of the National Academy of Sciences*, 119(52):e2211045119.

Safi, M. A. and Garba, S. M. (2017). Global stability analysis of seir model with holling type ii incidence function. *Computational and mathematical methods in medicine*, 2017(1):826052.

Schwalb, A., Horton, K. C., Emery, J. C., Harker, M. J., Goscé, L., Veeken, L. D., Garden, F. L., Viet Nguyen, H., Nguyen, T.-A., Luu Boi, K., et al. (2024). Potential impact, costs, and benefits of population-wide screening interventions for tuberculosis in viet nam: a mathematical modelling study. *medRxiv*, pages 2024–12.

Soliman, B. W. and Bueno, A. C. (2021). Modeling the spread of pneumonia in the philippines using sir model with demographic changes. *Journal of Technology Management and Business*, 5(1):28–34.

Sulayman, F., Abdullah, F. A., and Mohd, M. H. (2023). An sveire model of tuberculosis to assess the effect of an imperfect vaccine and other exogenous factors. *Mathematics*, 9(4):327.

Tilahun, G. T., Makinde, O. D., and Malonza, D. (2017). Modelling and optimal control of pneumonia disease with cost-effective strategies. *Journal of biological dynamics*, 11(sup2):400–426.

Trauer, J. M., Denholm, J. T., and McBryde, E. S. (2022). Construction of a mathematical model for tuberculosis transmission in highly endemic regions of the asia-pacific. *Journal of Theoretical Biology*, 358:74–84.

United Nations Environment Programme (UNEP) (2015). Sustainable development goals and the 2030 agenda: Why environmental sustainability and gender equality are so important to reducing poverty and inequalities – unep perspectives issue no. 17.

Verver, S., Cai, R., Vanhommerig, J. W., Vlas, S. J., Hontelez, J., Coffeng, L., et al. (2018). Mathematical modelling of programmatic screening strategies for latent tuberculosis infection in countries with low tuberculosis incidence.

Wilcox, B. A. and Colwell, R. R. (2019). Emerging and reemerging infectious diseases: biocomplexity as an interdisciplinary paradigm. *EcoHealth*, 2(4):244–257.

World Health Organization (2015). Global tuberculosis report 2014.

World Health Organization (2020a). Global tuberculosis report 2019.

World Health Organization (2020b). Who recommendations on the management of diarrhoea and pneumonia.

World Health Organization (2023). *Global Tuberculosis Report 2022*. World Health Organization, Geneva, Switzerland.

World Health Organization (2024). Global tuberculosis report 2023.

World Health Organization (2025). Report of the who consultation on asymptomatic tuberculosis, geneva, switzerland, 14–15 october 2024.

Xiao-Ying, L., Hong-Fei, D., Li-Mei, Y., and Wei-Min, L. (2016). Pulmonary tuberculosis and bacterial pneumonia co-infection: A clinical etiology investigation in china. *Chinese Journal of Zoonoses*, 30(4):364–372.

Zephaniah, O. C., Nwaugonma, U.-I. R., Chioma, I. S., and Adrew, O. (2020). A mathematical model and analysis of an sveir model for streptococcus pneumonia with saturated incidence force of infection. *Mathematical Modeling and Applications*, 5(1):16–38.

Zhang, H., Madhusudanan, V., Murthy, B., Srinivas, M., and Adugna, B. A. (2022). Fuzzy analysis of svirs disease system with holling type-ii saturated incidence rate and saturated treatment. *Mathematical Problems in Engineering*, (1).

APPENDICES

Appendix A: MATLAB Code for Parameter Estimation

function kirimifminsearch()

clear all; clc;

tdata=[2012,2013,2014,2015,2016,2017,2018,2019,2020,2021,2022];

ydata=[42440,48555,50599,54345,56795,59529,60615,62146,62022,66106,68100];

Q = 0.8;

lambda = 0.207; betta = 0.15; eta1 = 0.0003; eta2 = 0.000002; eta3 = 0.00000126; lambda1 = 0.3; lambda2 = 0.8; rho = 0.6; theta1 = 0.34; theta2 = 0.5; gamma1 = 0.5; gamma2 = 0.7; gamma3 = 0.21; gamma4 = 0.065; gamma5 = 0.3; theta3 = 0.68; theta4 = 0.023; theta5 = 0.175; phi1 = 0.6; phi2 = 0.5; phi3 = 0.6; phi4 = 0.1; n = 0.0; alpha1 = 0.85; alpha2 = 0.8; alpha3 = 0.75; mu = 0.0147; kapa = 0.003; episilon1 = 0.1; episilon2 = 0.03;

k(1) = Q; k(2) = rho; k(3) = miu; k(4) = e1; k(5) = e2; k(6) = eta1; k(7) = eta2; k(8) = eta3; k(9) = eta4; k(10) = gamma1; k(11) = gamma2; k(12) = gamma3; k(13) = gamma4; k(14) = gamma5; k(15) = gamma6; k(16) = alpha1; k(17) = alpha2; k(18) = alpha3; k(19) = phi1; k(20) = phi2; k(21) = phi3; k(22) = phi4; k(23) = kappa; k(24) = n; k(25) = beta1; k(26) = beta2; k(27) = omega1; k(28) = omega2;

fxn=@(k)(SEIRsol(k)-ydata); options = optimoptions('fminsearch','Algorithm','trust-region-reflective');

lb=0*ones(28,1); ub=1*ones(28,1); par = fminsearch(fxn,k,lb,ub,options); fprintf('

xlswrite('Parameter$\text{Value}_{E}stimates.xlsx', par', 1,' C2');$

figure(3);

ymodel = SEIRsol(k); Date = datetime(2012,1,1) + calyears(0:length(tdata)-1); hold on

plot(Date,ydata,'-*b','linewidth',2);

plot(Date,ymodel,'-*r','linewidth',2); xlabel('Year'); ylabel('TB-Pneumonia Prevalence');

legend('NSDCC Prevalence Data','Data Fitted','Location','northeast') hold off grid on

function ymodel = SEIRsol(k)

S0=50622914; V0=22780311; E0=16874305; R0=5705328; Ia0=30364; Is0=41733;

```
Ta0=21787; Ts0=39738; Iap0=0.25*42440; Isp0=0.25*42440;
Tap0=0.25*42440;Tsp0=0.25*42440;
yinit = [S0 V0 E0 Ia0 Is0 Iap0 Isp0 Ta0 Ts0 Tap0 Tsp0 R0
[T,Y] =
ode45(@(t,y,k)SEIRode(t,y,k),linspace(0,length(tdata)),yinit,[],k);
ymodel2=Y(:,6)+Y(:,7)+Y(:,10)+Y(:,11); ymodel=ymodel2(1:9:length(T)-1); end
function dy = SEIRode(t,y,k) L=1508563; dy =zeros(12,1);
ratios1=linspace(-1,1,5); Sig1=1./(1+exp(-1*ratios1));
ratios2=linspace(-1,1,8); Sig2=1./(1+exp(-1*ratios2));
X1=Sig1(4); X2=Sig1(3); X3=Sig1(2); n1=Sig2(8); n2=Sig2(7); n3=Sig2(6);
n4=Sig2(5); n5=Sig2(4); n6=Sig2(3); n7=Sig2(2);

lambda1=k(25)*(y(7)+n1*y(5)+n2*y(6)+n3*y(4)+n4*y(11)+n5*y(9)
+n6*y(10)+n7*y(8)); lambda2=k(26)*(y(7)+X1*y(6)+X2*y(11)+X3*y(10));

dy(1) = (1-Q)*lambda + kapa*y(13) - lambda1*y(1) - mu*y(1); dy(2) = Q*lambda - (1-
rho)*lambda1*y(2) - mu*y(2); dy(3) = lambda1*y(1) + (1-rho)*lambda1*y(2) ...
- (episilon1/(1+n*y(3)))*y(3) - (episilon2/(1+n*y(3)))*y(3) ... - theta1*y(3) - mu*y(3);
dy(4) = (episilon2/(1+n*y(3)))*y(3) - theta2*y(4) - phi1*y(4) - mu*y(4) - lambda2*y(4);
dy(5) = (episilon1/(1+n*y(3)))*y(3) + phi1*y(4) - theta3*y(5) - (mu+gamma1+lambda2)*y(5);
dy(6) = lambda2*y(4) - (mu+gamma5+phi2+theta4)*y(6); dy(7) = lambda2*y(5) + phi2*y(6)
- (gamma2+theta5+mu)*y(7); dy(8) = theta1*y(3) - alpha1*y(8) - mu*y(8); dy(9) = theta2*y(4)
+ phi3*y(11) - (alpha2+mu)*y(9);
dy(10) = theta3*y(5) + phi4*y(12) - (gamma4+alpha3+mu)*y(10);
dy(11) = theta4*y(6) - (phi3+mu)*y(11); dy(12) = theta5*y(7) - (mu+phi4+gamma3)*y(12);
dy(13) = alpha1*y(8) + alpha2*y(9) + alpha3*y(10) - (kapa+mu)*y(13);
```

Appendix B: MATLAB Code for Model Simulation

```
function dy = phd2(t,y) global pi p m sigma lambda mu rho alpha gamma theta1 theta2
omega delta1 theta3 psi1 psi2 global delta2 psi3 betta eta1 eta2 eta3
```

```
p = 0.78; pi = 0.02072; betta = 1.199883592e-6; eta1 = 0.002; eta2 = 0.00002; eta3 =
0.00000126; lambda = 0.3; rho = 0.6; theta1 = 0.2; theta2 = 0.5; delta1 = 0.02; theta3 =
0.2; omega = 0.8; m = 0.00004; psi1 = 0.6; psi2 = 0.5; delta2 = 0.05; psi3 = 0.3; gamma =
0.1; alpha = 0.3; sigma = 0.00003; mu = 0.0254;
dy = zeros(9,1);
dy(1) = (1-p)*pi + sigma*y(9) - lambda*y(1) - mu*y(1);
dy(2) = p*pi - (1-rho)*lambda*y(2) - mu*y(2);
dy(3) = lambda*y(1) + (1-rho)*lambda*y(2) ... - (alpha/(1+m*y(3)))*y(3)
- (gamma/(1+m*y(3)))*y(3) ... - theta1*y(3) - mu*y(3); dy(4) = (alpha/(1+m*y(3)))*y(3)
- theta2*y(4) - omega*y(4) - mu*y(4); dy(5) = (gamma/(1+m*y(3)))*y(3) + omega*y(4)
- theta3*y(5) - (mu+delta1)*y(5); dy(6) = theta1*y(3) - psi1*y(6) - mu*y(6); dy(7) =
theta2*y(4) - (psi2+mu)*y(7); dy(8) = theta3*y(5) - (delta2+psi3+mu)*y(8); dy(9) = psi1*y(6)
+ psi2*y(7) + psi3*y(8) - (sigma+mu)*y(9); end Script file clc; clear;
p = 0.8; pi = 0.0207; eta1 = 0.0003; eta2 = 0.00002; eta3 = 0.00000126; rho = 0.7; theta1=
0.34; theta2= 0.5; delta1= 0.5; theta3= 0.68; omega = 0.8; psi1 = 0.85; psi2 = 0.6; delta2=
0.065; psi3 = 0.75; chi1 = 0.05; chi2 = 0.1; sigma = 0.0003; mu = 0.0254;
betta = 0:0.1:1;
Rc = betta .* ... ( (eta1*chi1*(theta3+delta1+mu) + chi1*omega +
chi2*(theta2+mu+omega)) .* (psi3+delta2+mu) .* (psi2+mu) ... + eta3*theta2 ... +
chi1*(psi3+delta2+mu)*(theta3+delta1+mu) ...
+ eta2*theta3*(psi2+mu)*(chi1*omega+chi2*(theta2+omega+mu)) ) ... .* (((1-p)*pi)/mu
+ ((1-rho)*p*pi)/mu) ... ./ ( (chi1+chi2+theta1+mu) .* (theta2+omega+mu) .* (theta3+delta1+mu)
.* (psi2+mu) .* (delta2+psi3+mu) );
figure(1) plot(betta,Rc,'LineWidth',2) xlabel('\beta'); ylabel('R_c');
gridon; title('Reproductionnumbervstransmissionrate');
tspan = 0:0.001:20; t0 = [1182969 30920683 17923767 127595 200000 500000 50000
113155 2753131];
[t,y] = ode23(@phd2vary, tspan, t0);
```

figure(2) plot(t, y(:,1), 'r', 'LineWidth', 2); xlabel('time (years)'); ylabel('Asymptomatic infectious population'); box off; grid on;

Co-infection Code function dy = Cophd2vary(t,y)

global lambda Q n kapa lambda1 mu rho episilon1 episilon2 lambda2 phi1 theta1 theta2 gamma1 theta3 global theta4 phi2 gamma5 theta5 gamma2 alpha1 phi3 alpha2 phi4 gamma4 alpha3 gamma3

Q = 0.8; lambda = 0.207; betta = 0.15; eta1 = 0.0003; eta2 = 0.000002; eta3 = 0.00000126; lambda1 = 0.3; lambda2 = 0.8; rho = 0.6; theta1 = 0.34; theta2 = 0.5; gamma1 = 0.5; gamma2 = 0.7; gamma3 = 0.21; gamma4 = 0.065; gamma5 = 0.3; theta3 = 0.68; theta4 = 0.023; theta5 = 0.175; phi1 = 0.6; phi2 = 0.5; phi3 = 0.6; phi4 = 0.1; n = 0.0; alpha1 = 0.85; alpha2 = 0.8; alpha3 = 0.75; mu = 0.0147; kapa = 0.003; episilon1 = 0.1; episilon2 = 0.03;

dy = zeros(13,1);

dy(1) = (1-Q)*lambda + kapa*y(13) - lambda1*y(1) - mu*y(1); dy(2) = Q*lambda - (1-rho)*lambda1*y(2) - mu*y(2);

dy(3) = lambda1*y(1) + (1-rho)*lambda1*y(2) ... - (episilon1/(1+n*y(3)))*y(3) - (episilon2/(1+n*y(3)))*y(3) ... - theta1*y(3) - mu*y(3);

dy(4) = (episilon2/(1+n*y(3)))*y(3) - theta2*y(4) - phi1*y(4) - mu*y(4) - lambda2*y(4);

dy(5) = (episilon1/(1+n*y(3)))*y(3) + phi1*y(4) - theta3*y(5) - (mu+gamma1+lambda2)*y(5);

dy(6) = lambda2*y(4) - (mu+gamma5+phi2+theta4)*y(6); dy(7) = lambda2*y(5) + phi2*y(6) - (gamma2+theta5+mu)*y(7); dy(8) = theta1*y(3) - alpha1*y(8) - mu*y(8); dy(9) = theta2*y(4) + phi3*y(11) - (alpha2+mu)*y(9); dy(10) = theta3*y(5) + phi4*y(12) - (gamma4+alpha3+mu)*y(10);

dy(11) = theta4*y(6) - (phi3+mu)*y(11); dy(12) = theta5*y(7) - (mu+phi4+gamma3)*y(12);

dy(13) = alpha1*y(8) + alpha2*y(9) + alpha3*y(10) - (kapa+mu)*y(13);

end

Script file clc; clear;

tspan = 0:0.01:20;

t0 = [1182969 26294166 13442825 59557 37949 57427 66588 ... 300000 40000 91560 57427 66588 12279834];

[t,y] = ode23(@Cophd2vary, tspan, t0);

figure(3) plot(t, y(:,6), ’b’, ’LineWidth’, 2);

xlabel(’time (years)’); ylabel(’Asymptomatic TB-Pneumonia treated’); box off; grid on; hold on; Appendix C

Appendix C: Publication One

Hindawi
Discrete Dynamics in Nature and Society
Volume 2024, Article ID 5883142, 17 pages
https://doi.org/10.1155/2024/5883142

Research Article

A Model for the Propagation and Control of Pulmonary Tuberculosis Disease in Kenya

Erick Mutwiri Kirimi,[1] **Grace Gakii Muthuri**,[1] **Cyrus Gitonga Ngari**,[2] **and Stephen Karanja**[1]

[1]*Department of Mathematics, Meru University of Science and Technology, P.O. Box 972-60200, Meru, Kenya*
[2]*Department of Pure and Applied Sciences, Kirinyaga University, P.O. Box 143-10300, Kerugoya, Kenya*

Correspondence should be addressed to Erick Mutwiri Kirimi; ercmutwiri@gmail.com

Received 8 November 2023; Revised 10 March 2024; Accepted 21 March 2024; Published 31 March 2024

Academic Editor: Anibal Coronel

Pulmonary tuberculosis is among the leading infectious diseases causing mortality worldwide. Therefore, scaling up intervention strategies to reduce the spread of infections in the population is imperative. In this paper, a population-based compartmental approach has been employed to formulate a mathematical model of pulmonary tuberculosis that incorporates an asymptomatic infectious population. The model includes asymptomatic infectious individuals since they spread infections incessantly to susceptible populations without being noticed, thus contributing to the high rate of infection transmission. Qualitative and numerical analyses were performed to determine the impact of various intervention strategies on controlling infection transmission in the population. Sensitivity and numerical results indicate that increasing screening of latently infected and asymptomatic infectious individuals reduces infection transmission to the susceptible population. Numerical results demonstrate that the combination of vaccination, screening, and treatment of all forms of pulmonary tuberculosis is the most effective intervention in decreasing infection transmission. Furthermore, a combination of screening and treatment of all forms of pulmonary tuberculosis proves more effective than a combination of vaccination and treatment of symptomatic infectious individuals alone. Treating the symptomatic infectious population alone is identified as the least effective intervention for curtailing infection transmission in the susceptible population. These study findings will guide healthcare officials in making decisions regarding the screening of latently infected and asymptomatic infectious pulmonary tuberculosis patients, thereby aiding in the fight against epidemics of this disease.

1. Introduction

Mathematical modeling is one of the valuable tools that explore the transmission dynamics of infectious diseases and assess the impact of various control interventions. Therefore, mathematical modeling of infectious diseases is used to guide public health policies and inform decision-making during epidemics [1, 2]. This paper employs a classical SEIR transmission mechanism to formulate a novel model for pulmonary tuberculosis, aiming to accurately depict its natural progression. The SEIR model, a widely used compartmental model in epidemiology, is utilized to forecast the spread of infectious diseases with latent or exposed phases [3]. During the latent phase of a disease, individuals are neither infectious nor symptomatic [4]. The evolution of infectious diseases, taking into consideration the SEIR model, has been discussed by several authors [5–9]. Research suggests that around one-quarter of the global population harbors latent pulmonary tuberculosis infections [10]. Consequently, an epidemiological model for pulmonary tuberculosis must account for this latent population and hence adopts the classical SEIR framework. Within the SEIR model, the population is categorized into four compartments: Susceptible (S), Exposed (E), Infectious (I), and Recovered (R) [2].

Appendix D: Publication Two

Informatics in Medicine Unlocked 46 (2024) 101470

Contents lists available at ScienceDirect

Informatics in Medicine Unlocked

journal homepage: www.elsevier.com/locate/imu

Modeling the effects of vaccine efficacy and rate of vaccination on the transmission of pulmonary tuberculosis

Erick Mutwiri Kirimi [a,*], Grace Gakii Muthuri [a], Cyrus Gitonga Ngari [b], Stephen Karanja [a]

[a] Department of Mathematics, Meru University of Science and Technology, P.O Box, 972-60200, Meru, Kenya
[b] Department of Pure and Applied Sciences, Kirinyaga University, P.O Box, 143-10300, Kerugoya, Kenya

ARTICLE INFO

Keywords:
Pulmonary tuberculosis
Asymptomatic infectious
Control reproduction number
Vaccine efficacy
Vaccination rate
Numerical simulation

ABSTRACT

Numerous prevention intervention strategies have been developed to curtail the spread of pulmonary tuberculosis to susceptible populations. However, pulmonary tuberculosis continues to claim many lives worldwide. In this paper, a deterministic mathematical model incorporating an asymptomatic infectious population, considering vaccine efficacy, and vaccination rate, has been formulated. The model includes asymptomatic infectious individuals since they spread infections incessantly to susceptible populations without being noticed, thus contributing to the high transmission rate. Sensitivity and numerical analysis have been conducted to investigate the impact of varying vaccine efficacy and vaccination rates on the transmission of pulmonary tuberculosis infections from the asymptomatic infectious population. The sensitivity and numerical results show that an increase in vaccine efficacy reduces the asymptomatic infectious population and subsequently lowers the transmission rate of infections. Moreover, an increase in vaccine efficacy was shown to reduce the control reproduction number due to asymptomatic infectious individuals, thereby decreasing the transmission of pulmonary tuberculosis to susceptible populations. Further results indicate that an increase in vaccination rate reduces the control reproduction number due to asymptomatic infectious individuals, consequently lowering the rate of infection transmission. These findings emphasize the need to develop a vaccine of higher efficacy to reduce infection transmission to susceptible populations by the asymptomatic infectious individuals. Additionally, the results underscore the importance of increasing vaccination rates to eradicate pulmonary tuberculosis from the population.

1. Introduction

Pulmonary tuberculosis has claimed and continues to claim numerous lives worldwide. For instance, in Kenya alone, approximately 32,000 people succumbed to the disease in 2022 [1]. This high mortality rate persists despite the availability of effective treatment strategies to curb its spread. The efforts to eradicate pulmonary tuberculosis face challenges due to the inadequacy of tools for preventing infection transmission among susceptible populations [2]. Therefore, there is an urgent need for intensified research and innovation aimed at preventing infection transmission globally. Specifically, research focused on developing highly effective vaccines and implementing suitable vaccination strategies is paramount [3].

At present, Bacillus Calmette-Guérin (BCG) stands as the sole vaccine employed for preventing pulmonary tuberculosis transmission. However, its preventive efficacy is only approximately 50%, rendering it insufficient for curtailing infection transmission in susceptible populations [4]. Consequently, ongoing research endeavors aim to develop new and more efficacious vaccines against pulmonary tuberculosis, with several candidates undergoing various stages of clinical testing [3]. Mathematical modeling approaches can predict the potential impact of these novel vaccines on pulmonary tuberculosis containment [3]. For instance, such models are instrumental in assessing vaccine efficacies and furnishing insights into the long-term effectiveness of vaccination programs. Furthermore, mathematical models aid in determining optimal and cost-effective vaccination coverage necessary for disease eradication within the population [5].

Mathematical modeling approaches have been instrumental in studying complex biological processes [6–11]. The intricate and unpredictable transmission patterns of pulmonary tuberculosis can thus be elucidated through mathematical modeling techniques [12]. Mathematical modeling of infectious diseases plays a crucial role in

* Corresponding author.
E-mail address: ercmutwiri@gmail.com (E.M. Kirimi).

https://doi.org/10.1016/j.imu.2024.101470
Received 23 January 2024; Received in revised form 5 March 2024; Accepted 6 March 2024
Available online 15 March 2024

Appendix E: Plagiarism Report

DrillBit

The Report is Generated by DrillBit Plagiarism Detection Software

Submission Information

Author Name	ERICK MUTWIRI KIRIMI
Title	MODELING PULMONARY TUBERCULOSIS AND PNEUMONIA CO-INFECTION INCORPORATING AN ASYMPTOMATIC COMPONENT AND NATURAL IMMUNITY
Paper/Submission ID	4411486
Submitted by	mmusungu@must.ac.ke
Submission Date	2025-09-24 18:17:37
Total Pages, Total Words	166, 44795
Document type	Thesis

Result Information

Similarity **7 %**

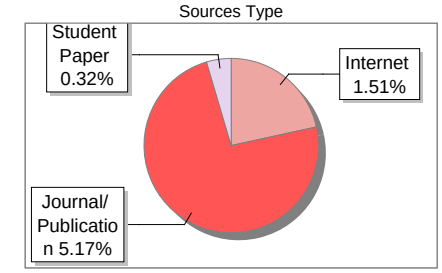

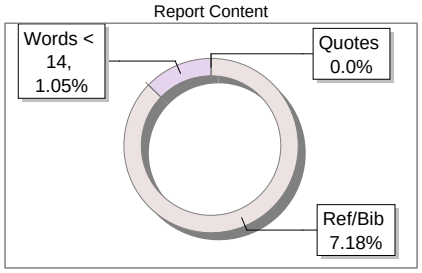

Exclude Information

Quotes	Not Excluded
References/Bibliography	Excluded
Source: Excluded < 14 Words	Not Excluded
Excluded Source	**0 %**
Excluded Phrases	Not Excluded

Database Selection

Language	English
Student Papers	Yes
Journals & publishers	Yes
Internet or Web	Yes
Institution Repository	Yes

A Unique QR Code use to View/Download/Share Pdf File

Appendix F: MIRERC Clearance

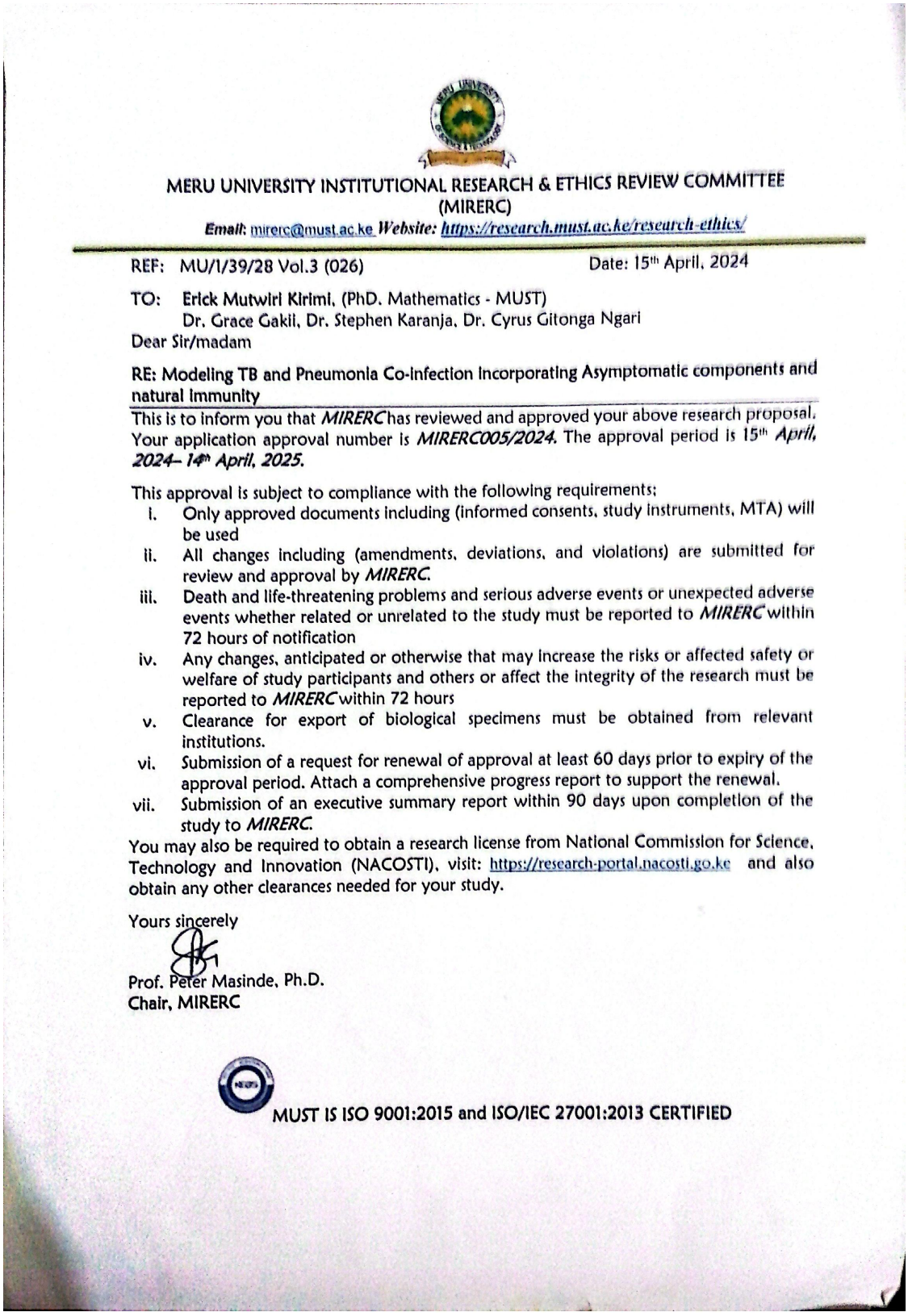

MERU UNIVERSITY INSTITUTIONAL RESEARCH & ETHICS REVIEW COMMITTEE
(MIRERC)
Email: mirerc@must.ac.ke *Website:* https://research.must.ac.ke/research-ethics/

REF: MU/I/39/28 Vol.3 (026) Date: 15th April, 2024

TO: Erick Mutwiri Kirimi, (PhD. Mathematics - MUST)
Dr. Grace Gakii, Dr. Stephen Karanja, Dr. Cyrus Gitonga Ngari

Dear Sir/madam

RE: Modeling TB and Pneumonia Co-infection Incorporating Asymptomatic components and natural Immunity

This is to inform you that *MIRERC* has reviewed and approved your above research proposal. Your application approval number is *MIRERC005/2024.* The approval period is 15th *April, 2024– 14th April, 2025.*

This approval is subject to compliance with the following requirements;

i. Only approved documents including (informed consents, study instruments, MTA) will be used
ii. All changes including (amendments, deviations, and violations) are submitted for review and approval by *MIRERC.*
iii. Death and life-threatening problems and serious adverse events or unexpected adverse events whether related or unrelated to the study must be reported to *MIRERC* within 72 hours of notification
iv. Any changes, anticipated or otherwise that may increase the risks or affected safety or welfare of study participants and others or affect the integrity of the research must be reported to *MIRERC* within 72 hours
v. Clearance for export of biological specimens must be obtained from relevant institutions.
vi. Submission of a request for renewal of approval at least 60 days prior to expiry of the approval period. Attach a comprehensive progress report to support the renewal.
vii. Submission of an executive summary report within 90 days upon completion of the study to *MIRERC.*

You may also be required to obtain a research license from National Commission for Science, Technology and Innovation (NACOSTI), visit: https://research-portal.nacosti.go.ke and also obtain any other clearances needed for your study.

Yours sincerely

Prof. Peter Masinde, Ph.D.
Chair, MIRERC

MUST IS ISO 9001:2015 and ISO/IEC 27001:2013 CERTIFIED

Appendix G: Research Permit

REPUBLIC OF KENYA

NATIONAL COMMISSION FOR SCIENCE, TECHNOLOGY & INNOVATION

Ref No: **729710**

Date of Issue: **25/April/2024**

RESEARCH LICENSE

This is to Certify that Mr. Erick Mutwiri Kirimi of Pan African University, has been licensed to conduct research as per the provision of the Science, Technology and Innovation Act, 2013 (Rev.2014) in Nairobi on the topic: MODELING PULMONARY TUBERCULOSIS AND PNEUMONIA CO-INFECTION INCORPORATING AN ASYMPTOMATIC COMPONENT AND NATURAL IMMUNITY for the period ending: 25/April/2025.

License No: **NACOSTI/P/24/414417**

729710

Applicant Identification Number

Director General
NATIONAL COMMISSION FOR SCIENCE,TECHNOLOGY & INNOVATION

Verification QR Code

NOTE: This is a computer generated License. To verify the authenticity of this document, Scan the QR Code using QR scanner application.

See overleaf for conditions